

AN ABSTRACT OF THE DISSERTATION OF

Khaled Husain G. Almabruk for the degree of Doctor of Philosophy in
Pharmaceutical Sciences presented on September 2, 2016.

Title: Development of Novel Agents to Combat Tuberculosis and Malaria.

Abstract approved:

Taifo Mahmud

Abstract

Despite the advance of biomedical science, infectious diseases remain one of the number one killers in the world. They claim the lives of millions of people annually, particularly in underdeveloped and developing countries. In fact, more than 32% of the health burden in Africa is caused by infectious diseases, e.g., tuberculosis, malaria, and HIV/AIDS, as well as other neglected tropical diseases.

Tuberculosis (TB), one of the most devastating infectious diseases, is caused by *Mycobacterium tuberculosis*. In 2014, 9.6 million people were diagnosed with active TB, 1.5 million of whom died from the disease (WHO). Most of these deaths occur in HIV patients who are more vulnerable to the infection due to a weakened immune system. Moreover, the emergence of multi-drug resistant strains of *M. tuberculosis* in recent years has rendered some of the

first-line anti-TB drugs, such as isoniazid (INH) and rifampin, less effective. Consequently, TB is becoming a bigger problem worldwide.

Similar to TB, malaria also causes a significant health burden in tropical countries. It is a parasitic disease transmitted by *Anopheles* mosquitoes. The main malarial parasites that infect humans are *Plasmodium falciparum* and *P. vivax*. In 2015, there were an estimated 214 million new cases of malaria and 438,000 deaths (WHO). Furthermore, the development of resistant strains of *P. falciparum* to chloroquine and artemisinin has raised a public concern. Therefore, the development of new anti-malarial agents is urgently needed.

Our research focuses on the discovery of new drug candidates that can be developed as new anti-tubercular and anti-malarial drugs. Using a combination of contemporary biosynthetic approaches and semisynthetic modifications, we have produced analogs of rifampin, a clinically used first-line anti-tubercular drug. Rifampin is derived from rifamycin B, a complex natural polyketide compound produced by the soil bacterium *Amycolatopsis mediterranei* S699. This polyketide natural product is biosynthesized by a type I modular polyketide synthase (PKS) system. While simple modifications of the functional groups of rifamycin can be done chemically, alterations of its polyketide backbone are difficult to achieve, thus requiring alternative approaches, e.g., biosynthetic engineering. In collaboration with the group of Professor Rup Lal at the University of Delhi, we designed a strategy to

construct mutant strains of *A. mediterranei* S699, in which the acyltransferase (AT) domain of module 6 of the rif-PKS (recognizes methylmalonyl-CoA as substrate) was replaced with the AT domain of module 2 of the rapamycin PKS (recognizes malonyl-CoA). The mutant strain was able to produce a novel rifamycin analog, 24-desmethylrifamycin B, which was confirmed by mass spectroscopy, NMR and X-ray crystallography. The product was subsequently modified semi-synthetically to 24-desmethylrifampin. The latter compound was then tested against a panel of Gram-positive and Gram-negative bacteria such as *Staphylococcus aureus*, *Pseudomonas aeruginosa*, and *Mycobacterium smegmatis*, and the results showed that 24-desmethylrifampin has antibacterial activity comparable to the commercially used antibiotic rifampin. More interestingly, 24-desmethylrifampin showed excellent activity against both rifampin-sensitive and rifampin-resistant strains of *M. tuberculosis*.

As a part of our efforts to discover potential candidates for anti-TB drugs, we also investigated a prenylated isoflavanone, perbergin, which was isolated from the Madagascar plant *Dalbergia pervillei*. Perbergin was found to have a virulence factor quenching activity in the plant pathogen *Rhodococcus fascians*. *R. fascians* to some extent is similar to *M. tuberculosis* in that their cell walls are rich in mycolic acids. Also, structurally, perbergin is somewhat similar to trehalose monomycolate (TMM), which is involved in the *M. tuberculosis* cell wall biosynthesis and virulence. Thus, it is intriguing to

investigate the use of perbergin as a trehalose monomycolate mimetic, which may disrupt the cell wall structures or act as an inhibitor of enzymes involved in the biosynthesis of acyltrehaloses. To this end, we synthesized the reported perbergin in nine steps with an overall yield of 13.5%. However, the NMR data for the synthetic products are inconsistent with those published for perbergin. Analysis of the raw data for perbergin, which was kindly provided by Prof. Mondher Eljaziri at Université Libre De Bruxelles, revealed that the natural perbergin contains a geranyl moiety at C-6 instead of C-8, and the geranyl moiety has an *E* configuration instead of a *Z* configuration. Moreover, the synthetic products (±)-(Z)- and (E)-isoperbergins showed good antibacterial activity against the Gram-positive bacteria *S. aureus* and *M. smegmatis*, but not the Gram-negative bacteria *Escherichia coli* and *P. aeruginosa*. Furthermore, we tested the activity of the synthetic compounds against both rifampin-sensitive and rifampin-resistant strains of *M. tuberculosis*; however, they were not active at a concentration lower than 10 µg/mL.

The fourth part of this dissertation is to develop novel agents to combat malaria. Previously, our research group has generated a number of novel pactamycin analogs through manipulations of the pactamycin biosynthetic pathway. Pactamycin, a bacterial-derived natural product discovered by the Upjohn Company in the early 1960s, has broad-spectrum growth inhibitory activity against mammalian cells, viruses, bacteria and protozoa. However, it

is also highly toxic. Inactivation of the *ptmH* gene, which encodes a radical SAM-dependent protein, in the pactamycin producing strain of *Streptomyces pactum* resulted in a mutant that produced pactamycin analogs, TM-025 and TM-026. Both of these compounds showed excellent anti-malarial activity and were 10-30 fold less toxic than pactamycin.

To improve the biological and pharmaceutical properties of TM-025 and TM-026, we employed a mutasynthetic strategy to generate their fluorinated analogs. We created a double knockout mutant, *S. pactum* $\Delta ptmTH$, which lacks the *ptmH* gene and also lacks the ability to produce 3-aminobenzoic acid (a precursor of pactamycin). The mutant was then fed with synthetically prepared 2-fluoro-5-aminobenzoic acid to give two fluorinated analogs, TM-025F and TM-026F. The compounds were tested against chloroquine-sensitive and chloroquine-resistant strains of *P. falciparum*, and the results showed that TM-025F and TM-026F have excellent activity against all plasmodial strains tested.

In conclusion, we have applied genetic, mutasynthetic, and synthetic approaches to produce new analogs of complex natural products with promising activity against tuberculosis and malaria. The study also provided insights into the biosynthetic machinery and the modes of formation of those compounds in nature. Furthermore, using a total synthesis approach, we generated geranylated isoflavanones that showed good activity and selectivity

toward Gram-positive bacteria, including *M. smegmatis*. However, they lack activity against *M. tuberculosis* at concentrations lower than 10 µg/mL. It is noteworthy that this synthetic study led to the revision of the published chemical structure of perbergin.

©Copyright by Khaled Husain G. Almabruk
September 2, 2016
All Rights Reserved

Development of Novel Agents to Combat Tuberculosis and Malaria

by

Khaled Husain G. Almaghrabi

A DISSERTATION

submitted to

Oregon State University

in partial fulfillment of
the requirements for the
degree of

Doctor of Philosophy

Presented September 2, 2016
Commencement June 2017

Doctor of Philosophy dissertation of Khaled Husain G. Almabruk presented on
September 2, 2016

APPROVED:

Major Professor, representing Pharmaceutical Sciences

Dean of the College of Pharmacy

Dean of the Graduate School

I understand that my dissertation will become part of the permanent collection of Oregon State University libraries. My signature below authorizes release of my dissertation to any reader upon request.

Khaled Husain G. Almabruk, Author

ACKNOWLEDGEMENTS

I would like to express my sincere appreciation to my academic advisor, Dr. Taifo Mahmud, for having me in his laboratory and directing me throughout my graduate studies. Also, for his unlimited support, help and advice whenever I needed them. His supervision, enthusiasm and encouragements are greatly appreciated.

I would like to thank my committee members, Dr. Philip Proteau, Dr. Adam Alani, Dr. Benjamin Philmus, and Dr. Daniel Rockey for their time and advice in directing me during my PhD studies.

I am also grateful to all former and current members of Dr. Mahmud's group for their friendship, encouragements and sharing expertise whenever needed. Also, I would like to appreciate the friendships of the members of the Zabriskie, McPhail, Proteau, Philmus, and Sikora groups. I am in debt to the Department of Pharmaceutical Sciences for their support and help. I would like to express my sincere gratitude to the government of Libya for a scholarship to pursue my PhD study.

I am in great debt to my mother, brothers and sisters for their unlimited love, help, and support, may Allah bless them all and keep them safe. My friends, Marie Alsairei, Yousef Alanazi, Abdullah Alanzi, Sultan Alshahrani, Adel Al Fatease and Saeed Banawas, are acknowledged for their friendship and advice.

CONTRIBUTIONS OF AUTHORS

Dr. Taifo Mahmud designed the studies and edit the manuscripts in Chapters 2, 3 and 4. In Chapter 2, Aeshna Nigam, Anjali Saxena, Udit Mukherjee, Hardeep Kaur, Puneet Kohli, Rashmi Kumari, and Priya Singh did the genetic manipulation of *Amycolatopsis mediterranei* S699, and Dr. Rup Lal designed the study and edit the manuscript. Dr. Jongtae Yang helped with the screening for AT6 mutant. Dr. Lev N. Zakharov did the X-ray analysis of 24-desmethylrifamycin SV. In Chapter 3, the manuscript was written through contributions of all authors. In Chapter 4, Drs. Wanli Lu and Mostafa Abugrain prepared and characterized the double knockout mutant *ptmT/H*, and Drs. Yuexin Li and Jane X. Kelly did the anti-malarial assay. Khaled H. Almabruk performed all other experiments. Khaled H. Almabruk and Dr. Taifo Mahmud analyzed the data and wrote the manuscripts for Chapters 2, 3, and 4.

TABLE OF CONTENTS

	<u>Page</u>
CHAPTER I: General Introduction.....	1
1.1 Tuberculosis.....	2
1.1.2 TB History.....	3
1.1.3 Transmission and Stages of TB	4
1.1.4 <i>Mycobacterium tuberculosis</i>	5
1.1.5 Diagnosis and Current Treatment	7
1.1.5.1 Diagnosis.....	7
1.1.5.2 Current Treatment	7
1.1.6 <i>Mycobacterium tuberculosis</i> Resistance	10
1.1.7 Development of Novel Anti-tubercular Agents and Newly Approved Anti-TB Agents	11
1.2 Malaria.....	16
1.2.2 Malaria Life Cycle.....	16
1.2.3 Malaria Symptoms.....	18
1.2.5 Malaria Treatment and Resistance	18
1.2.6 Natural Products and Anti-malarial Activity	20
1.2.7 Candidates in Pre-clinical and Clinical Trails	21
1.3 Dissertation Background	25
1.3.1 Genetic and Semisynthetic Approaches Toward Novel Rifamycins.....	25
1.3.1.1 Rifamycin.....	25
1.3.1.2 Rifamycin Biosynthesis	26
1.3.1.3 Semisynthetic and Mutasynthetic Approaches to Novel Rifamycins	27
1.3.2 Synthesis of Geranylated Isoflavanones as Potential Anti-TB Drugs	32
1.3.2.1 Perbergin as a Potential Anti-TB Drug	33
1.3.3 Mutasynthesis of Pactamycin Analogs as Anti-malarial Agents	35
1.3.3.1 Pactamycin.....	35

TABLE OF CONTENTS (Continued)

	<u>Page</u>
1.3.3.2 Novel Pactamycin Analogs with Excellent Anti-malarial Activity	36
1.4 Thesis Overview.....	38
1.5 References.....	39
CHAPTER II: Modification of Rifamycin Polyketide Backbone Leads to Improved Drug Activity Against Rifampicin-Resistant <i>Mycobacterium Tuberculosis</i>	46
2.1 Abstract.....	47
2.2 Introduction.....	48
2.3 Results and Discussion.....	52
2.3.1 AT6 domain substitution in <i>A. mediterranei</i> S699	52
2.3.2 Production of rifamycin analogs by rifAT6::rapAT2 mutant	54
2.3.3 Structure determination of 24-desmethylrifamycin B and 24-desmethylrifamycin SV	55
2.3.4 Conversion of 24-desmethylrifamycin B to 24-desmethylrifamycin S	56
2.3.5 Synthesis of 24-desmethylrifampicin	57
2.3.6 Antibacterial activity of 24-desmethylrifamycin S and 24-desmethylrifampicin.....	59
2.4 Discussion.....	61
2.5 Material and Methods.....	66
2.5.1 General Experimental Procedures	66
2.4.2 Bacterial strains, plasmids, and culture media	66
2.4.3 Construction and screening of a genomic cosmid library and selection of the rifamycin cluster	67
2.4.4 Construction of pAT6F	68
2.4.5 Genetic manipulation of <i>A. mediterranei</i> S699.....	69
2.4.6 PCR and sequence analysis of the AT6 mutant.....	70
2.4.7 Isolation and purification of 24-desmethylrifamycin B	70
2.4.8 Conversion of 24-desmethylrifamycin B to 24-desmethylrifamycin S	72

TABLE OF CONTENTS (Continued)

	<u>Page</u>
2.4.9 X-ray crystallography of 24-desmethylrifamycin S	73
2.4.10 Synthesis of 24-desmethylrifampicin	74
2.4.11 Antibacterial assay	75
2.5 Supplemental Data	77
2.6 References	93
CHAPTER III: Total Synthesis Of (±)-Isoperbergins and Correction of The Chemical Structure of Perbergin	97
3.1 Abstract	98
3.2 Results and Discussion	100
3.3 Experimental Section	110
3.3.1 General Experimental Procedures	110
3.3.2 Synthesis of 2,3-Bis(benzyloxy)-4-methoxybenzaldehyde (2)	111
3.3.3 Synthesis of 1-(2,4,6-Tris(benzyloxy)phenyl)ethan-1-one (4)	112
3.3.4 Synthesis of (E)-3-(2,3-Bis(benzyloxy)-4-methoxyphenyl)-1-(2,4,6- tris(benzyloxy)phenyl)prop-2-en-1-one (5)	112
3.3.5 Synthesis of 2-(2,3-Bis(benzyloxy)-4-methoxyphenyl)-3,3- dimethoxy-1-(2,4,6-tris(benzyloxy)phenyl)propan-1-one (6)	113
3.3.6 Synthesis of 5,7-Bis(benzyloxy)-3-(2,3-bis(benzyloxy)-4- methoxyphenyl)-4H-chromen-4-one (7)	114
3.3.7 Synthesis of (±)-3-(2,3-Dihydroxy-4-methoxyphenyl)-5,7- dihydroxychroman-4-one ((±)- 8)	115
3.3.8 Synthesis of 5-Hydroxy-3-(4-methoxy-2,3- bis(methoxymethoxy)phenyl)-7-(methoxymethoxy)chroman-4-one (9) ..	116
3.3.9 Synthesis of (E)-5-((3,7-Dimethylocta-2,6-dien-1-yl)oxy)-3-(4- methoxy-2,3-bis(methoxymethoxy)phenyl)-7-(methoxymethoxy)chroman- 4-one (10)	117
3.3.10 Synthesis of (E)- and (Z)-8-(3,7-Dimethylocta-2,6-dien-1-yl)-5- hydroxy-3-(4-methoxy-2,3-bis(methoxymethoxy)phenyl)-7- (methoxymethoxy)chroman-4-one (11)	118
3.3.11 Synthesis of (±)- Z-12 and (±)- E-12	119
3.3.12 Antibacterial Activity Assay	120

TABLE OF CONTENTS (Continued)

	<u>Page</u>
3.4 Acknowledgment.....	120
3.5 Supplemental Data.....	122
3.7 References.....	134
CHAPTER IV: Mutasythesis of Fluorinated Pactamycin Analogues and Their Antimalarial Activity	136
4.1 Abstract.....	137
4.2 Introduction.....	138
4.3 Results and Discussion.....	140
4.4 Experimental Section.....	148
4.4.1 Bacterial strains and plasmids.....	148
4.4.2 General DNA manipulations	148
4.4.3 Construction of ptmA and ptmT knock-out plasmids	149
4.4.4 Feeding experiments with 3-aminobenzoic acid and [7- ¹³ C]-3-aminobenzoic acid.....	150
4.4.5 Feeding experiments with 2-, 3-, and 4-aminobenzoic acids	151
4.4.6 Synthesis of 2-fluoro-5-aminobenzoic acid	152
4.4.7 Synthesis of 3-amino-4-methyl-5-fluorobenzoic acid	153
4.4.8 Feeding experiments with 2-fluoro-5-aminobenzoic acid and 3-amino-4-methyl-5-fluorobenzoic acid	153
4.4.9 Isolation of TM-025F and TM-026F	153
4.4.10 In vitro Antimalarial Activity Assay.....	155
4.4.11 Antibacterial Activity Assay	156
4.5 Supplemental Data.....	157
4.5 References.....	171
CHAPTER V: General Conclusion	173
Appendices.....	177

LIST OF FIGURES

<u>Figure</u>	<u>Page</u>
Figure 1.1.1. Schematic of cell wall envelope of <i>Mycobacterium tuberculosis</i>	6
Figure 1.1.2. Sites and Mechanisms of Action of Antimycobacterial Agents.....	8
Figure 1.1.3. Chemical structures of first-line drugs for TB treatment...10	10
Figure 1.2.1. Malarial parasite life cycle.....	17
Figure 1.3.1. Genetic organization of rifamycin B biosynthesis.....	27
Figure 1.3.2. Conversion of rifamycin B to clinically used anti-TB.....	28
Figure 1.3.3. The feeding of 3-amino-4-bromobenzoic acid to the AHBA blocked mutant of <i>A. mediterranei</i>	30
Figure 1.3.4. Feeding <i>rifK</i> mutant with four SNAC-AHBA diketide derivatives.....	31
Figure 1.3.5. Feeding β -hydroxyl SNAC derivative of AHBA to RM01 mutant.....	32
Figure 1.3.6. Chemical structure of the isoflavanone core and some biologically active isoflavanoids. C-5 and C-7 usually each bear a hydroxy group.....	33
Figure 1.3.7. Chemical structures of reported perbergin, trehalose, trehalose momomycolate (TMM), and trehalose dimycolate (TDM).....	34
Figure 1.3.8. Chemical structures of different pactamycin analogs.....	36
Figure 1.3.9. Chemical structures of TM0-26 and TM-025.....	37
Figure 2.1. Chemical structures of rifamycins and rapamycin.....	48
Figure 2.2. Genetic organization of polyketide synthase gene cluster of rifamycin B biosynthesis.....	50
Figure 2.3. Construction of AT6 mutant of <i>Amycolatopsis mediterranei</i> S699.....	53
Figure 2.4. Mass spectrometry analysis of ethyl acetate extracts of wild-type and AT6 mutant strains of <i>A. mediterranei</i> S699.....	56
Figure 2.5. X-ray crystal structure of 24-desmethylrifamycin S dimer in complex with Ca^{2+}	57

LIST OF FIGURES (Continued)

<u>Figure</u>	<u>Page</u>
Figure 2.S1. Domain replacement strategy for the formation of 24-desmethylrifamycin B.....	78
Figure 2.S2. Schematic overviews of plasmid pAT6F construction.....	79
Figure 2.S3. Phenotypic appearances of single- and double-crossover mutants of <i>A. mediterranei</i> S699 on solid media.....	80
Figure 2.S4. Southern blot hybridization of single and double crossover clones.....	81
Figure 2.S5. Nucleotide sequence of PCR1/rapAT2/PCR2 of pAT6.....	82
Figure 2.S6. Restriction map of hybrid DNA obtained from nucleotide sequences (Figure 2.S1) formed in the double cross over clones.....	83
Figure 2.S7. Purification of 24-desmenthylrifampicin using HPLC. Peaks were detected at 254 nm.....	84
Figure 2.S8. Comparative MS/MS Analyses of rifampicin and 24-desmethylrifampicin.....	85
Figure 2.S9. Characteristic MS fragments of rifampicin and 24-desmethylrifampicin in ESI negative ion mode.....	86
Figure 2.S10. ¹ H NMR spectrum of 24-desmethylrifamycin B.....	87
Figure 2.S11. ¹³ C NMR spectrum of 24-desmethylrifamycin B.....	88
Figure 2.S12. ¹ H NMR spectrum of 24-desmethylrifamycin SV.....	89
Figure 2.S13. (-)-ESI-MS spectra of rifamycin S.....	90
Figure 2.S14. ¹ H NMR of 24-desmethylrifampicin.....	91
Figure 2.S15. Agar diffusion assay of rifamycin S, rifampicin, 24-desmethylrifamycin S, and 24-desmethylrifampicin against <i>Staphylococcus aureus</i> (A) and <i>Mycobacterium smegmatis</i> (B).....	92
Figure 3.1. Proposed chemical structures of perbergin and tetrapterol C.....	100
Figure 3.2. Key NOESY correlations of (±)- E-12 and (±)- Z-12	105
Figure 3.3. HMBC correlations of (±)- E-12 , (±)- Z-12 , and natural perbergin.....	107
Figure 3.S1. ¹ H NMR spectrum of (±)- E-12 (500 MHz, CDCl ₃).....	122

LIST OF FIGURES (Continued)

<u>Figure</u>	<u>Page</u>
Figure 3.S2. ^{13}C NMR spectrum of (\pm)- E-12 (125 MHz, CDCl_3).....	123
Figure 3.S3. HSQC spectrum of (\pm)- E-12 (500 MHz, CDCl_3).....	124
Figure 3.S4. HMBC spectrum of (\pm)- E-12 (500 MHz, CDCl_3).....	125
Figure 3.S5. NOESY spectrum of (\pm)- E-12 (500 MHz, CDCl_3).....	126
Figure 3.S6. ^1H NMR spectrum of (\pm)- Z-12 (500 MHz, CDCl_3).....	127
Figure 3.S7. ^{13}C NMR spectrum of (\pm)- Z-12 (125 MHz, CDCl_3).....	128
Figure 3.S8. HSQC spectrum of (\pm)- Z-12 (500 MHz, CDCl_3).....	129
Figure 3.S9. HMBC spectrum of (\pm)- Z-12 (500 MHz, CDCl_3).....	130
Figure 3.S10. NOESY spectrum of (\pm)- Z-12 (500 MHz, CDCl_3).....	131
Figure 3.S11. UV spectra of (\pm)- E-12 and (\pm)- Z-12	132
Figure 3.S12. Chiral HPLC traces of (\pm)- E-12 and (\pm)- Z-12	132
Figure 3.S13. Antibacterial assay of (\pm)- E-12 and (\pm)- Z-12 against <i>R. fascians</i> (A), <i>M. smegmatis</i> (B), and <i>S. aureus</i> (C).....	133
Figure 4.1. Identification of genes responsible for the production of pactamycin precursor.....	139
Figure 4.2. HPLC analysis of EtOAc extracts of the wild-type and the mutant strains of <i>S. pactum</i>	142
Figure 4.3. Mass spectral data for EtOAc (A–C) and n-BuOH (D–F) extracts of <i>S. pactum</i> mutants with and without chemical complementations	143
Figure 4.4. Chemical structures of pactamycin analogs.....	146
Figure 4.S1. Gel electrophoreses of PCR products that confirm ΔptmA and ΔptmT mutant strains of <i>S. pactum</i>	158
Figure 4.S2. MS data for n-BuOH extracts from $\Delta\text{ptmT}/H$ cultures complemented with external precursors.....	169
Figure 4.S3. Preparation of fluorinated precursors and chemical complementation experiments with $\Delta\text{ptmT}/H$ mutants.....	160
Figure 4.S4. MS/MS analysis of TM-025, TM-026, and their fluorinated analogs.....	161
Figure 4.S5. ^1H NMR spectrum of 2-fluoro-5-aminobenzoic acid.....	162
Figure 4.S6. ^{13}C NMR spectrum of 2-fluoro-5-aminobenzoic acid.....	163

LIST OF FIGURES (Continued)

<u>Figure</u>	<u>Page</u>
Figure 4.S7. ^1H NMR spectrum of 3-amino-4-methyl-5-fluorobenzoic acid.....	164
Figure 4.S8. ^{13}C NMR spectrum of 3-amino-4-methyl-5-fluorobenzoic acid.....	165
Figure 4.S9. ^1H NMR spectrum of TM-026F.....	166
Figure 4.S10. ^{13}C NMR spectrum of TM-026F.....	167
Figure 4.S11. ^1H NMR spectrum of TM-025F.....	168
Figure 4.S12. ^{13}C NMR spectrum of TM-025F.....	169
Figure 4.S13. Agar diffusion assay of pactamycin	170

LIST OF TABLES

<u>Table</u>	<u>Page</u>
Table 1.1.1. Drugs currently in use to treat TB.....	9
Table 1.1.2. Recently approved anti-TB drugs and other potential candidates for TB treatment.....	15
Table 1.2.1. Current potential candidates for malaria treatment.....	24
Table 2.1. Drug sensitivity assay of various <i>M. tuberculosis</i> strains toward rifamycins.....	60
Table 2.2. Crystal data and structure refinement for 24-desmethyrrifamycin S.....	74
Table 2.S1. Bacterial strains and plasmids used in this study.....	77
Table 2.S2. Primers used to amplify flanking regions of <i>rifAT6</i>	78
Table 3.1. ¹ H (500 MHz, CDCl ₃) and ¹³ C (125 MHz, CDCl ₃) NMR Spectroscopic Data for Perbergin, (±)- E-12 , and (±)- Z-12	106
Table 3.2. Antibacterial Activity of (±)- E-12 , (±)- Z-12 , and the (±)-Isoflavanone 8^a	109
Table 4.1. Antimalarial Activity of Pactamycin Analogues.....	147
Table 4.S1. Strains and plasmids used in this study.....	157
Table 4.S2. Primers used in this study.....	158

LIST OF SCHEMES

<u>Scheme</u>	<u>Page</u>
Scheme 2.1. Conversion of 24-desmethylrifamycin B to 24-desmethylrifamycin S and chemical synthesis of 24-desmethylrifampicin.....	59
Scheme 3.1. Synthetic strategy for isoflavanone (±)-8.....	101
Scheme 3.2. Conversion of isoflavanone 9 to (±)-E-12 and (±)Z-12...	103

CHAPTER I

General Introduction

Khaled H. Almabruk

Introduction

Infectious diseases remain one of the major causes of morbidity and mortality worldwide. They affect children and adults of all ages. In fact, a large number of annual deaths around the world are due to infectious diseases, among which are HIV/AIDS, tuberculosis (TB), and malaria. However, since the introduction of the Millennial Development Goals (MDGs) in year 2000, which primarily focused on combating HIV/AIDS, TB, and malaria, the mortality rates caused by these diseases have been steadily declining. Yet, in many low- and middle-income countries, they are still responsible for significant health burdens and deaths. Additionally, the encouraging progress by MDGs is clouded by the increased number of cases of multidrug-resistant (MDR)-TB and malaria, which have rendered many currently available treatments ineffective. Therefore, new drugs to treat MDR-TB and malaria are acutely needed.

1.1 Tuberculosis

Tuberculosis (TB) is an infectious disease caused by the pathogenic bacterium *Mycobacterium tuberculosis*. More than 95% of TB patients were reported in third world countries, particularly in countries where HIV infection is prevalent, because HIV patients are more susceptible to the disease. In fact, as of 2015, 1 in 3 HIV deaths were due to TB (WHO). Although TB is a treatable and preventable disease, when not detected and/or treated properly due to improper diagnosis or patient non-compliance with the drug regimen, it

may develop into a serious public health problem. In addition, the development of multidrug-resistant (MDR) and extensively drug-resistant (XDR)-TB has caused most of the currently available first-line drugs to no longer be effective.

1.1.2 TB History

Tuberculosis is an old disease. It has been postulated that the genus *Mycobacterium* originated in East Africa over 150 million years ago (Hayman 1984). The ancestors of the current mycobacteria were present 3 million years ago (Gutierrez et al. 2005). Also, *M. tuberculosis* has been found in ancient Egyptian mummies, as shown by molecular genetic evidence (Zimmerman 1979, Nerlich et al. 1997). TB, before the late nineteenth century, was called the White Death, because it caused much suffering and many deaths since there was no cure.

The first discovery of the transmissibility of *M. tuberculosis* infection was made by a French physician Jean-Antoine Villemin in 1865. In 1885, Robert Koch perfected a staining technique that enabled him to see the microbe that caused TB. Also, X-rays, which were discovered in 1895, enabled the accurate diagnosis of the disease. In the early twentieth century, Albert Calmette and his colleague Camille Guérin introduced the BCG (Bacillus Calmette-Guérin) vaccine. In 1921, the vaccine was first used in France on an infant whose mother had pulmonary tuberculosis. Indeed, the infant did not develop TB. The BCG vaccine has dramatically reduced TB infections and

the resulting deaths. Many years later, the development of antibiotics created a belief that TB could be controlled and perhaps even eradicated.

1.1.3 Transmission and Stages of TB

TB is an airborne disease which can be transmitted from person to person upon the exposure to air droplets carrying the microbes from the infected person. *M. tuberculosis* can remain inactive (dormant) for years without causing any obvious symptoms. The most common symptoms associated with a TB infection are general fatigue, cough, chest pain, and night sweats. If left untreated, this could lead to high fever, bloody coughing, and eventually death. Multiple stage processes are involved in a TB infection. When a person inhales the droplets containing the microbe, *M. tuberculosis* is localized in the alveoli. After 7-21 days, the bacteria multiply within the inactivated pulmonary macrophage, which then bursts and triggers the accumulation of more macrophages. During this stage, the patient becomes tuberculin positive. Also, T-cells are activated, causing the release of γ -interferon (IFN). A tubercle center starts to grow because of the release of cytokines and IFN. While the macrophages present around the tubercle are in an active form, those inside the tubercle itself are inactive and become the host for *M. tuberculosis*. The final stage in a TB infection is the bursting of lesion sacs, which release mycobacterial cells that can easily transmit and infect neighboring tissues of the lungs.

1.1.4 *Mycobacterium tuberculosis*

Mycobacterium belongs to the class of *Actinobacteria*, which has many subclasses, some of which can cause serious illness to humans and animals. *M. tuberculosis*, *M. leprae* and *M. bovis* are different *Mycobacterium* species that cause human diseases. *M. tuberculosis* is of particular concern, because it can lead to a serious threat to global public health. Morphologically, *M. tuberculosis* is a non-motile, non-spore forming, rod shaped bacterium. *M. tuberculosis* grows slowly with a doubling-time of 20-51 hours. Despite the fact that the crystal violet stain does not remain on its cell wall, because of its high lipid content, *M. tuberculosis* is classified as a Gram-positive bacterium with a high GC content.

With the recent developments in gene technology and the corresponding analytical tools, more information is now available on the structure of and the metabolic pathways in *M. tuberculosis*, that are necessary for its survival. The cell envelope of *M. tuberculosis* is composed of a complex structure made of peptidoglycan, arabinogalactan, and mycolic acids, which are surrounded by a mixture of non-covalently bonded lipids, glycans and proteins. The *M. tuberculosis* cell wall is characterized by its thickness, which confers impermeability and resistance to some therapeutic agents. The cell wall core contains large amounts of short (up to C₂₀) and long (up to C₆₀-C₉₀) chains of mycolic and fatty acids, which have cross-linked with arabinogalactan that is attached to peptidoglycan. Across the cell wall, there are cell-wall proteins, phthiocerol dimycocerosate, cord factors (trehalose mono- and dimycolates),

sulfolipids, phosphatidylinositol mannosides (PIMs), and lipoarabinomannan (LAM). The soluble portion of extractable lipids, sugars, and proteins are thought to be involved in *M. tuberculosis* signaling and pathogenesis. Furthermore, the high lipid content in the cell wall provides *M. tuberculosis* with a natural resistance that protects it from any external pressure. Also, across the cell membrane are porins, which allow the hydrophilic nutrients to enter the cell (Figure 1.1.1).

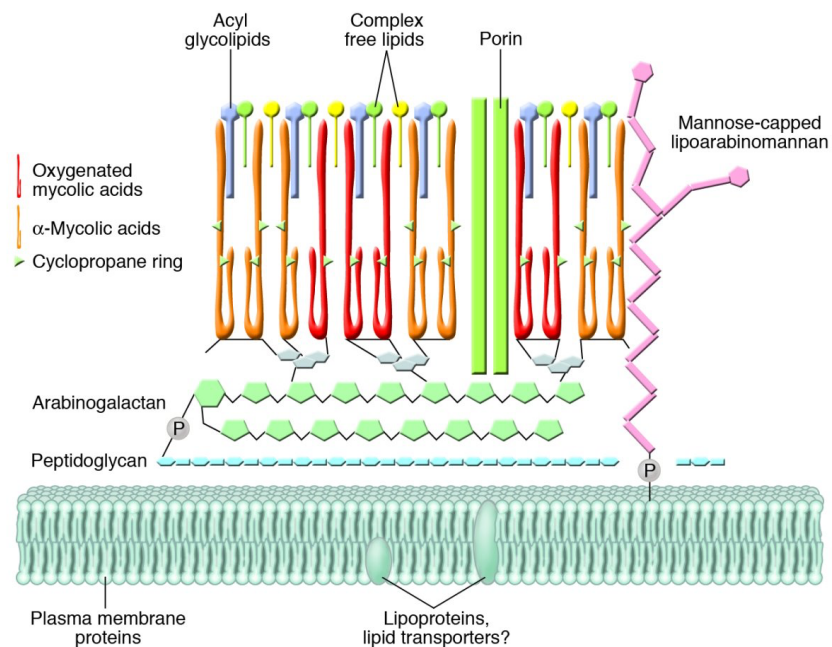


Figure 1.1.1. Schematic of cell wall envelope of *Mycobacterium tuberculosis* (Riley 2006).

1.1.5 Diagnosis and Current Treatment

1.1.5.1 Diagnosis

Microbiological testing of sputum for acid bacilli remains one of the major tests in the diagnosis of TB. Also, the tuberculin skin test (TST) and X-rays are still used in the diagnosis of TB; however, if the patient is TB positive, TST cannot distinguish between a latent and an active TB infection. TST is a cutaneous delayed-type hypersensitivity response to the purified protein derivative (PPD) from a mixture of about 200 *M. tuberculosis* proteins. This assay could cross react with BCG and give false positive results. However, a more recently developed test, the so-called interferon gamma release assay (IGRA), has helped in the accurate diagnosis of patients with a TB infection (LTBI or active TB) and does not cross react with BCG. This test uses 2 to 3 specific TB antigens (Blumberg et al. 2014).

1.1.5.2 Current Treatment

For decades, treatment of tuberculosis has been challenging and hundreds of anti-TB drugs have been synthesized; yet, only a few of them have been used successfully in clinics to treat TB patients. Some of these drugs target *M. tuberculosis* cell wall biosynthesis, while others target different sites in the cell (Figure 1.1.2). A six-month regimen has been used as a standard treatment protocol for drug-susceptible *M. tuberculosis*.

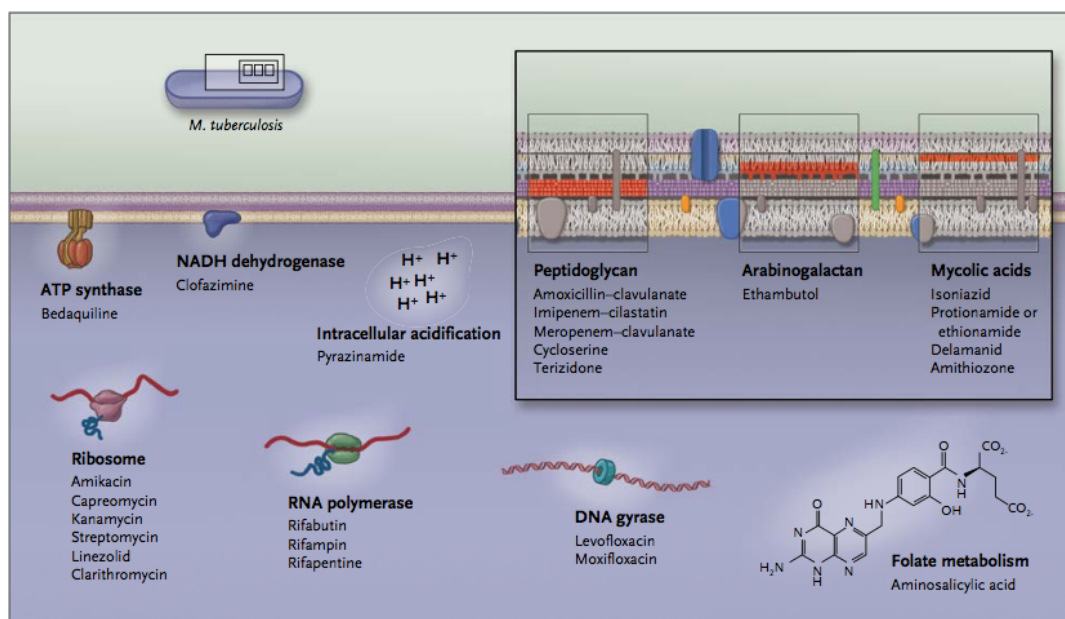


Figure 1.1.2. Sites and Mechanisms of Action of Antimycobacterial Agents (Horsburgh et al. 2015).

In the United States, four-dose regimens are used in the treatment of drug-susceptible *M. tuberculosis*, depending on the nature of the infecting strain whether it is drug-sensitive or -resistant *M. tuberculosis* and the pathological conditions of the patient. The combination of the drugs and the timing of the treatment may also be different. Each regimen has an initial phase of 2 months, followed by another phase that varies between 4-7 months (Blumberg et al. 2003).

Table 1.1.1. Drugs currently in use to treat TB.

First-line drugs	Second-line drugs
Isoniazid	Streptomycin
Rifampin	Amikacin
Rifabutin	Capreomycin
Rifapentine	Levofloxacin
Ethambutol	Cycloserine
Pyrazinamide	<i>p</i> -Aminosalicylic acid
	Ethionamide
	Linezolid

Drugs currently available for the treatment of TB are divided into two groups, the first-line and the second-line drugs (Table 1.1.1). The second-line drugs are usually used when the first-line drugs fail to treat the disease. However, the cytotoxicity of some of the second-line drugs limits their use. A patient with latent TB infection is usually treated with isoniazid to prevent TB from developing into the active state. MDR TB, on the other hand, is treated based on its susceptibility to the drug sensitivity test. Isoniazid-resistant TB is usually treated with rifamycin, ethambutol, and pyrazinamide, with or without fluoroquinolones, for 6 to 12 months; while in the case of rifampin resistance (with the absence of isoniazid resistance), a combination of isoniazid, pyrazinamide, and streptomycin has been shown to be effective.

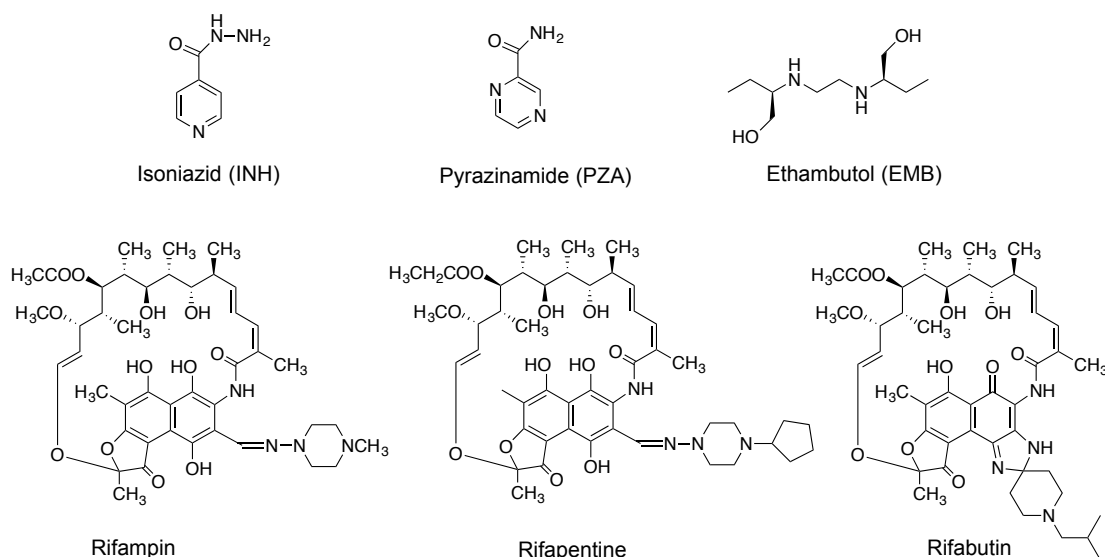


Figure 1.1.3. Chemical structures of first-line drugs for TB treatment

1.1.6 *Mycobacterium tuberculosis* Resistance

In the 1980s, only a few cases of MDR-TB were reported in Europe and in the United States. However, in 1997, WHO declared the spread of MDR-TB, as thousands of cases were no longer responding to rifampin and/or isoniazid. Isoniazid is a pro-drug which has to be activated inside the bacterium to reactive species that form adducts with NADP^+ in the enoyl-acyl carrier protein reductase (InhA), thus inhibiting mycolic acid biosynthesis. Mutations of the catalase-peroxidase (*katG*) gene, which is involved in the activation of isoniazid in susceptible *M. tuberculosis*, were found to confer the bacterium resistance to isoniazid. More than 40% of isoniazid-resistant strains of *M. tuberculosis* were found to have a mutation(s) in this gene (Zhang et al. 1992).

Strains of *Mycobacterium* that are resistant to rifampin gained their resistance

through mutations in the β -subunit of RNA polymerase, the molecular target of rifampin. Some of the major mutations are D516V, H526Y, and S531L with frequencies of occurrence at 6.8%, 8.5% and 57.6%, respectively (Sougakoff et al. 2004).

Pyrazinamide is another first-line drug used to treat *M. tuberculosis* infections. It is also a pro-drug; upon administration, it is converted to the active form pyrazinoic acid (POA) by the action of the pyrazinamidase enzyme found in *M. tuberculosis*. A mutation in the *pncA* gene, a gene that encodes pyrazinamidase, confers *M. tuberculosis* resistance to pyrazinamide (Raynaud et al. 1999). It was proposed that pyrazinamide inhibits the fatty acid synthesis in *M. tuberculosis* by acting on fatty acid synthase-I (FAS-I), thus affecting their growth (Zimhony et al. 2000). However, there were no mutations found in FAS-I from isolates resistant to pyrazinamide. Another study showed that the activity of pyrazinamide is pH dependent (Zhang et al. 1999). More recently, Zhang and co-workers showed that POA binds to RpsA, a ribosomal protein S1 involved in protein translation and trans-translation. The trans-translation is an important process for degradation of toxic proteins in non-replicating bacteria, thus pyrazinamide can kill non-replicating *M. tuberculosis* (Shi et al. 2011).

1.1.7 Development of Novel Anti-tubercular Agents and Newly Approved Anti-TB Agents

The completion of the *M. tuberculosis* genome sequence in the late 1990s

and the availability of new genetic, analytical, and medicinal chemistry tools in recent years have opened a new era in anti-TB drug development (Woong Park et al. 2011, Tahlan et al. 2012, Iøerger et al. 2013). Using more accurate information on the biology of *M. tuberculosis*, many drug candidates with good anti-TB activity have been developed, some of which have found their way into clinical trials. In addition, the re-development of old antibiotics that are only weakly active against *M. tuberculosis* into antibiotics with good anti-TB activity has been explored. One example of the successful outcomes of this approach is spectinomycin, which is an aminoglycoside antibiotic produced by *Streptomyces spectabilis*. It inhibits ribosomal translocation, thus inhibiting protein synthesis. While the natural product shows weak anti-TB activity (MIC = ~50 µg/mL), the chemically modified analogs (the spectinamides) have significantly improved anti-TB activity (MIC = 0.8 µg/mL) (Lee et al. 2014).

Other potential candidates for drug targets are proteins that are involved in cell wall biosynthesis such as MmpL3 and InhA. MmpL proteins are a group of mycobacterial membrane proteins involved in a cell's survival. Among them is MmpL3, which plays an important role in exporting mycolic acid in the form of trehalose monomycolate. Drugs under development that can inhibit this protein include SQ109, an ethylenediamine derivative containing 1-adamantanamine and geranyl moieties. This drug is active against drug-susceptible and -resistant *M. tuberculosis* (Protopopova et al. 2005, Tahlan et al. 2012). On the other hand, InhA is a mycobacterial enoyl reductase, which

is involved in the synthesis of mycolic acid. InhA inhibitors that are still in preclinical evaluations include NITD-916, a member of the 4-hydroxy-2-pyridones family that showed good bactericidal activity against isoniazide-resistant TB (Ng et al. 2015).

Due to their safe pharmacological profile, β -lactam antibiotics have also been investigated for their potential use as anti-TB drugs, e.g., meropenem–clavulanate in the treatment of XDR-TB (Hugonnet et al. 2009). However, the long-term use of β -lactam antibiotics may disturb the microbiome of the intestine and cause gastrointestinal upsets, which may lead to loss of compliance.

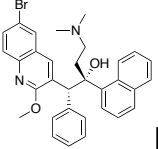
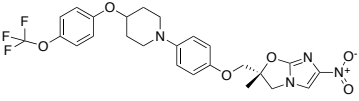
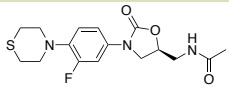
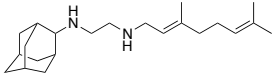
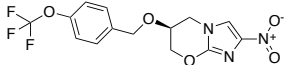
The first new anti-TB drug approved by the FDA in more than 40 years is bedaquiline, an anti-TB agent belonging to the diarylquinolones family. It acts by targeting F_0F_1 ATP synthase. It works on both mutated and dormant *M. tuberculosis* but not on other prokaryotic and eukaryotic cells. However, bedaquiline has drug-drug interaction with rifampicin, as the latter induces CYP3A4 enzyme, which is involved in bedaquiline metabolism, leading to 50% reduction of the plasma concentration of the drug (Lounis et al. 2008).

Another drug that has been approved in Europe for the treatment of MDR-TB is delamanid, which was discovered by Otsuka Pharmaceutical Co. (Matsumoto et al. 2006). It inhibits mycolic acid synthesis in *M. tuberculosis*, thus interfering with cell wall biosynthesis.

Despite the extensive work on anti-TB drug discovery, MDR- and XDR-TB remain a serious threat to global public health. Therefore, continued efforts

are needed to discover novel drugs that have either novel mechanisms of action or the same old molecular targets with higher selectivity and sensitivity toward both sensitive and MDR strains of *M. tuberculosis*.

Table 1.1.2. Recently approved anti-TB drugs and other potential candidates for TB treatment.

Drug	Class	Status	Proposed Mode of Action
 Bedaquiline	Diarylquinoline	Approved in 2012	Affects the proton pump for ATP synthase.
 Delamanid	Nitroimidazole	Approved in EU	Inhibition of mycolic acid biosynthesis.
 Sutezolid	Oxazolidione	Phase II	Inhibition of protein synthesis (Barbachyn et al. 1996)
 SQ109	Ethylenediamine	Phase II	Inhibition of MmpL3 (Protopopova et al. 2005).
 Pretomanid	Nitroimidazole	Phase II	Cell wall inhibitors; Nitric oxide stimulants; Protein synthesis inhibitors (Stover et al. 2000).

1.2 Malaria

Malaria is a parasitic infection transmitted by *Anopheles* mosquitoes. Most human malarial infections are caused by *Plasmodium falciparum*, *P. vivax*, *P. ovale* or *P. malariae*. *P. falciparum* is considered the most dangerous species because if not treated properly, it could lead to death. Whereas *P. vivax* rarely causes severe disease and can be treated with chloroquine, recent multiple mortalities associated with *P. vivax* infections in some tropical areas have raised public concerns (Poespoprodjo et al. 2009, Price et al. 2009, Battle et al. 2012). In 2015, there were an estimated 214 million new cases of malaria and 438,000 deaths (WHO). Since the eradication of malaria in the 1950s in the USA, only a few cases were reported which either were imported by immigrants or from visiting abroad where malaria is epidemic. However, malaria is still a major problem in third world countries. Over 80% of the reported cases were from Africa and 10% were from South Asia. Malaria takes the lives of children, especially those who are younger than five. Furthermore, the development of malarial strains resistant to commonly used drugs like chloroquine and artemisinin and the evolution of mosquitoes resistant to insecticides have increased the number of deaths. Therefore, the development of new antimalarial drugs with novel mechanisms of action is needed.

1.2.2 Malaria Life Cycle

A female mosquito transmits malaria during blood feeding through minute sporozoites, which invade the hepatocytes. These sporozoites can replicate

in hepatocytes to produce 10,000 to 30,000 merozoites in 5-8 days; this cycle is referred to as the liver cycle. When the schizonts burst, merozoites invade the erythrocytes. In 48 hours, an asexual cycle takes place for both *P. falciparum* and *P. vivax* infections. The growing parasites start to consume red blood cells and convert a toxic heme product to non-toxic hemozoin through lipid-mediated crystallization. The sexual form develops within the host during the blood stage, producing male and female gametocytes, which can be taken up by *Anopheles* mosquitoes. The male and female gametocytes, each containing half of the chromosomes, fuse together in the midgut of *Anopheles* mosquitoes forming zygotes, which can develop further to form sporozoites, which are able to infect a new human host (Figure 1.2.1).

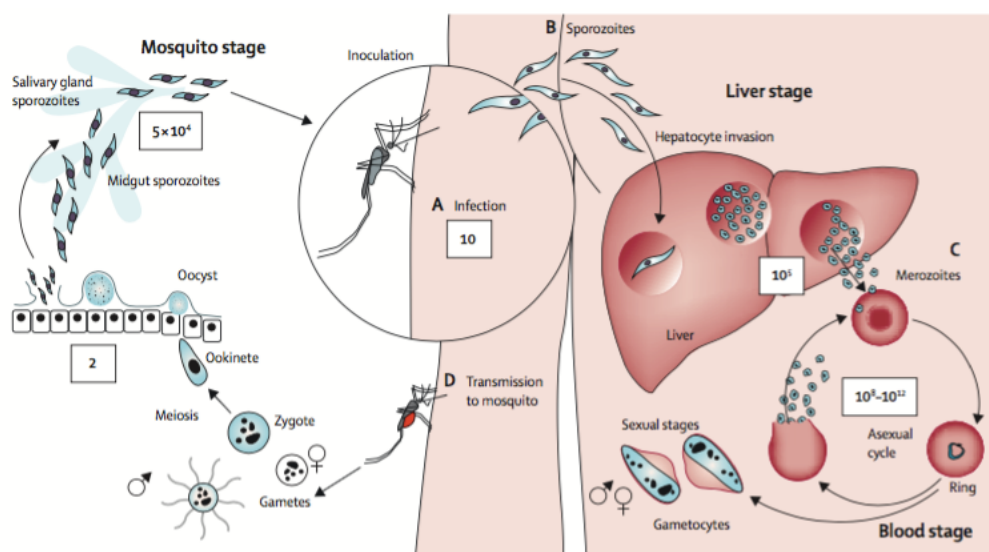


Figure 1.2.1. Malarial parasite life cycle (White et al. 2014).

1.2.3 Malaria Symptoms

Malaria is classified into two categories, which differ in the symptoms presented by the patient. Uncomplicated or classical malaria has three stages: a cold stage, a hot stage, and a sweating stage. A patient presents with fever, chills, nausea, vomiting, general weakness, mild jaundice and a headache. The complicated or severe malaria is more dangerous in that the patient is presented with very severe symptoms such as found in cerebral malaria. The patient with cerebral malaria can have abnormal behavior, impairment of consciousness, seizures, and/or a coma. Also, it is usually combined with one or more of the following: severe anemia because of hemolysis, acute respiratory distress syndrome (ARDS), hemoglobinuria, abnormalities in blood coagulation, low blood pressure, acute kidney failure, and metabolic acidosis. Complicated malaria is fatal if not treated properly.

1.2.5 Malaria Treatment and Resistance

Artemisinin-based combination therapies (ACTs) are recommended by WHO for the treatment of uncomplicated malaria caused by the *P. falciparum* parasite. Two drugs with different mechanisms of action should be given. The choice of the drug is controlled by a safety profile and the nature of the malarial strain. On the other hand, the treatment of severe malaria is given by intramuscular or intravenous injection of artesunate for at least 24 hours and followed by a complete three-day course of an ACT. Other common drugs used to treat the blood stage of malaria are chloroquine, quinine, quinidine,

atovaquone, mefloquine, and primaquine. Primaquine is also active against the dormant parasite hypnozoites.

In the 1930s, the use of chloroquine (CQ) almost brought malarial infection to an end and helped save thousands of lives. However, 10 years of heavy use of CQ was enough for the malaria parasite to develop resistance to the drug. The first cases of resistant strains of *P. falciparum* were reported in Thailand and Colombia (Payne 1987). Shortly after, the resistant strain became common in areas where malaria is endemic such as Africa, South America and India. *P. falciparum* resistant strains were found to obtain their resistance by reducing the concentration of CQ in the digestive vacuole of the parasite. The mechanism by which this happens is still elusive. One important gene, *pfcr*, was found to be responsible for *P. falciparum* resistance and the gene product, PfCRT, was predicted to be involved in drug efflux and/or pH regulation. A recent comparative study of the resistant and the wild-type forms of PfCRT found that the resistant form of PfCRT transports chloroquine while the wild type does not (Wellems et al. 1991, Martin et al. 2009, Chinappi et al. 2010).

Artemisinin is one of the most powerful anti-malarial agents isolated from the *Artemisia annua* plant (qinghaosu). The extract of the plant was used by the Chinese as a medicine to treat fever and malaria. In 1977, Tu Youyou, a Chinese scientist, was able to isolate the active ingredient responsible for the anti-malarial activity. Since then, other semi-synthetic derivatives have been developed, e.g., artesunate and artemether, which are excellent anti-malarial

drugs. The drugs were effective for the treatment of chloroquine-resistant *P. falciparum* and MDR *P. falciparum*. An early mechanistic study has demonstrated that the endoperoxide bridge of artemisinin is crucial for its anti-malarial activity (Brossi et al. 1988). Since peroxide is a rich source of free radicals, the anti-malarial activity may be due to an interaction between the endoperoxide bridge and the intraparasitic heme-iron complex (Meshnick 1998). Additionally, it has been shown that artemisinins are potent inhibitors of *P. falciparum* phosphatidylinositol-3-kinase (PfPI3K) in a ring stage form, suggesting a new mechanism of action for this group of agents. PfPI3K is present in vesicular compartments at the parasite membrane and in the food vacuole. It is believed to play a role in hemoglobin endocytosis and trafficking (Vaid et al. 2010). In 2008, a case study from the Thailand-Combodian border has shown a decrease in the clearance rate of the parasite upon the initial dose of artesunate monotherapy (Noedl et al. 2008). The mechanism of artemisinin resistance was unknown, however, recently Kasturi Haldar and colleagues found that mutations in PfKelch13, a previously identified resistance marker, play a key role in the resistance to artemisinins (Winzeler et al. 2014, Mbengue et al. 2015).

1.2.6 Natural Products and Anti-malarial Activity

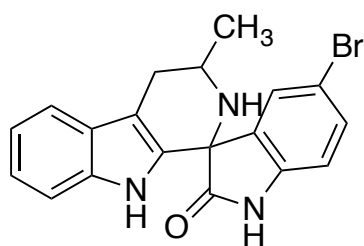
For decades, natural products have been the inspiration for the development of biologically active compounds against malaria (Kumari et al. 2009, Gupta et al. 2010). For example, the *Cinchona* bark alkaloid quinine, which was historically used as an anti-malarial, has inspired scientists to develop

structurally similar compounds (e.g., chloroquine and mefloquine) with better pharmacological activity. Artemisinin, from the *Artemisia annua* plant, is another example whose excellent anti-malarial activity and unique structure have urged scientists to develop derivatives with improved activity and pharmacological properties. Some of those compounds, such as artesunate and artemether, are currently used as a component of the first-line therapy for the treatment of malaria. Other examples of natural products that are used to treat malaria include extracts of *Argemone mexicana* and *Nauclea pobeguinii* plants (Graz et al. 2010, Mesia et al. 2010). The *A. mexicana* plant extract is now in Phase II clinical trials, and it appears to be safe at a wide range of doses (Graz et al. 2010).

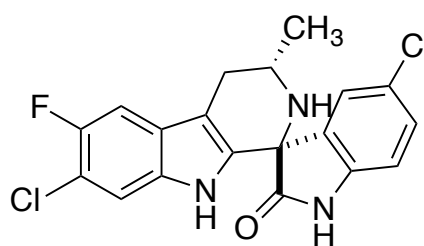
1.2.7 Candidates in Pre-clinical and Clinical Trails

As more methods for high-throughput anti-malarial screening became available, such as blood screen assays, liver stage screens, and transmission assay screens, more anti-malarial hits were discovered, some of which are still in pre-clinical evaluation, while others have reached clinical trials.

NITD-609 (Rottmann et al. 2010) was discovered based on a screening of a blood-stage proliferating assay, in which 10,000 compounds were screened and identified as a first novel class of spiroindolones. A racemic spiroazepineindole was identified as a major lead of this family (Yeung et al. 2010). NITD-609 was found to inhibit the outer membrane transporter, P-type ATPase, of the malarial parasite. NITD-609 is now in Phase II clinical trials.

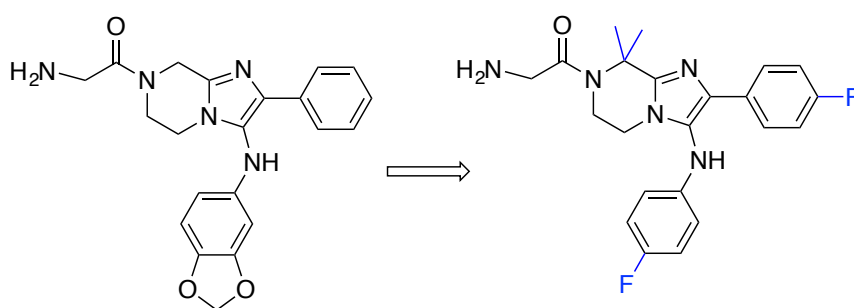


Spiroazepineindole



NITD-609

Another class of anti-malarial agents was discovered based on a high-throughput screening of a library of compounds having an imidazolopiperazine scaffold using a cell-based proliferation assay. GNF156 was one of the most potent hits against the malarial parasite in this class of compounds, and it was found to be effective against the blood stage and the liver stage of the *Plasmodium yoelii*. GNF156 is in Phase I clinical trials (Wu et al. 2011, Nagle et al. 2012).

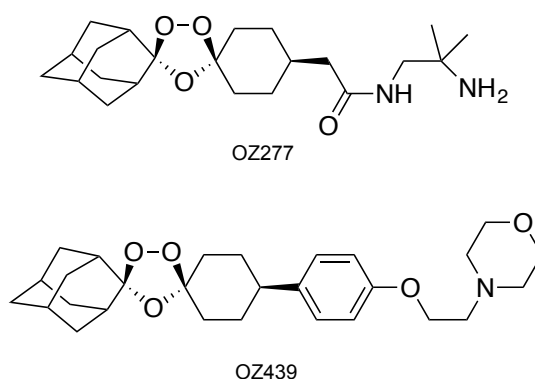


Imidazolopiperazines

GNF156

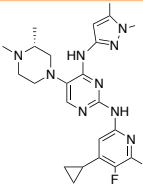
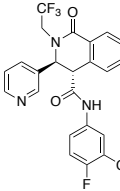
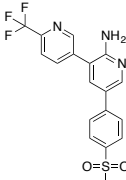
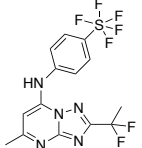
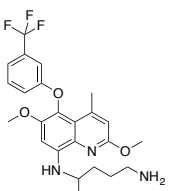
Another class of newly discovered anti-malarial agents is 1,2,4-troxolanes, such as OZ277 (Dong et al. 2010) and OZ439 (Charman et al. 2011). OZ277 is also known as arterolone, which is a synthetic ozonide believed to have the same mechanism of action as artemisinin where their activity is due to the reaction of the peroxide with the iron and heme to generate free radicals,

which leads to alkylating the parasite proteins, thus leading to parasite death. Due to the promising results obtained from OZ277, which is now in Phase II clinical trials, a second-generation ozonide, OZ439, has been synthesized, which acts by the same mechanism of action as OZ277. OZ439 was found to act fast with improved bioavailability. OZ439 is now in Phase I clinical trials.



Research toward the development of novel anti-malarial agents that could fight the sensitive and multi-drug resistant strains of malarial parasites continues unabated. In the scheme provided below are some of the important hits that have reached pre-clinical studies and advanced clinical trials as potential candidates for malaria treatment (Table 1.2.1). Information in the table was adapted from the Medicines for Malaria Venture (MMV) web site.

Table 1.2.1. Current potential candidates for malaria treatment.

Drug	Class	Status	Mechanism of Action
 MMV253	triaminopyrimidine	Pre-clinical studies	<ul style="list-style-type: none"> • Mutants identified in vacuolar ATP-synthase sub-unit D indicating possible biological target
 SJ733	dihydroisoquinolones	Pre-clinical studies	<ul style="list-style-type: none"> • PfATP4 inhibitor
 MMV048	aminopyridine	Phase I	<ul style="list-style-type: none"> • P/PfPI4K inhibitor
 DSM265	triazolopyrimidine	Phase IIa in Peru	<ul style="list-style-type: none"> • Plasmodium dihydroorotate dehydrogenase (DHODH) inhibitor
 Tafenoquine	8-aminoquinoline	Phase III	<ul style="list-style-type: none"> • Inhibits dihydroorotate dehydrogenase • Oxidative impact

1.3 Dissertation Background

As part of an effort to discover new anti-TB and anti-malarial drugs, we used a combination of biosynthetic and synthetic approaches to produce analogs of natural products that have good activity against multi-drug resistant strains of *M. tuberculosis* or *P. falciparum*. In this dissertation, three lines of research related to this effort are presented: 1) genetic and semisynthetic approaches toward novel rifamycins, 2) synthesis of geranylated isoflavonones as potential anti-TB drugs, and 3) mutasynthesis of pactamycin analogs as antimalarial drugs. The followings are brief backgrounds for each of these projects.

1.3.1 Genetic and Semisynthetic Approaches Toward Novel Rifamycins

1.3.1.1 Rifamycin

Rifamycin B is a polyketide natural product that was first isolated from the soil bacterium *Ammycolatopsis mediterranei* by Piero Sensi at Lepetit Pharmaceuticals Research Laboratory in 1959. It is the precursor of rifampin, the most powerful antibiotic for TB treatment to date (Maggi et al. 1966). This class of antibiotics binds to bacterial RNA polymerases and prevents mRNA extension. The clinical use of rifamycin derivatives has resulted in a considerable reduction in mortality rates due to TB. However, a long period of use, in combination with poor compliance and poor medical supervision, has resulted in the emergence of strains of *M. tuberculosis* that are resistant to rifampin. Thus, there is an urgent need to produce rifamycin analogs that can overcome this resistance problem. However, the structural complexity of

rifamycin B limits the use of chemical tools to generate different rifamycin analogs, e.g., modifications of the backbone structure. Therefore, we aimed to use genetic approaches to create novel rifamycin scaffolding that could be subsequently modified by semi-synthesis approaches.

1.3.1.2 Rifamycin Biosynthesis

The rifamycin biosynthetic gene clusters have been identified in a number of strains of *Amycolatopsis* and *Salinispora* (Kaur et al. 2001, Kim et al. 2006, Wilson et al. 2010). Rifamycin polyketide backbone is assembled by Type I modular polyketide synthases using 3-amino-5-hydroxybenzoic acid (AHBA) as a starter unit and malonyl- and methylmalonyl-CoA as extender units. The AHBA unit is derived from the aminoshikimate pathway, which is encoded by 8 genes (*rifG-rifJ*) within the cluster (Figure 1.3.1) (Floss et al. 2011). Upstream of the AHBA genes are the rif-PKS genes (*rifA-rifE*) and an amide synthase gene (*rifF*). The Rif-PKS comprises of a loading domain and ten chain extension modules. Each module consists of a minimal set of domains that includes a ketosynthase (KS) that is responsible for catalyzing condensation reaction, an acyltransferase (AT), which loads the extender unit malonyl-CoA or methylmalonyl-CoA, and an acyl carrier protein (ACP) domain, which tethers the growing polyketide chain. In addition, there are ketoreductase and dehydratase domains in some of the modules. The amide synthase is responsible for the macrolactamization of a fully extended polyketide (undecaketide) structure to give proansamycin X, which is subsequently modified by a number of tailoring proteins. Those tailoring

enzymes add functional groups to decorate the architecture of the rifamycin B backbone (Floss et al. 2005, Xiong et al. 2005, Xu et al. 2005) (Figure 1.3.1).

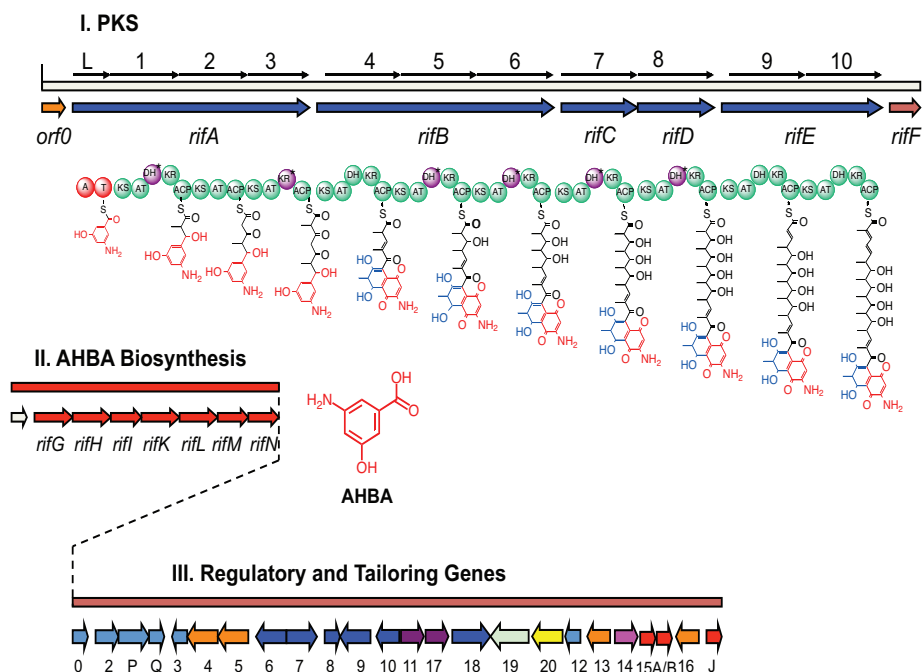


Figure 1.3.1. Genetic organization of rifamycin B biosynthesis (August et al. 1998).

1.3.1.3 Semisynthetic and Mutasynthetic Approaches to Novel

Rifamycins

Since the discovery of rifamycin B, hundreds of its semisynthetic derivatives have been generated, but only a few of them have found their way to commercial use. This is due to the complex structure of rifamycin and the rigid structural requirements for rifamycin to maintain its binding to bacterial RNA polymerase. Most rifamycin derivatives are developed from rifamycin S, an oxidative product of rifamycin B, by adding a side chain at C-3 and/or C-4. Among those derivatives are rifampin, rifabutin, and rifapentine, which

demonstrate good pharmacological profiles, and are currently used in clinics as first-line anti-tubercular drugs (Figure 1.3.2).

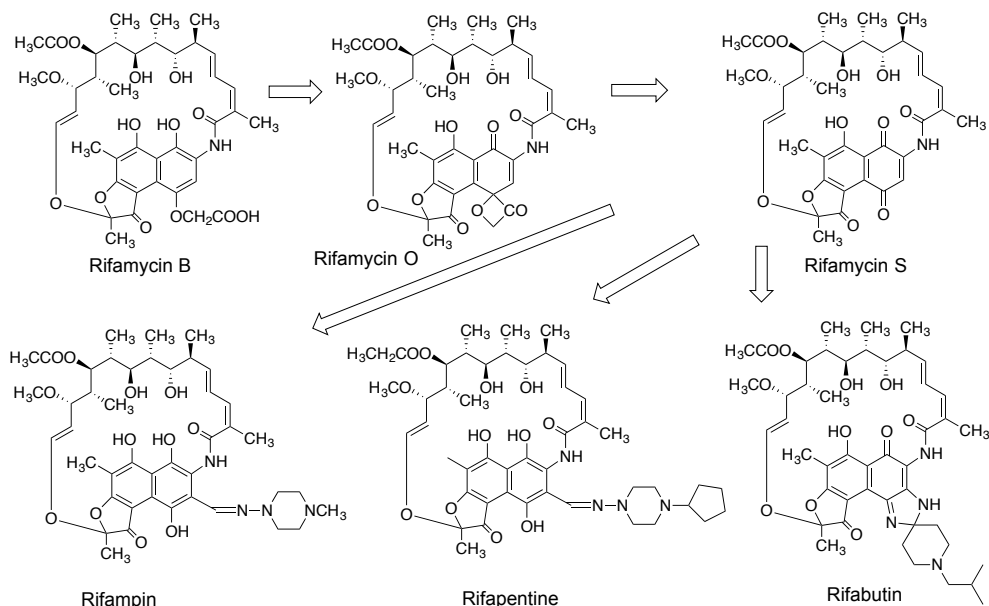


Figure 1.3.2. Conversion of rifamycin B to clinically used anti-TB.

More recently, many semisynthetic routes to new rifamycin derivatives with improved activity have also been published (Barluenga et al. 2006, Figueiredo et al. 2009, Garcia et al. 2010). Some of these derivatives have proved to be useful against rifampin-sensitive or rifampin-resistant strains of *M. tuberculosis*, whereas others showed comparable activity to rifampin against *S. epidermidis*, *S. aureus* and MRSA (Gill et al. 2012, Czerwonka et al. 2016). The advancements of molecular genetic techniques and genome sequencing technology, as well as the development of tools for genetic manipulations have made it possible for scientists to study natural product biosynthesis at the molecular level and use the knowledge to produce new analogs of natural products. Gene knockout and domain swapping proved to be useful in

generating libraries of novel “unnatural” natural products with enhanced bioactivity, at least in some cases (Hopwood et al. 1985, Nguyen et al. 2006). One successful example was the generation of erythromycin analogs with a broad range of activity (Jacobsen et al. 1997). Also another combinatorial biosynthetic approach, in which the deoxyerythronolide B synthase acyltransferase (ATs) domains were swapped with the AT domains from the rapamycin PKS (RAPS) that encode alternative substrate specificities, lead to the generation of more than 50 macrolides (McDaniel et al. 1999).

A number of new rifamycin analogs have also been generated through biosynthetic manipulations. Inactivation of *rif orf14*, a methyltransferase gene, in *A. mediterranei* S699 resulted in the production of 27-O-demethylrifamycin SV and 25-desacetyl-27-O-demethylrifamycin SV (Xu et al. 2003). Inactivation of other tailoring genes within the rifamycin biosynthetic gene cluster in *A. mediterranei* S699 not only gave other analogs of rifamycin, e.g., rifamycins W and SV, but also provided insights into the tailoring steps in rifamycin biosynthesis (Xu et al. 2005). Recently, an attempt to produce new pactamycin analogs by feeding a mutant strain of *A. mediterranei* that lacks the ability to produce AHBA with different synthetic AHBA derivatives (e.g., 3-amino-4-bromobenzoic acid) was carried out. However, this experiment failed to produce novel rifamycins; instead, a tetraketide was isolated and a linear undecaketide was detected by mass spectrometry (Figure 1.3.3)(Bulyszko et al. 2015).

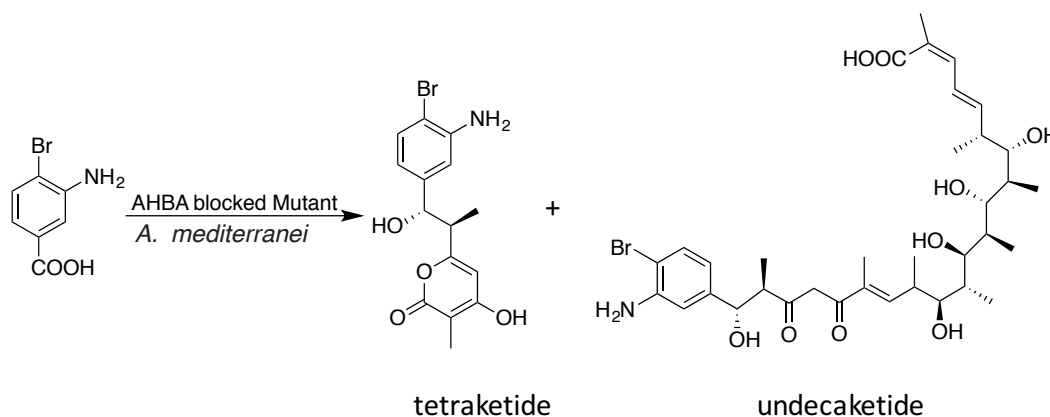


Figure 1.3.3. The feeding of 3-amino-4-bromobenzoic acid to the AHBA blocked mutant of *A. mediterranei*.

The accumulation of the tetraketide intermediate suggests that manipulations of the rif PKSs prior to module 5 would significantly diminish the production of rifamycin. This may be due to strict substrate specificity of Rif Orf19, which is involved in the naphthalene ring formation in module 4 (Figure 1.3.1.) (Xu et al. 2005, Bulyszko et al. 2015).

A successful chemical reconstitution of rifamycin biosynthesis using an N-acetylcysteamine (NAC) thioester of the natural diketide intermediate in the AHBA mutant was reported by Khosla and co-workers. The group investigated the stereospecificity of the ketoreductase domain of the rif PKS module 1 using synthetically prepared NAC thioesters of the four possible diketide intermediates. Feeding experiments with these compounds to the *rifK* mutant, which lacks the ability to produce AHBA, showed that only one of them could rescue the production of rifamycin B (Figure 1.3.4), indicating the high stereospecificity of the KR domain. This result also suggests that enzymes that are involved in the early steps of rifamycin biosynthesis have high substrate specificity (Hartung et al. 2005).

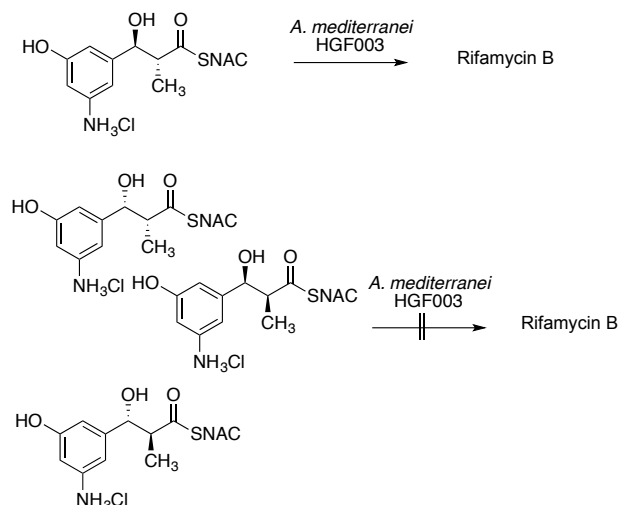


Figure 1.3.4. Feeding *rifK* mutant with four SNAC-AHBA diketide derivatives.

Independently, we have also attempted to use a NAC thioester of a diketide analog to generate 7-desmethyrrifamycin SV in the *rifL* mutant strain of *A. mediterranei*, which also lacks the ability to produce AHBA. However, we were not able to obtain the desired 7-desmethyl product (unpublished data) (Figure 1.3.5).



Figure 1.3.5. Feeding β -hydroxyl SNAC derivative of AHBA to RM01 mutant.

Despite the rigidity and substrate specificity of Rif Orf19, which is involved in the naphthalene ring formation in module 4, PKS modules from 5-10 may be amendable for genetic manipulations. Gene swapping and gene inactivation

(dehydratase, ketoreductase) could still be carried out in order to generate novel rifamycin scaffolds for further semi-synthetic modifications.

1.3.2 Synthesis of Geranylated Isoflavanones as Potential Anti-TB Drugs

Isoflavanones are plant secondary metabolites that belong to the flavonoid class of natural products. Isoflavanones exhibit a wide range of biological activity that includes anti-cancer activity (Chin et al. 2006), anti-bacterial activity (Tanaka et al. 2009), and inhibitors of α -glucosidases (Valentova et al. 2011). The chemical structures of isoflavanones contain a three ring system (A, B, and C). Rings A and B are fused and substituted with functional groups (usually on ring A). Additionally, some isoflavanones are prenylated with either prenyl or geranyl substitution at C-6 or C-8. The other aromatic ring (C) is pendent from the C-3 position of ring B.

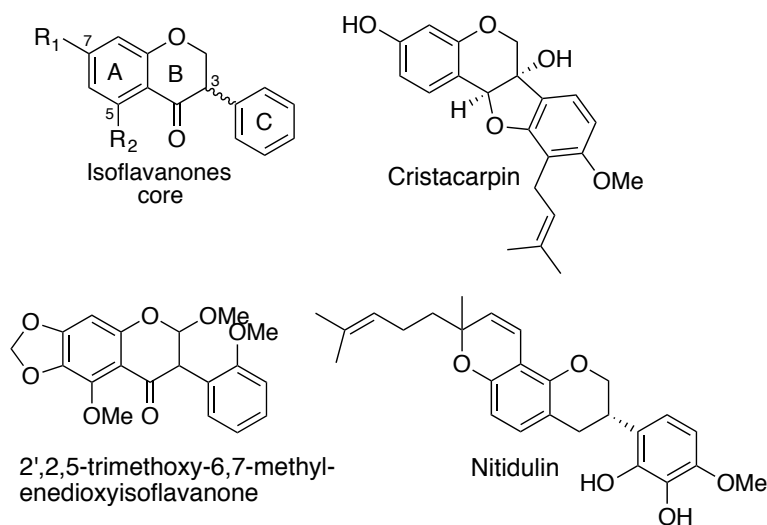


Figure 1.3.6. Chemical structure of the isoflavanone core and some biologically active isoflavanoids. C-5 and C-7 usually each bear a hydroxy group.

The ring C is usually found with different functional groups such as hydroxy, methoxy, prenyl, or geranyl groups (Figure 1.3.6). Due to their broad range biological activity, many synthetic methodologies have been developed to access this class of compounds. Those include palladium-catalyzed arylation, addition of C-O bond to arynes, gold-catalyzed annulation, or direct reduction of isoflavone (Skouta et al. 2007, Dubrovskiy et al. 2010, Lessi et al. 2011).

1.3.2.1 Perbergin as a Potential Anti-TB Drug

Perbergin is a geranylated isoflavanone that was isolated from the Madagascar plant *Dalbergia pervillei* (Rajaonson et al. 2011). This natural product has attracted our attention because of its ability to quench a virulence factor in the plant pathogen *Rhodococcus fascians*. It exhibits its action by targeting the AttR regulon, which is involved in the regulation of *R. fascians* pathogenic behavior. *R. fascians* is a mycolic acid-producing Gram-(+) bacterium from the class of Actinobacteria. It shares a similar cell wall envelope and mycolic acid content with a number of other bacteria, such as *Mycobacterium*, *Norcardia* and *Corynebacterium*, all of which have pathogenic species (Daffe et al. 1993).

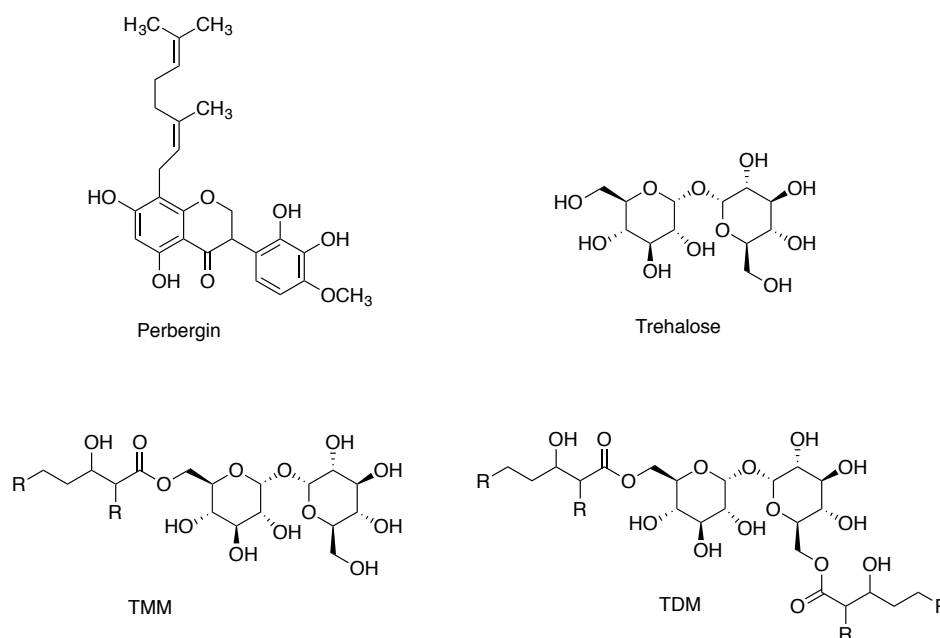


Figure 1.3.7. Chemical structures of reported perbergin, trehalose, trehalose monomycolate (TMM), and trehalose dimycolate (TDM).

One key similarity between *Rhodococcus* and *Mycobacterium* is the presence of trehalose mono- and di-mycolates (TMM and TDM) in their cell walls. Trehalose was found to be the carrier of mycolic acids from the cytosol to the cell wall and both TDM and TMM are important components of the outer layer of the *M. tuberculosis* envelope. Since perbergin structurally resembles trehalose monomycolate (TMM) (Figure 1.3.7), we postulated that perbergin may exhibit anti-bacterial activity against those that are rich in mycolic acids. However, the known source of this compound is *Dalbergia pervillei*, which grows in Madagascar, and a large amount of the plant will be needed to isolate enough perbergin to pursue further testing on its activity. Therefore, we set out to develop a route for the total synthesis of perbergin, and test its activity against a suite of Gram-positive and Gram-negative bacteria including *Mycobacterium smegmatis* as described in Chapter 2.

1.3.3 Mutasyntesis of Pactamycin Analogs as Anti-malarial Agents

1.3.3.1 Pactamycin

Pactamycin is a bacterial-derived natural product which was discovered by the Upjohn Company in the early 1960s. It has broad-spectrum inhibitory activity against viruses, bacteria, mammalian cells, and protozoa. This broad-spectrum activity is primarily due to its strong binding to a conserved region within the ribosomes of most organisms, leading to non-selective inhibition of protein synthesis in those organisms. Furthermore, due to its structural complexity and instability, semisynthetic modifications of pactamycin have been difficult to achieve (Figure 1.3.8). These challenges have attracted many synthetic chemists to pursue the total synthesis of pactamycin. In 2011, Hanessian and co-workers reported the first total synthesis of pactamycin, involving 33 linear steps with an overall yield of 3%. Two years later, Johnson and co-workers reported the total synthesis of pactamycin in 15 steps with a reported yield of 1.9% (Hanessian et al. 2011, Sharpe et al. 2013).

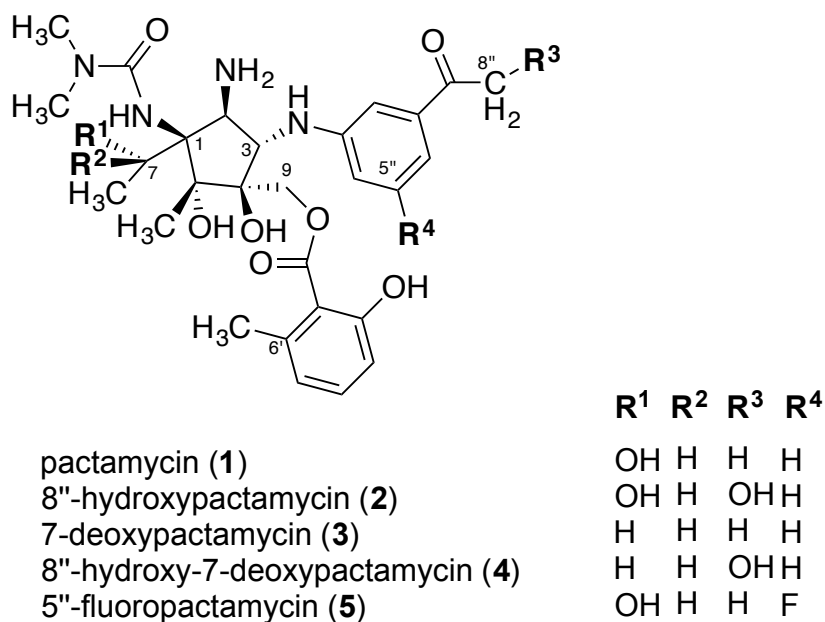


Figure 1.3.8. Chemical structures of different pactamycin analogs.

Although pactamycin can be chemically synthesized and semi-synthetically modified to generate libraries of analogs, the applicability of these routes toward clinical use is still limited by their overall yields and/or many step syntheses.

1.3.3.2 Novel Pactamycin Analogs with Excellent Anti-malarial Activity

As part of a continued effort to study pactamycin biosynthesis, we were able to generate a number of mutant strains of *Streptomyces pactum* ATCC 27456 that produce novel analogs of pactamycin. Some of those new analogs have better chemical stability and pharmacological properties than pactamycin. For example, Δ ptmH mutant, in which the ptmH gene that encodes a radical SAM-dependent protein has been inactivated, produces two novel analogs of pactamycin, TM-025 and TM-026 (Figure 1.3.9) (Lu et al. 2011). These new

analogues showed potent anti-malarial activity at low nanomolar concentrations, have less cytotoxicity, and are structurally more stable than pactamycin. Most importantly, the production yield of these analogues was 10 to 20-fold higher than that of pactamycin.

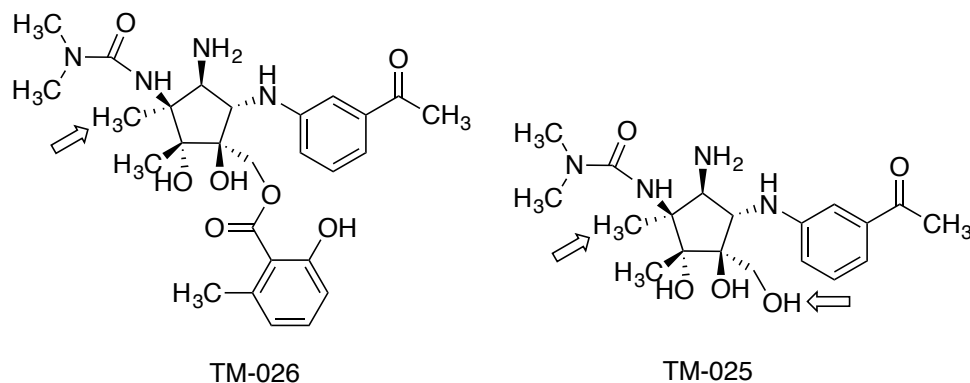


Figure 1.3.9. Chemical structures of TM0-26 and TM-025.

To further improve the pharmacological properties of these analogues, we applied a mutasynthetic approach to generate fluorinated derivatives of TM-025 and TM-026. This was done by blocking the synthesis of 3-aminobenzoic acid (the precursor of pactamycin) in *S. pactum* and performing precursor-directed structure modifications as described in Chapter 3.

1.4 Thesis Overview

This dissertation describes our ongoing efforts to develop novel anti-tubercular and antimalarial agents. Chapter 1 contains a general introduction, which includes a general background of tuberculosis and malaria, as well as a research background of this dissertation. Chapter 2 describes the application of genetic and semisynthetic methodologies to generate novel rifamycin analogs and the activity of the new compounds against rifampin-sensitive and rifampin-resistant strains of *M. tuberculosis*. Chapter 3 describes a linear total synthesis of geranylated isoflavanones, which are structurally similar to the natural product perbergin, and the revision of the chemical structure of the reported perbergin. Chapter 4 describes the application of a mutasynthetic approach to generate fluorinated pactamycin analogs and its selectivity against plasmodium parasites. Chapter 5 contains general conclusion. Other published scientific work that were done during my Ph.D. program but are not discussed as the main part of this dissertation are presented as appendices.

1.5 References

August, P. R., L. Tang, Y. J. Yoon, S. Ning, R. Muller, T. W. Yu, M. Taylor, D. Hoffmann, C. G. Kim, X. Zhang, C. R. Hutchinson and H. G. Floss (1998). "Biosynthesis of the ansamycin antibiotic rifamycin: deductions from the molecular analysis of the rif biosynthetic gene cluster of *Amycolatopsis mediterranei* S699." Chem Biol **5**(2): 69-79.

Barbachyn, M. R., D. K. Hutchinson, S. J. Brickner, M. H. Cynamon, J. O. Kilburn, S. P. Klemens, S. E. Glickman, K. C. Grega, S. K. Hendges, D. S. Toops, C. W. Ford and G. E. Zurenko (1996). "Identification of a novel oxazolidinone (U-100480) with potent antimycobacterial activity." J Med Chem **39**(3): 680-685.

Barluenga, J., F. Aznar, A. B. Garcia, M. P. Cabal, J. J. Palacios and M. A. Menendez (2006). "New rifabutin analogs: synthesis and biological activity against *Mycobacterium tuberculosis*." Bioorg Med Chem Lett **16**(22): 5717-5722.

Battle, K. E., P. W. Gething, I. R. Elyazar, C. L. Moyes, M. E. Sinka, R. E. Howes, C. A. Guerra, R. N. Price, K. J. Baird and S. I. Hay (2012). "The global public health significance of *Plasmodium vivax*." Adv Parasitol **80**: 1-111.

Blumberg, H. M., W. J. Burman, R. E. Chaisson, C. L. Daley, S. C. Etkind, L. N. Friedman, P. Fujiwara, M. Grzemska, P. C. Hopewell, M. D. Iseman, R. M. Jasmer, V. Koppaka, R. I. Menzies, R. J. O'Brien, R. R. Reves, L. B. Reichman, P. M. Simone, J. R. Starke, A. A. Vernon, C. f. D. C. American Thoracic Society, Prevention and S. the Infectious Diseases (2003). "American Thoracic Society/Centers for Disease Control and Prevention/Infectious Diseases Society of America: treatment of tuberculosis." Am J Respir Crit Care Med **167**(4): 603-662.

Blumberg, H. M. and R. R. Kempker (2014). "Interferon-gamma release assays for the evaluation of tuberculosis infection." JAMA **312**(14): 1460-1461.

Brossi, A., B. Venugopalan, L. Dominguez Gerpe, H. J. Yeh, J. L. Flippen-Anderson, P. Buchs, X. D. Luo, W. Milhous and W. Peters (1988). "Arteether, a new antimalarial drug: synthesis and antimalarial properties." J Med Chem **31**(3): 645-650.

Bulyszko, I., G. Drager, A. Klenge and A. Kirschning (2015). "Evaluation of the Synthetic Potential of an AHBA Knockout Mutant of the Rifamycin Producer *Amycolatopsis mediterranei*." Chemistry **21**(52): 19231-19242.

Charman, S. A., S. Arbe-Barnes, I. C. Bathurst, R. Brun, M. Campbell, W. N. Charman, F. C. Chiu, J. Chollet, J. C. Craft, D. J. Creek, Y. Dong, H. Matile, M. Maurer, J. Morizzi, T. Nguyen, P. Papastogiannidis, C. Scheurer, D. M. Shackelford, K. Sriraghavan, L. Stingelin, Y. Tang, H. Urwyler, X. Wang, K. L. White, S. Wittlin, L. Zhou and J. L. Vennerstrom (2011). "Synthetic ozonide drug candidate OZ439 offers new hope for a single-dose cure of uncomplicated malaria." Proc Natl Acad Sci U S A **108**(11): 4400-4405.

Chin, Y. W., L. K. Mdee, Z. H. Mbwambo, Q. Mi, H. B. Chai, G. M. Cragg, S. M. Swanson and A. D. Kinghorn (2006). "Prenylated flavonoids from the root bark of *Berchemia discolor*, a Tanzanian medicinal plant." J Nat Prod **69**(11): 1649-1652.

Chinappi, M., A. Via, P. Marcatili and A. Tramontano (2010). "On the mechanism of chloroquine resistance in *Plasmodium falciparum*." PLoS One **5**(11): e14064.

Czerwonka, D., J. Domagalska, K. Pyta, M. M. Kubicka, P. Pecyna, M. Gajacka and P. Przybylski (2016). "Structure-activity relationship studies of new rifamycins containing l-amino acid esters as inhibitors of bacterial RNA polymerases." Eur J Med Chem **116**: 216-221.

Daffe, M., M. McNeil and P. J. Brennan (1993). "Major structural features of the cell wall arabinogalactans of *Mycobacterium*, *Rhodococcus*, and *Nocardia* spp." Carbohydr Res **249**(2): 383-398.

Dong, Y., S. Wittlin, K. Sriraghavan, J. Chollet, S. A. Charman, W. N. Charman, C. Scheurer, H. Urwyler, J. Santo Tomas, C. Snyder, D. J. Creek, J. Morizzi, M. Koltun, H. Matile, X. Wang, M. Padmanilayam, Y. Tang, A. Dorn, R. Brun and J. L. Vennerstrom (2010). "The structure-activity relationship of the antimalarial ozonide arterolane (OZ277)." J Med Chem **53**(1): 481-491.

Dubrovskiy, A. V. and R. C. Larock (2010). "Intermolecular C-O addition of carboxylic acids to arynes." Org Lett **12**(14): 3117-3119.

Figueiredo, R., C. Moiteiro, M. A. Medeiros, P. A. da Silva, D. Ramos, F. Spies, M. O. Ribeiro, M. C. Lourenco, I. N. Junior, M. M. Gaspar, M. E. Cruz, M. J. Curto, S. G. Franzblau, H. Orozco, D. Aguilar, R. Hernandez-Pando and M. C. Costa (2009). "Synthesis and evaluation of rifabutin analogs against *Mycobacterium avium* and H(37)Rv, MDR and NRP *Mycobacterium tuberculosis*." Bioorg Med Chem **17**(2): 503-511.

Floss, H. G. and T. W. Yu (2005). "Rifamycin-mode of action, resistance, and biosynthesis." Chem Rev **105**(2): 621-632.

Floss, H. G., T. W. Yu and K. Arakawa (2011). "The biosynthesis of 3-amino-5-hydroxybenzoic acid (AHBA), the precursor of mC7N units in ansamycin and mitomycin antibiotics: a review." J Antibiot (Tokyo) **64**(1): 35-44.

Garcia, A. B., J. J. Palacios, M. J. Ruiz, J. Barluenga, F. Aznar, M. P. Cabal, J. M. Garcia and N. Diaz (2010). "Strong in vitro activities of two new rifabutin analogs against multidrug-resistant *Mycobacterium tuberculosis*." Antimicrob Agents Chemother **54**(12): 5363-5365.

Gill, S. K., H. Xu, P. D. Kirchhoff, T. Cierpicki, A. J. Turbiak, B. Wan, N. Zhang, K. W. Peng, S. G. Franzblau, G. A. Garcia and H. D. Showalter (2012). "Structure-based design of novel benzoxazinorifamycins with potent binding affinity to wild-type and rifampin-resistant mutant *Mycobacterium tuberculosis* RNA polymerases." J Med Chem **55**(8): 3814-3826.

Graz, B., M. L. Willcox, C. Diakite, J. Falquet, F. Dackuo, O. Sidibe, S. Giani and D. Diallo (2010). "Argemone mexicana decoction versus

artesanate-amodiaquine for the management of malaria in Mali: policy and public-health implications." Trans R Soc Trop Med Hyg **104**(1): 33-41.

Gupta, P. and N. Vasudeva (2010). "In vitro antiplasmodial and antimicrobial potential of *Tagetes erecta* roots." Pharm Biol **48**(11): 1218-1223.

Gutierrez, M. C., S. Brisse, R. Brosch, M. Fabre, B. Omais, M. Marmiesse, P. Supply and V. Vincent (2005). "Ancient origin and gene mosaicism of the progenitor of *Mycobacterium tuberculosis*." PLoS Pathog **1**(1): e5.

Hanessian, S., R. R. Vakiti, S. Dorich, S. Banerjee, F. Lecomte, J. R. DelValle, J. Zhang and B. Deschenes-Simard (2011). "Total synthesis of pactamycin." Angew Chem Int Ed Engl **50**(15): 3497-3500.

Hartung, I. V., M. A. Rude, N. A. Schnarr, D. Hunziker and C. Khosla (2005). "Stereochemical assignment of intermediates in the rifamycin biosynthetic pathway by precursor-directed biosynthesis." J Am Chem Soc **127**(32): 11202-11203.

Hayman, J. (1984). "Mycobacterium ulcerans: an infection from Jurassic time?" Lancet **2**(8410): 1015-1016.

Hopwood, D. A., F. Malpartida, H. M. Kieser, H. Ikeda, J. Duncan, I. Fujii, B. A. Rudd, H. G. Floss and S. Omura (1985). "Production of 'hybrid' antibiotics by genetic engineering." Nature **314**(6012): 642-644.

Horsburgh, C. R., Jr., C. E. Barry, 3rd and C. Lange (2015). "Treatment of Tuberculosis." N Engl J Med **373**(22): 2149-2160.

Hugonnet, J. E., L. W. Tremblay, H. I. Boshoff, C. E. Barry, 3rd and J. S. Blanchard (2009). "Meropenem-clavulanate is effective against extensively drug-resistant *Mycobacterium tuberculosis*." Science **323**(5918): 1215-1218.

Ioerger, T. R., T. O'Malley, R. Liao, K. M. Guinn, M. J. Hickey, N. Mohaideen, K. C. Murphy, H. I. Boshoff, V. Mizrahi, E. J. Rubin, C. M. Sassetti, C. E. Barry, 3rd, D. R. Sherman, T. Parish and J. C. Sacchettini (2013). "Identification of new drug targets and resistance mechanisms in *Mycobacterium tuberculosis*." PLoS One **8**(9): e75245.

Jacobsen, J. R., C. R. Hutchinson, D. E. Cane and C. Khosla (1997). "Precursor-directed biosynthesis of erythromycin analogs by an engineered polyketide synthase." Science **277**(5324): 367-369.

Kaur, H., J. Cortes, P. Leadlay and R. Lal (2001). "Cloning and partial characterization of the putative rifamycin biosynthetic gene cluster from the actinomycete *Amiclatopsis mediterranei* DSM 46095." Microbiol Res **156**(3): 239-246.

Kim, T. K., A. K. Hewavitharana, P. N. Shaw and J. A. Fuerst (2006). "Discovery of a new source of rifamycin antibiotics in marine sponge actinobacteria by phylogenetic prediction." Appl Environ Microbiol **72**(3): 2118-2125.

Kumari, P., K. Misra, B. S. Sisodia, U. Faridi, S. Srivastava, S. Luqman, M. P. Darokar, A. S. Negi, M. M. Gupta, S. C. Singh and J. K. Kumar (2009). "A promising anticancer and antimalarial component from the leaves of *Bidens pilosa*." Planta Med **75**(1): 59-61.

Lee, R. E., J. G. Hurdle, J. Liu, D. F. Bruhn, T. Matt, M. S. Scherman, P. K. Vaddady, Z. Zheng, J. Qi, R. Akbergenov, S. Das, D. B. Madhura, C. Rathi, A. Trivedi, C. Villellas, R. B. Lee, Rakesh, S. L. Waidyarachchi, D. Sun, M. R. McNeil, J. A. Ainsa, H. I. Boshoff, M. Gonzalez-Juarrero, B. Meibohm, E. C. Bottger and A. J. Lenaerts (2014). "Spectinamides: a new class of semisynthetic antituberculosis agents that overcome native drug efflux." Nat Med **20**(2): 152-158.

Lessi, M., T. Masini, L. Nucara, F. Bellina and R. Rossi (2011). "Highly Selective Palladium-Catalyzed Direct C-H α -Monoarylation of Carbonyl Compounds using Water Containing the Surfactant Polyoxyethylene- α -Tocopheryl Sebacate (PTS) as a Solvent." Advanced Synthesis & Catalysis **353**(2-3): 501-507.

Lounis, N., T. Gevers, J. Van Den Berg and K. Andries (2008). "Impact of the interaction of R207910 with rifampin on the treatment of tuberculosis studied in the mouse model." Antimicrob Agents Chemother **52**(10): 3568-3572.

Lu, W., N. Roongsawang and T. Mahmud (2011). "Biosynthetic studies and genetic engineering of pactamycin analogs with improved selectivity toward malarial parasites." Chem Biol **18**(4): 425-431.

Maggi, N., C. R. Pasqualucci, R. Ballotta and P. Sensi (1966). "Rifampicin: a new orally active rifamycin." Chemotherapy **11**(5): 285-292.

Martin, R. E., R. V. Marchetti, A. I. Cowan, S. M. Howitt, S. Broer and K. Kirk (2009). "Chloroquine transport via the malaria parasite's chloroquine resistance transporter." Science **325**(5948): 1680-1682.

Matsumoto, M., H. Hashizume, T. Tomishige, M. Kawasaki, H. Tsubouchi, H. Sasaki, Y. Shimokawa and M. Komatsu (2006). "OPC-67683, a nitro-dihydro-imidazooxazole derivative with promising action against tuberculosis in vitro and in mice." PLoS Med **3**(11): e466.

Mbengue, A., S. Bhattacharjee, T. Pandharkar, H. Liu, G. Estiu, R. V. Stahelin, S. S. Rizk, D. L. Njimoh, Y. Ryan, K. Chotivanich, C. Nguon, M. Ghorbal, J. J. Lopez-Rubio, M. Pfrender, S. Emrich, N. Mohandas, A. M. Dondorp, O. Wiest and K. Haldar (2015). "A molecular mechanism of artemisinin resistance in *Plasmodium falciparum* malaria." Nature **520**(7549): 683-687.

McDaniel, R., A. Thamchaipenet, C. Gustafsson, H. Fu, M. Betlach and G. Ashley (1999). "Multiple genetic modifications of the erythromycin polyketide synthase to produce a library of novel "unnatural" natural products." Proc Natl Acad Sci U S A **96**(5): 1846-1851.

Meshnick, S. R. (1998). "Artemisinin antimalarials: mechanisms of action and resistance." Med Trop (Mars) **58**(3 Suppl): 13-17.

Mesia, K., R. K. Cimanga, L. Dhooche, P. Cos, S. Apers, J. Totte, G. L. Tona, L. Pieters, A. J. Vlietinck and L. Maes (2010). "Antimalarial activity and toxicity evaluation of a quantified *Nauclea pobeguinii* extract." J Ethnopharmacol **131**(1): 10-16.

Nagle, A., T. Wu, K. Kuhen, K. Gagaring, R. Borboa, C. Francek, Z. Chen, D. Plouffe, X. Lin, C. Caldwell, J. Ek, S. Skolnik, F. Liu, J. Wang, J. Chang, C.

Li, B. Liu, T. Hollenbeck, T. Tuntland, J. Isbell, T. Chuan, P. B. Alper, C. Fischli, R. Brun, S. B. Lakshminarayana, M. Rottmann, T. T. Diagana, E. A. Winzeler, R. Glynn, D. C. Tully and A. K. Chatterjee (2012). "Imidazolopiperazines: lead optimization of the second-generation antimalarial agents." *J Med Chem* **55**(9): 4244-4273.

Nerlich, A. G., C. J. Haas, A. Zink, U. Szeimies and H. G. Hagedorn (1997). "Molecular evidence for tuberculosis in an ancient Egyptian mummy." *Lancet* **350**(9088): 1404.

Ng, P. S., U. H. Manjunatha, S. P. Rao, L. R. Camacho, N. L. Ma, M. Herve, C. G. Noble, A. Goh, S. Peukert, T. T. Diagana, P. W. Smith and R. R. Kondreddi (2015). "Structure activity relationships of 4-hydroxy-2-pyridones: A novel class of antituberculosis agents." *Eur J Med Chem* **106**: 144-156.

Nguyen, K. T., D. Ritz, J. Q. Gu, D. Alexander, M. Chu, V. Miao, P. Brian and R. H. Baltz (2006). "Combinatorial biosynthesis of novel antibiotics related to daptomycin." *Proc Natl Acad Sci U S A* **103**(46): 17462-17467.

Noedl, H., Y. Se, K. Schaecher, B. L. Smith, D. Socheat, M. M. Fukuda and C. Artemisinin Resistance in Cambodia 1 Study (2008). "Evidence of artemisinin-resistant malaria in western Cambodia." *N Engl J Med* **359**(24): 2619-2620.

Payne, D. (1987). "Spread of chloroquine resistance in *Plasmodium falciparum*." *Parasitol Today* **3**(8): 241-246.

Poespoprodjo, J. R., W. Fobia, E. Kenangalem, D. A. Lampah, A. Hasanuddin, N. Warikar, P. Sugiarto, E. Tjitra, N. M. Anstey and R. N. Price (2009). "Vivax malaria: a major cause of morbidity in early infancy." *Clin Infect Dis* **48**(12): 1704-1712.

Price, R. N., N. M. Douglas and N. M. Anstey (2009). "New developments in *Plasmodium vivax* malaria: severe disease and the rise of chloroquine resistance." *Curr Opin Infect Dis* **22**(5): 430-435.

Protopopova, M., C. Hanrahan, B. Nikonenko, R. Samala, P. Chen, J. Gearhart, L. Einck and C. A. Nacy (2005). "Identification of a new antitubercular drug candidate, SQ109, from a combinatorial library of 1,2-ethylenediamines." *J Antimicrob Chemother* **56**(5): 968-974.

Rajaonson, S., O. M. Vandeputte, D. Vereecke, M. Kiendrebeogo, E. Ralambofetra, C. Stevigny, P. Duez, C. Rabemanantsoa, A. Mol, B. Diallo, M. Baucher and M. El Jaziri (2011). "Virulence quenching with a prenylated isoflavanone renders the Malagasy legume *Dalbergia pervillei* resistant to *Rhodococcus fascians*." *Environmental Microbiology* **13**(5): 1236-1252.

Raynaud, C., M. A. Laneelle, R. H. Senaratne, P. Draper, G. Laneelle and M. Daffe (1999). "Mechanisms of pyrazinamide resistance in mycobacteria: importance of lack of uptake in addition to lack of pyrazinamidase activity." *Microbiology* **145** (Pt 6): 1359-1367.

Riley, L. W. (2006). "Of mice, men, and elephants: *Mycobacterium tuberculosis* cell envelope lipids and pathogenesis." *J Clin Invest* **116**(6): 1475-1478.

Rottmann, M., C. McNamara, B. K. Yeung, M. C. Lee, B. Zou, B. Russell, P. Seitz, D. M. Plouffe, N. V. Dharia, J. Tan, S. B. Cohen, K. R. Spencer, G.

E. Gonzalez-Paez, S. B. Lakshminarayana, A. Goh, R. Suwanarusk, T. Jegla, E. K. Schmitt, H. P. Beck, R. Brun, F. Nosten, L. Renia, V. Dartois, T. H. Keller, D. A. Fidock, E. A. Winzeler and T. T. Diagana (2010). "Spiroindolones, a potent compound class for the treatment of malaria." Science **329**(5996): 1175-1180.

Sharpe, R. J., J. T. Malinowski and J. S. Johnson (2013). "Asymmetric synthesis of the aminocyclitol pactamycin, a universal translocation inhibitor." J Am Chem Soc **135**(47): 17990-17998.

Shi, W., X. Zhang, X. Jiang, H. Yuan, J. S. Lee, C. E. Barry, 3rd, H. Wang, W. Zhang and Y. Zhang (2011). "Pyrazinamide inhibits trans-translation in *Mycobacterium tuberculosis*." Science **333**(6049): 1630-1632.

Skouta, R. and C. J. Li (2007). "Gold(I)-catalyzed annulation of salicylaldehydes and aryl acetylenes as an expedient route to isoflavanones." Angew Chem Int Ed Engl **46**(7): 1117-1119.

Sougakoff, W., M. Rodrigue, C. Truffot-Pernot, M. Renard, N. Durin, M. Szpytma, R. Vachon, A. Troesch and V. Jarlier (2004). "Use of a high-density DNA probe array for detecting mutations involved in rifampicin resistance in *Mycobacterium tuberculosis*." Clin Microbiol Infect **10**(4): 289-294.

Stover, C. K., P. Warrener, D. R. VanDevanter, D. R. Sherman, T. M. Arain, M. H. Langhorne, S. W. Anderson, J. A. Towell, Y. Yuan, D. N. McMurray, B. N. Kreiswirth, C. E. Barry and W. R. Baker (2000). "A small-molecule nitroimidazopyran drug candidate for the treatment of tuberculosis." Nature **405**(6789): 962-966.

Tahlan, K., R. Wilson, D. B. Kastrinsky, K. Arora, V. Nair, E. Fischer, S. W. Barnes, J. R. Walker, D. Alland, C. E. Barry, 3rd and H. I. Boshoff (2012). "SQ109 targets MmpL3, a membrane transporter of trehalose monomycolate involved in mycolic acid donation to the cell wall core of *Mycobacterium tuberculosis*." Antimicrob Agents Chemother **56**(4): 1797-1809.

Tanaka, H., H. Hattori, T. Oh-Uchi, M. Sato, M. Sako, Y. Tateishi and G. H. Rizwani (2009). "Three new isoflavanones from *Erythrina costaricensis*." Nat Prod Res **23**(12): 1089-1094.

Vaid, A., R. Ranjan, W. A. Smythe, H. C. Hoppe and P. Sharma (2010). "PfPI3K, a phosphatidylinositol-3 kinase from *Plasmodium falciparum*, is exported to the host erythrocyte and is involved in hemoglobin trafficking." Blood **115**(12): 2500-2507.

Valentova, M., R. Marek, E. Svajdenka, R. Kubinova and V. Suchy (2011). "A new isoflavanone from *Iresine herbstii*." Fitoterapia **82**(2): 272-275.

Wellems, T. E., A. Walker-Jonah and L. J. Panton (1991). "Genetic mapping of the chloroquine-resistance locus on *Plasmodium falciparum* chromosome 7." Proc Natl Acad Sci U S A **88**(8): 3382-3386.

White, N. J., S. Pukrittayakamee, T. T. Hien, M. A. Faiz, O. A. Mokuolu and A. M. Dondorp (2014). "Malaria." Lancet **383**(9918): 723-735.

Wilson, M. C., T. A. Gulder, T. Mahmud and B. S. Moore (2010). "Shared biosynthesis of the saliniketals and rifamycins in *Salinispora arenicola* is controlled by the sare1259-encoded cytochrome P450." J Am Chem Soc **132**(36): 12757-12765.

Winzeler, E. A. and M. J. Manary (2014). "Drug resistance genomics of the antimalarial drug artemisinin." Genome Biol **15**(11): 544.

Woong Park, S., M. Klotzsche, D. J. Wilson, H. I. Boshoff, H. Eoh, U. Manjunatha, A. Blumenthal, K. Rhee, C. E. Barry, 3rd, C. C. Aldrich, S. Ehrh and D. Schnappinger (2011). "Evaluating the sensitivity of *Mycobacterium tuberculosis* to biotin deprivation using regulated gene expression." PLoS Pathog **7**(9): e1002264.

Wu, T., A. Nagle, K. Kuhen, K. Gagaring, R. Borboa, C. Francek, Z. Chen, D. Plouffe, A. Goh, S. B. Lakshminarayana, J. Wu, H. Q. Ang, P. Zeng, M. L. Kang, W. Tan, M. Tan, N. Ye, X. Lin, C. Caldwell, J. Ek, S. Skolnik, F. Liu, J. Wang, J. Chang, C. Li, T. Hollenbeck, T. Tuntland, J. Isbell, C. Fischli, R. Brun, M. Rottmann, V. Dartois, T. Keller, T. Diagana, E. Winzeler, R. Glynn, D. C. Tully and A. K. Chatterjee (2011). "Imidazolopiperazines: hit to lead optimization of new antimalarial agents." J Med Chem **54**(14): 5116-5130.

Xiong, Y., X. Wu and T. Mahmud (2005). "A homologue of the *Mycobacterium tuberculosis* PapA5 protein, rif-orf20, is an acetyltransferase involved in the biosynthesis of antitubercular drug rifamycin B by *Amycolatopsis mediterranei* S699." Chembiochem **6**(5): 834-837.

Xu, J., T. Mahmud and H. G. Floss (2003). "Isolation and characterization of 27-O-demethylrifamycin SV methyltransferase provides new insights into the post-PKS modification steps during the biosynthesis of the antitubercular drug rifamycin B by *Amycolatopsis mediterranei* S699." Arch Biochem Biophys **411**(2): 277-288.

Xu, J., E. Wan, C. J. Kim, H. G. Floss and T. Mahmud (2005). "Identification of tailoring genes involved in the modification of the polyketide backbone of rifamycin B by *Amycolatopsis mediterranei* S699." Microbiology **151**(Pt 8): 2515-2528.

Yeung, B. K., B. Zou, M. Rottmann, S. B. Lakshminarayana, S. H. Ang, S. Y. Leong, J. Tan, J. Wong, S. Keller-Maerki, C. Fischli, A. Goh, E. K. Schmitt, P. Krastel, E. Francotte, K. Kuhen, D. Plouffe, K. Henson, T. Wagner, E. A. Winzeler, F. Petersen, R. Brun, V. Dartois, T. T. Diagana and T. H. Keller (2010). "Spirotetrahydro beta-carbolines (spiroindolones): a new class of potent and orally efficacious compounds for the treatment of malaria." J Med Chem **53**(14): 5155-5164.

Zhang, Y., B. Heym, B. Allen, D. Young and S. Cole (1992). "The catalase-peroxidase gene and isoniazid resistance of *Mycobacterium tuberculosis*." Nature **358**(6387): 591-593.

Zhang, Y., A. Scorpio, H. Nikaido and Z. Sun (1999). "Role of acid pH and deficient efflux of pyrazinoic acid in unique susceptibility of *Mycobacterium tuberculosis* to pyrazinamide." J Bacteriol **181**(7): 2044-2049.

Zimhony, O., J. S. Cox, J. T. Welch, C. Vilcheze and W. R. Jacobs, Jr. (2000). "Pyrazinamide inhibits the eukaryotic-like fatty acid synthetase I (FAS I) of *Mycobacterium tuberculosis*." Nat Med **6**(9): 1043-1047.

Zimmerman, M. R. (1979). "Pulmonary and osseous tuberculosis in an Egyptian mummy." Bull N Y Acad Med **55**(6): 604-608.

CHAPTER II

Modification of Rifamycin Polyketide Backbone Leads to Improved Drug Activity Against Rifampicin-Resistant *Mycobacterium tuberculosis*

Aeshna Nigam¹, Khaled H. Almabruk¹, Anjali Saxena, Jongtae Yang, Udit Mukherjee, Hardeep Kaur, Puneet Kohli, Rashmi Kumari, Priya Singh, Lev N. Zakharov, Yogendra Singh, Taifo Mahmud,* and Rup Lal*

¹ These authors contributed equally to the work

2.1 Abstract

Rifamycin B, a product of *Amycolatopsis mediterranei* S699, is the precursor of clinically used antibiotics that are effective against tuberculosis, leprosy and AIDS related mycobacterial infections. However, prolonged usage of these antibiotics has resulted in the emergence of rifamycin resistant strains of *Mycobacterium tuberculosis*. As part of our effort to generate better analogs of rifamycin, we substituted the acyltransferase (AT) domain of module 6 of rifamycin polyketide synthase (*rifPKS*) with that of module 2 of rapamycin PKS. The resulting mutants (*rifAT6::rapAT2*) of *A. mediterranei* S699 produced new rifamycin analogs, 24-desmethylrifamycin B and 24-desmethylrifamycin SV, which contained modification in the polyketide backbone. 24-desmethylrifamycin B was then converted to 24-desmethylrifamycin S, whose structure was confirmed by MS, NMR, and X-ray crystallography. Subsequently, 24-desmethylrifamycin S was converted to 24-desmethylrifampicin, which showed excellent antibacterial activity against several rifampicin-resistant *M. tuberculosis* strains.

2.2 Introduction

Rifamycin B, a product of the soil bacterium *Amycolatopsis mediterranei* S699, is a clinically important precursor of the broad-spectrum macrolide antibiotics, rifampicin, rifabutin, rifapentine and rifaximin (Figure 2.1). Rifampicin, rifabutin, and rifapentine are effective against tuberculosis (TB), leprosy, and AIDS related mycobacterial infections, whereas rifaximin is used to treat enteroaggregative *E. coli* infections. This class of antibiotics binds to bacterial RNA polymerases (RNAPs) and blocks the extension of RNA chain (Hartmann et al. 1985, Campbell et al. 2001). However, a long period of use and a combination of poor compliance and poor medical supervision have resulted in the rifamycin resistant strains of *Mycobacterium tuberculosis*. Therefore, there is an urgent need to produce rifamycin analogs that can overcome this resistance problem.

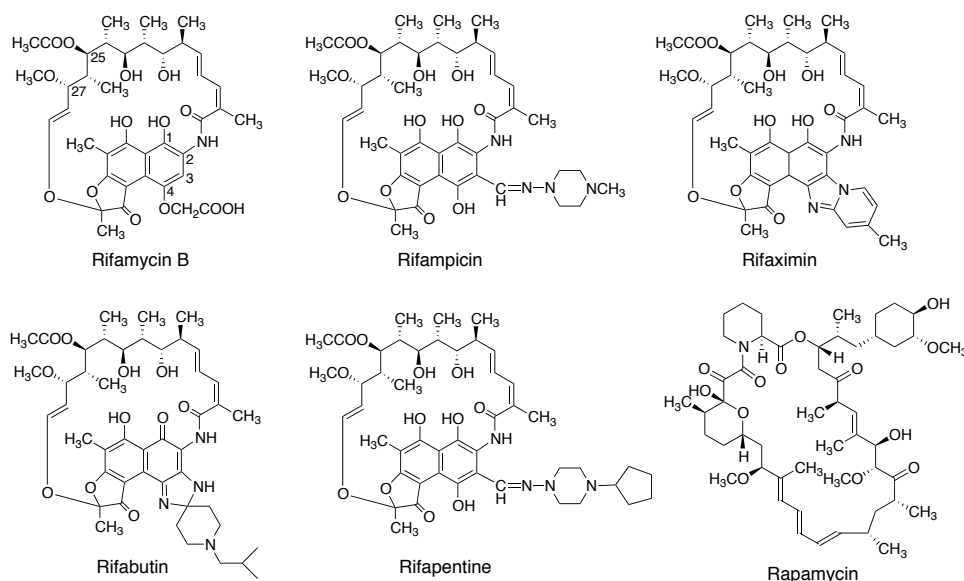
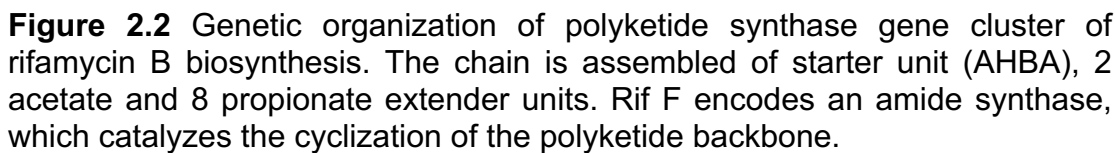


Figure 2.1. Chemical structures of rifamycins and rapamycin.

However, structural complexity of rifamycin B limits the use of chemical tools to generate fundamentally different rifamycin analogs, such as modifications of the backbone structure.

Structurally, rifamycin belongs to the ansamycin class of antibiotics, characterized by a naphthalene moiety spanned by an aliphatic chain (Figure 2.1). The carbon skeleton of rifamycin B is built by a type I polyketide synthase (PKS) machinery from two acetate and eight propionate units using 3-amino-5-hydroxybenzoic acid (AHBA) as a starter molecule (August et al. 1998). The rifamycin (*rif*) biosynthetic gene cluster (AF040570.3) was first independently identified in *Amycolatopsis mediterranei* S699 (August et al. 1998, Verma et al. 2011) and LBG A3136 (Schupp et al. 1998), which was then confirmed by genome sequencing of *A. mediterranei* S699 (Verma et al. 2011) (Figure 2.2). The cluster consists of five type I PKS genes, *rifA* to *rifE*, an amide synthase (*rifF*), the AHBA biosynthetic genes, and genes responsible for regulation, efflux, and tailoring processes. The *Rif*-PKS is comprised of a non-ribosomal peptide synthetase-like loading domain (Admiraal et al. 2001, Admiraal et al. 2003) and ten chain extension modules. Each module consists of a minimal set of domains that includes ketosynthase (KS), responsible for catalyzing a condensation reaction, acyltransferase (AT), which loads the extender unit malonyl-CoA or methylmalonyl-CoA, and an acyl carrier protein (ACP) domain, which tethers the growing polyketide chain. The AT domains of module 2 and 9 recruit malonyl-CoA (incorporating acetate) and the remaining eight modules recruit methylmalonyl-CoA



Type I PKSs, such as *ery*PKS, have been shown to be amendable to

combinatorial biosynthetic modifications to give new analogs of antibiotics (Oliynyk et al. 1996, Jacobsen et al. 1998, Ranganathan et al. 1999, Xue et al. 1999). For instance, replacement of *debs*AT1 and AT2 with *rap*AT14 (Ruan et al. 1997), *debs*AT1 with *rap*AT2, *debs*AT6 with *rap*AT2 (Lau et al. 1999), *debs*AT4 with AT5 domain of nidamycin PKS (Stassi et al. 1998), have resulted in the formation of their respective novel hybrid analogs. Despite these early successes, many attempts to alter PKSs in other systems appeared to be less successful. In the case of rifamycin, ever since the discovery of *rif* PKS, no modifications of this PKS system have been reported. One of the reasons for this is that *A. mediterranei* S699 is less amenable to genetic manipulations. Nevertheless, our early efforts in this direction have resulted in cloning vectors transformation protocol for *A. mediterranei* (Lal et al. 1991, Lal et al. 1994, Lal et al. 1995, Lal et al. 1996, Khanna et al. 1998, Lal et al. 1998, Lal 1999, Lal et al. 2000, Tuteja et al. 2000). In addition, we have demonstrated that gene manipulations in this strain are possible (Xu et al. 2003, Xu et al. 2005). However, whether the *rif*PKS is amenable to genetic manipulations to produce new rifamycin analogs with altered polyketide backbone remains uncertain.

In this paper, we describe for first time the replacement of AT6 of *rif*PKS (which adds propionate) with AT2 of rapamycin (*rap*) PKS (which adds acetate to the growing polyketide chain) in *A. mediterranei* S699. The mutant produced 24-desmethylrifamycin B and 24-desmethylrifamycin SV, which were then converted to their semisynthetic derivative 24-desmethylrifamycin

S and 24-desmethyrrifampicin. These compounds were found to be effective against a number of pathogenic bacteria, including rifampicin-resistant strains of *M. tuberculosis*.

2.3 Results and Discussion

2.3.1 AT6 domain substitution in *A. mediterranei* S699

It has been reported that the formation of naphthalene moiety in rifamycin biosynthesis occurs during chain elongation, specifically on module 4, as opposed to a result of a post PKS modification process (Stratmann et al. 1999, Yu et al. 1999, Xu et al. 2005). This reaction is catalyzed by *Rif-Orf19*, a 3-(3-hydroxyphenyl) propionate hydroxylase-like protein, which introduces a hydroxy group into the acyl carrier protein (ACP)-bound tetraketide and sets the stage for a cyclization reaction to form the naphthalene ring (Xu et al. 2005). Based on this, we designed a strategy to construct mutant strains of *A. mediterranei* S699 that might produce new rifamycin analogs, in which modification of the polyketide backbone occurs after the naphthalene ring formation (Figure 2.2). We replaced the AT domain of module 6 (AT6) of the *rif*PKS (recognizes methylmalonyl-CoA as substrate) with the AT domain of module 2 (AT2) of the rapamycin PKS (recognizes malonyl-CoA) (Figure 2.3). For this purpose, the *rap*AT2 domain excised from pMO2 (Oliynyk et al. 1996), was sandwiched between PCR-I and PCR-II, 1.68kb and 1.5 kb DNA regions upstream and downstream of the AT6 domain of *rif*PKS, respectively. The resulting cassette (PCR-I/*rap*AT2/PCR-II) was then introduced into the vector pIJ4026 to give pAT6F (Figure 2.3B). This non-replicative plasmid

(containing erythromycin resistance gene *ermE*) was electroporated into *A. mediterranei* S699 and the transformants were selected under erythromycin pressure.

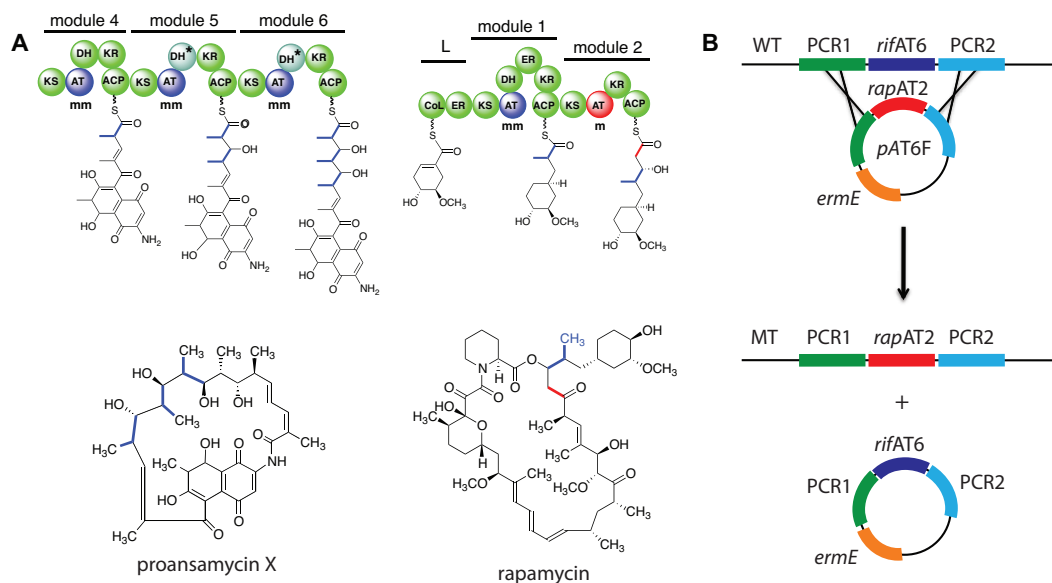


Figure 2.3. Construction of AT6 mutant of *Amycolatopsis mediterranei* S699. **A.** Partial polyketide assembly lines in rifamycin and rapamycin biosynthesis. AT6 domain of rifamycin PKS adds propionate, whereas AT2 domain of rapamycin PKS adds acetate to the growing polyketide chains. Proansamycin X is a precursor of rifamycin B. **B.** Schematic overview of homologous recombination events postulated to occur in *A. mediterranei* S699 to give an AT6 mutant.

Screening of first homologous recombinants yielded four single crossover (SCO) clones, which did not produce rifamycin, as indicated by the lack of brown pigmentation even after three weeks of incubation on agar plates (Figure 2. S3). Southern blot hybridization of their genomic DNA using [α - 32 P]-labeled pIJ4026 as probe confirmed the integration of PCR-I/*rapAT2*/PCR-II cassette in the chromosome (Figure 2.S4A). The mutants were then grown on agar plates without antibiotic pressure for 3-4 generations to allow a second homologous recombination to occur.

Screening of the colonies yielded three positive double crossover (DCO) clones, which were sensitive to erythromycin and produced brown pigmentation (Figure 2.S3E-G). These clones were confirmed by Southern blot hybridization using DIG labeled *rapAT2* (Figure 2.S6B). The DCO clones were also confirmed using PCR amplification and sequencing (data not shown). The *rapAT2* amplicons from these DCOs were identical to the *rapPKS* from *Streptomyces hygroscopicus*, indicating that the *rapAT2* domain has successfully replaced the *rifAT6* domain in *A. mediterranei* S699.

2.3.2 Production of rifamycin analogs by *rifAT6::rapAT2* mutant

To investigate if the *rifAT6::rapAT2* mutant could produce rifamycin analogs, the wild-type and the mutant strains of *A. mediterranei* were grown in YMG medium (50 mL) for 7 days. The cultures were centrifuged and the supernatants were fractionated with ethyl acetate and analyzed by electrospray ionization mass spectrometry (Thermo Finnigan liquid chromatograph-ion trap mass spectrophotometer). Whereas the wild-type produced rifamycin B and rifamycin SV, the mutants produced compounds that gave *quasi*-molecular ions of m/z 740 and 682, which were 14 atomic mass units (amu) less than those of rifamycin B (m/z 754 [M-H]⁻) and rifamycin SV (m/z 696 [M-H]⁻), respectively (Figure 2.4). The results were consistent with the expected molecular masses for desmethyl analogs of rifamycin B and SV, although on the basis of these data alone it was not clear if the missing methyl group occurred at the expected C-24 position of the polyketide backbone.

2.3.3 Structure determination of 24-desmethyrrifamycin B and 24-desmethyrrifamycin SV

To confirm the chemical structure of the products, a 1 L scale culture of *rifAT6::rapAT2* mutant was prepared. The culture was extracted with EtOAc and the extract was subjected to SiO₂ column chromatography and HPLC (YMC C₁₈ 250 x 10 mm 5 micron, acetonitrile-0.5 M aq. ammonium formate 40:60, flow rate 2 mL/min, 254 nm). The major product (m/z 740 [M-H]⁻) was isolated (yield, 20 mg/L) and analyzed by ¹H and ¹³C NMR. The ¹H NMR spectrum of the compound revealed the presence of three pendant methyl groups [δ 0.72 (d, J = 6.5 Hz, 3H), 0.85 (d, J = 7 Hz, 3H), 0.92 (d, J = 6.5 Hz, 3H)], instead of four in rifamycin B [δ -0.30 (d, J = 4.5 Hz, 3H), 0.57 (d, J = 6 Hz, 3H), 0.97 (d, J = 6 Hz, 6H)], confirming the lack of a pendant methyl group in the mutant product (Figure 2.5C-D). This is consistent with the expected product 24-desmethyrrifamycin B. Interestingly, 24-desmethyrrifamycin B is chemically rather unstable and can partially convert to 24-desmethyrrifamycin SV and S in MeOH. ¹H NMR analyses of the latter compounds revealed the lack of signals for the glycolate moiety (Figure 2.S10).

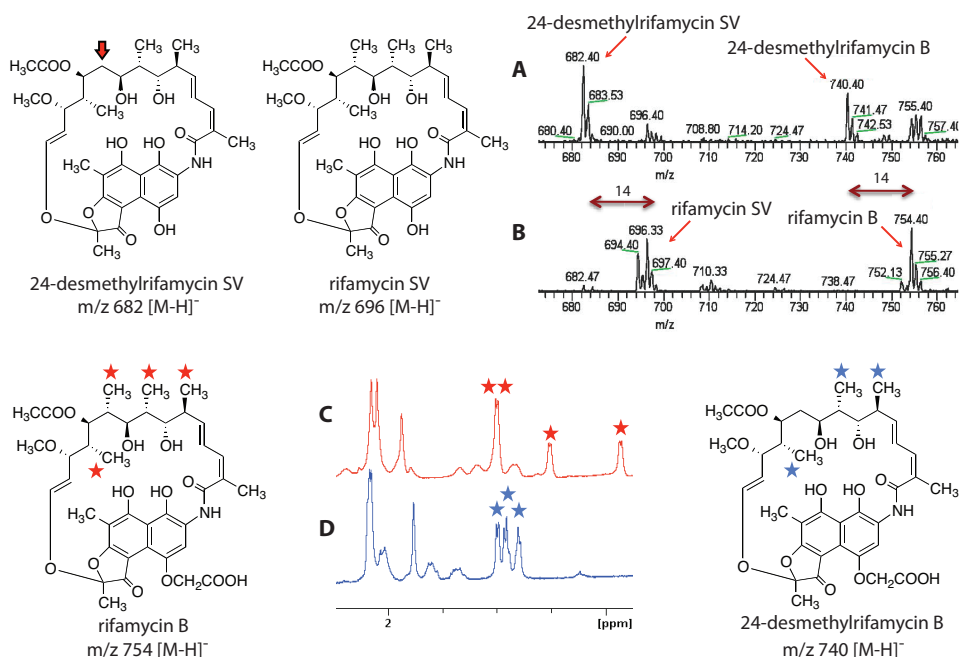


Figure 2.4. Mass spectrometry and NMR spectroscopy analyses of rifamycin B and 24-desmethylrifamycin B. **A.** (-)-ESI-MS analysis of ethyl acetate extract of the AT6 mutant strain of *A. mediterranei* S699 that shows prominent peaks at m/z 740 (desmethylrifamycin B) and 682 (desmethylrifamycin SV). **B.** (-)-ESI-MS analysis of ethyl acetate extract of the wild-type strain that shows prominent peaks at m/z 754 (rifamycin B) and 696 (rifamycin SV). **C.** Partial 1H NMR spectrum of rifamycin B. **D.** Partial 1H NMR spectrum of 24-desmethylrifamycin B. Red stars show the four pendant methyl group in rifamycin B and blue stars show three pendant methyl groups in 24-desmethylrifamycin B.

2.3.4 Conversion of 24-desmethylrifamycin B to 24-desmethylrifamycin S

S

To further confirm the chemical structure of the products, 24-desmethylrifamycin B was oxidized to 24-desmethylrifamycin S using $CuCl_2$ as catalyst. The product was analyzed by (-)-ESI-MS (m/z of 680 $[M-H]^-$, indicating the lack of the glycolate moiety and the presence of a naphthoquinone unit in the molecule) and 1H NMR spectrum. Interestingly, during storage in CD_3OD at $-20\text{ }^\circ C$, transparent red brown orthorhombic crystals were formed. These crystals were washed with cooled *n*-hexane and

subsequently subjected to X-ray crystallographic analysis. The crystal structures revealed a dimeric form of 24-desmethylrifamycin S coordinating with Ca^{2+} through C-1, C-8, C-21, and C-23 oxygen atoms (Figure 2.5). The results unambiguously confirmed the identity of the compound as 24-desmethylrifamycin S.

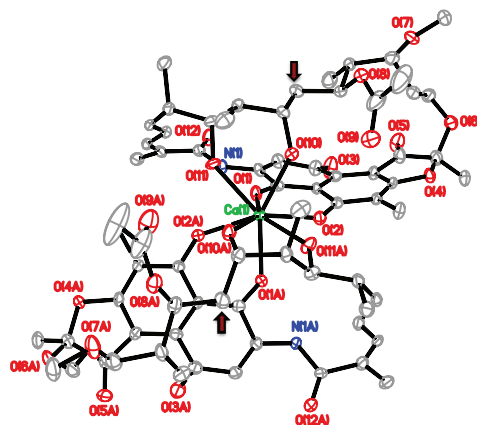
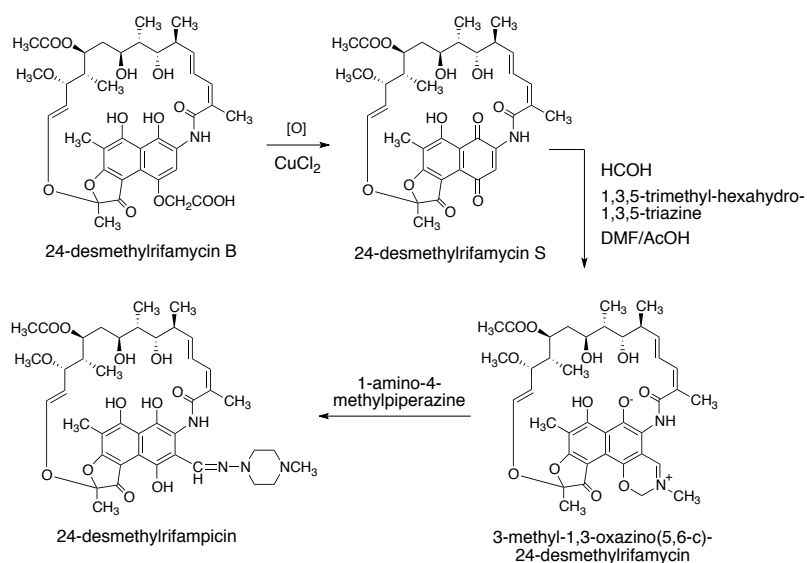


Figure 2.5. X-ray crystal structure of 24-desmethylrifamycin S dimer in complex with Ca^{2+} . Broad red arrows indicate the missing methyl groups.

2.3.5 Synthesis of 24-desmethylrifampicin

To compare the biological activity of the new compound with the clinically used rifampicin, 24-desmethylrifamycin S was converted to 24-desmethylrifampicin by chemical synthesis. The synthesis was carried out according to the published method for the preparation of rifampicin (Marsili et al. 1984). Thus, treatment of 24-desmethylrifamycin S with paraformaldehyde and 1,3,5-trimethyl-hexahydro-1,3,5-triazine in the presence of acetic acid gave 3-methyl-1,3-oxazino(5,6-c)-24-desmethylrifamycin (Scheme 1). The product was then treated with 1-amino-4-methylpiperazine to give 24-

desmethylrifampicin. Despite high purity of the product, as determined by TLC, HPLC, and ESI-MS (Figure S7 and S13), we were not able to obtain good quality NMR spectra of 24-desmethylrifampicin. This quandary might have been due to either partial oxidation of hydroquinone to quinone or reversible conformational changes of the compound that led to more than one conformer in the solution. However, attempts to improve the quality of the ^1H NMR spectrum by adding a trace amount of the reducing agent ascorbic acid, which is commonly used to reduce quinone to hydroquinone forms of rifampicin, or increasing the temperature during ^1H NMR measurements were unsuccessful. To confirm the utility of the synthetic method, we employed the same method to convert rifamycin S to rifampicin. The later compound gave an excellent ^1H NMR spectrum, identical to that of commercially available rifampicin (Figure 2. S14). As there is no indication of quinone formation in rifampicin, it is predicted that the reversible conformational changes of 24-desmethylrifampicin is a more likely scenario. Nevertheless, to validate the identity of 24-desmethylrifampicin, a comparative MS/MS analysis was carried out (Supplemental Fig. S13). The result showed that 24-desmethylrifampicin (m/z 807 \rightarrow 676 \rightarrow 616 \rightarrow 490 \rightarrow 420) and rifampicin (m/z 821 \rightarrow 690 \rightarrow 630 \rightarrow 490 \rightarrow 420) have identical fragmentation patterns, albeit most of the fragments of 24-desmethylrifampicin are 14 atomic mass units less than the corresponding fragments from rifampicin (Figure 2.S8 and 2.S9). These fragmentation patterns are also consistent with those previously reported for rifampicin (Prasad et al. 2009).



Scheme 2.1. Conversion of 24-desmethylrifamycin B to 24-desmethylrifamycin S and chemical synthesis of 24-desmethylrifampicin.

2.3.6 Antibacterial activity of 24-desmethylrifamycin S and 24-desmethylrifampicin

An antibacterial assay was carried out using 24-desmethylrifampicin, 24-desmethylrifamycin S and commercially available rifampicin and rifamycin S against *Mycobacterium smegmatis* and *Staphylococcus aureus*. The results showed that 24-desmethylrifamycin S and 24-desmethylrifampicin are active against *M. smegmatis* and *S. aureus*, comparable to rifamycin S and rifampicin, respectively (Figure 2.S15). This prompted us to carry on the study using multidrug resistant strains of *M. tuberculosis*. For this, MDR strains were procured from Open Source Drug Discovery (OSDD) (www.osdd.net/) and the drug testing was performed at Premas Biotech, Haryana, India, according to WHO guidelines. The drug sensitivity tests were carried out against two rifampicin-sensitive (OSDD 209 and H37Rv) and three rifamycin-resistant (OSDD 55, OSDD 206, and OSDD 321) strains of *M. tuberculosis*.

(Table 2.1). Rifampicin (HiMedia), 24-desmethylrifampicin and 24-desmethylrifamycin S were tested against the above-mentioned pathogenic strains. The tests were done at various concentrations (0.01 – 50 µg/mL) of drugs using BacT/ALERT MB System (Crump et al. 2011). The results revealed that 24-desmethylrifamycin S and 24-desmethylrifampicin showed strong antibacterial activity against both rifampicin-sensitive and -resistant strains of *M. tuberculosis*.

Table 2.1. Drug sensitivity data for rifampicin-resistant and -susceptible strains of *Mycobacterium tuberculosis* (procured from OSDD) against commercially available rifampicin and the novel compounds 24-desmethylrifamycin S and 24-desmethylrifampicin.

<i>M. tuberculosis</i> strain		rifampicin (HiMedia) (µg/ml)	24-desmethyl- rifamycin S (µg/ml)	24-desmethyl- rifampicin (µg/ml)
OSDD 55 (H526T)	Rifampicin- resistant	>50	0.1	<0.01
OSDD 206 (S531L)		>50	0.05	0.05
OSDD 321 (S531L)		>50	0.1	0.05
OSDD 209*	Rifampicin- susceptible	0.1	<0.01	<0.01
H37Rv*		0.05	<0.01	0.05

* no rpoB mutation

2.4 Discussion

Although many derivatives of rifamycin have been synthesized by chemical methods in the past 40 years (Aristoff et al. 2010), only a handful of rifamycin derivatives are currently used for treating tuberculosis. Most rifamycin derivatives, including those used in the clinics, are chemically modified at the C-3 and/or the C-4 positions of the naphthalene moiety. Chemical modifications of other parts of the compound appear to be difficult to achieve due to the complexity of the molecule. In addition, X-ray crystallography studies of *Thermus aquaticus* RNAP in complex with rifampicin revealed that the four free hydroxy groups in the molecule are important for RNAP binding (Campbell et al. 2001). Consequently, modifications of these hydroxyl groups are undesirable. Thus, this work focuses on the design of a strategy that gains access to rifamycin analogs, in which modifications take place in the polyketide backbone.

However, many complex polyketide systems similar to *rif*PKS have been reported to be less amenable to pathway engineering, either due to inflexibility of the downstream enzymes to accept modified substrates, or incompatibility in architectural modularity of the modified PKS systems (Khosla et al. 2009). Therefore, efforts to genetically engineer the *rif*PKS of *A. mediterranei* S699 were a somewhat risky and challenging endeavor. Additionally, the post PKS tailoring processes in rifamycin biosynthesis involving cytochrome P450-dependent hydroxylation and oxidative cleavage and rearrangement of the ansa chain (Xu et al. 2005, Wilson et al. 2010)

further augment the degree of complications in rifamycin biosynthesis. However, the most challenging aspect in the current study was the construction of the mutant strains of *A. mediterranei* S699. Gene transfer into this strain has so far only been successful through electroporation with undesirably low efficiency (Xu et al. 2003, Xu et al. 2005).

Nevertheless, the consideration of the formation of the naphthaquinone ring, which takes place during polyketide chain elongation (Yu et al. 1999, Xu et al. 2005), let us to target the replacement of the *rifAT6* domain with that of *rapAT2*. Using this domain-replacement strategy, we successfully demonstrated that the *rifPKS* gene cluster is amenable to genetic manipulations and the mutants (*rifAT6::rapAT2*) can produce new rifamycin analogs, 24-desmethyrrifamycin B and 24-desmethyrrifamycin SV. While not completely unexpected, it is rather surprising that this complex biosynthetic system is adaptable to such a modification. However, whether this approach is applicable to the other *rifPKS* modules remains to be explored. More importantly, their semi-synthetic product, 24-desmethyrrifampicin, showed comparable or better antibacterial activity than the clinically used rifampicin against various pathogenic bacteria, including rifampicin-sensitive and -resistant *M. tuberculosis*. This finding is significant because such a compound may be developed as a promising lead to cure MDR-TB.

Rifamycin resistance is associated with genetic alterations in an 81-bp region of the *rpoB* gene encoding the DNA-dependent RNAP β -subunit (Williams et al. 1998). In this study, we used rifampicin-resistant *M. tuberculosis* strains,

OSDD 321 and OSDD 206, which contain the S531L mutation, and OSDD 55, which has the H526T mutation in the RNAP β -subunit. These mutations appear to alter the affinity of the RNAPs to rifampicin. In addition, on the basis of the reported crystal structures of bacterial RNAPs in complex with rifampicin (Campbell et al. 2001), and the sequence data for rifampicin-resistant RNAPs (Williams et al. 1998), we hypothesize that drug resistant mutations disrupt hydrogen bonding in the polyketide ansa chain. This was in part confirmed by the fact that 24-desmethyrrifampicin showed improved activity against rifampicin-resistant *M. tuberculosis*. The loss of the methyl group in this compound is postulated to lead to conformational changes in the ansa chain that allow for more flexibility of the compound to bind mutated RNAPs. This conceivable conformational flexibility may be connected to the unsettled ^1H and ^{13}C NMR spectra of 24-desmethyrrifampicin.

While 24-desmethyrrifampicin showed improved efficacy against *M. tuberculosis*, compared to rifampicin it presents only a small structural change. Therefore, it is possible that resistant strains to 24-desmethyrrifamycin can quickly develop. However, interestingly, even among the clinically used rifamycin derivatives, the tendency of bacterial resistance to those drugs is significantly different. For example, although rifampicin resistant strains of *M. tuberculosis* are now emerging, resistance to rifabutin has yet to be widely seen. In fact, some bacterial strains that confer resistance to rifampicin are still susceptible to rifabutin. X-ray crystal structural studies of the *T. thermophilus* RNAP in complex with rifapentin or rifabutin

revealed additional interactions between their C-3/C-4 side chains and the enzyme (Artsimovitch et al. 2005). A more recent study on the crystal structures of the *E. coli* RNAP complexes with benzoxazinorifamycins has also demonstrated the role of the C-3/C-4 side chains in their improved binding to the protein (Molodtsov et al. 2013). In the case of 24-desmethyrlrifamycin, we anticipate that conformational flexibility of the ansa chain may provide some advantages against mutated RNAPs. This may be further improved by chemical modifications of the C-3/C-4 positions of the compound, e.g., adding benzoxazine moiety or other side chains, which can be effectively done by semi-synthesis using the mutant product as a scaffold. Currently, the *rifAT6::rapAT2* mutant produces about 20 mg/L 24-desmethyrlrifamycin B, which is lower than the yield of rifamycin B produced by the wild-type strain S699 (50-100 mg/L). This is consistent with the common phenomenon observed in many genetically engineered strains, which often produce combinatorial products in lower yields than the natural product (Floss 2006). However, the yield may be increased through a classical strain improvement program, or by adopting the PKS domain replacement strategy to modify industrial strains, which can produce rifamycin B up to 24 g/L (Lal et al. 1995).

Furthermore, it is desirable to successfully apply the 'proof-of-concept' methodology developed in this study to further garner new rifamycin analogs by modifying its polyketide backbone. This may include replacement of the AT domains of other modules (loss or gain of a methyl group at other C-

positions), inactivation of a dehydratase domain (introduction of an additional hydroxyl group) or a ketoreductase domain (introduction of a ketone). In addition, double or multiple modifications may also be pursued to generate more diverse analogs of rifamycin. Whereas effective strategies to achieve multiple genetic modifications still have yet to be developed, the combined genetic-synthetic approach applied in this study holds great potential to generate more rifamycin analogs to combat the threat of MDR strains of *M. tuberculosis* and/or other life-threatening pathogens.

2.5 Material and Methods

2.5.1 General Experimental Procedures

General - All chemicals were obtained either from Sigma Aldrich, EMD, TCI, or Pharmacia. Analytical thin-layer chromatography (TLC) was performed using silica gel plates (60 Å), which were visualized using a UV lamp and ceric ammonium molybdate (CAM) solution. Chromatographic purification of products was performed on silica gel (60 Å, 72–230 mesh). Proton NMR spectra were recorded on Bruker 300, 500, or 700 MHz spectrometers. Proton chemical shifts are reported in ppm (δ) relative to the residual solvent signals as the internal standard (CD_3OD : δ_{H} 3.35). Multiplicities in the ^1H NMR spectra are described as follows: s = singlet, bs = broad singlet, d = doublet, bd = broad doublet, t = triplet, bt = broad triplet, q = quartet, m = multiplet; coupling constants are reported in Hz. Carbon NMR spectra were recorded on Bruker 125 or 175 MHz spectrometers. Carbon chemical shifts are reported in ppm (δ) relative to the residual solvent signals as the internal standard. Low-resolution electrospray ionization (ESI) mass spectra were recorded on a Thermo-Finnigan liquid chromatograph-ion trap mass spectrometer. High-resolution mass spectra were recorded on an AB SCIEX TripleTOFTM 5600 equipped with an electrospray ionization source.

2.4.2 Bacterial strains, plasmids, and culture media

Amycolatopsis mediterranei S699 (wild-type), a producer of rifamycin B, was obtained from Professor Giancarlo Lancini at the former Lepetit Laboratories, Geranzano, Italy. For sporulation, it was grown at 30 °C on agar plates

containing YMG (4 g yeast extract, 10 g malt extract, 4 g glucose, and 15 g agar per liter, pH 7.2-7.4) medium (Kim et al. 1998). pUC18 and pUC19 were used for subcloning and pMO2 and pIJ4026 were used for domain replacement. *E. coli* XL-1 Blue was used for the propagation and isolation of plasmids. Rifamycin-sensitive and -resistant strains of *Mycobacterium tuberculosis* were acquired from Open Source Drug Discovery (OSDD) (www.osdd.net/) in association with CSIR- Institute of Genomics and Integrative Biology, India (<http://www.igib.res.in/>). The plasmids and bacterial strains that were used in the present study are listed in Supplemental Table S1.

2.4.3 Construction and screening of a genomic cosmid library and selection of the rifamycin cluster

The genomic library of *A. mediterranei* S699 was prepared in the cosmid vector pWE15 (Kaur et al. 2001). This involves isolation of high molecular weight DNA of *A. mediterranei* by Kirby's method (Kieser et al. 2000). The genomic DNA was partially digested with *Sau*3AI and subjected to size fractionation with sucrose gradient. The fractions were pooled and used for ligation with linearized and dephosphorylated pWE15. The ligated DNA was transferred into *E. coli* XL-1 Blue MR. About 2,000 clones were screened using [α -³²P]dATP labeled DNA probes obtained from PCR amplification of the loading domain of *rif*PKS and *rif*K (AHBA synthase gene) of S699. About 10 clones were selected after hybridization. End sequencing of the positive cosmid clones was performed. Finally, three cosmid clones, pRIF13, pRIF21

and pRIF24, which represent the entire *rif* gene cluster were selected and enlisted in Supplemental Table S1.

2.4.4 Construction of pAT6F

For the construction of the pAT6F replacement cassette, AT6 flanking regions, a 1.6 kb DNA fragment upstream of AT6 (AF040570.3) with engineered XbaI/BalI sites and a 1.5 kb DNA fragment downstream of AT6 (AF040570.3) with AvrII/XbaI sites, were obtained by PCR amplification from the cosmid pRIF13. The two amplicons, PCR-I and PCR-II, were treated with kinase and individually cloned into pUC18, which had been digested with SmaI at 28 °C and treated with shrimp alkaline phosphatase. The inserts and vector were ligated together and the ligation mix was electroporated into *E. coli* XL-1 Blue competent cells. The constructs containing PCR-I and PCR-II were named pAT6A and pAT6B, respectively. However, due to the cloning of PCR-I in only one orientation, the PCR-I insert was retrieved from pAT6A by digestion with EcoRI and HindIII and cloned into pUC19, which was predigested with EcoRI and HindIII. The ligation product was electroporated into *E. coli* XL-1 Blue competent cells. The pUC19 plasmid harboring the PCR-I insert was named pAT6C.

The *rapAT2* (X86780.1) fragment was excised from plasmid pMO2, by AvrII and HindIII digestion. The resulting 0.85 kb DNA fragment was ligated with AvrII/HindIII-digested pAT6B to give plasmid pAT6D. Subsequently, the PCR-I fragment was excised from pAT6C by BalI/NdeI digestion and cloned into the BalI/NdeI site of pAT6D to give pAT6E. The later plasmid was

subsequently digested with XbaI to give a 3.85 kb PCR1/*rapAT2*/PCR2 fragment, which was then inserted into the XbaI site of pIJ4026 to give pAT6F (Figures 2.S2, S5 and S6). pAT6F was constructed for the implementation of domain replacement (Figure 2.S4) in *A. mediterranei* S699. All clones (pAT6A, pAT6B, pAT6C, pAT6D, pAT6E & pAT6F) were sequenced using the 3100 Avant Genetic Analyzer (Applied Biosystems) at the University of Delhi, India.

2.4.5 Genetic manipulation of *A. mediterranei* S699

Routine genetic procedures, such as genomic DNA isolation [according to CTAB (cetyltrimethylammonium bromide) method], plasmid isolation (Promega DNA purification kit), and restriction endonuclease digestion, were carried out by standard techniques. pAT6F was electroporated (using BioRad GenePulser) into *A. mediterranei* S699 using the method described previously (Tuteja et al. 2000), and the electroporated mixture was plated on YMG agar plates, incubated for 12-16 h, and overlaid with soft agar (5 g/L, Difco™ agar, granulated) containing 500 µg/mL of erythromycin. The transformants, obtained after 5-7 days, were grown in YMG medium containing 50 µg/mL erythromycin (Sigma Aldrich) to confirm resistance. The integration of pAT6F in these single crossover (SCO) clones was confirmed by Southern blot hybridization. In order to stimulate replacement of AT6 with *rapAT2*, these SCOs were cultured for 3-4 rounds in YMG medium without erythromycin. The cells were plated on YMG agar plates with and without erythromycin pressure and antibiotic sensitive colonies were selected. The

double cross-over (DCO) clones were further confirmed by Southern blot hybridization. For Southern hybridization, the genomic DNA was immobilized on a Hybond N+ membrane (Amersham Biosciences). Hybridization was performed using [$\alpha^{32}\text{P}$]-labeled DNA probes at 65 °C for 12 h. For non-radioactive methods, hybridization was carried out using DIG-labeled DNA probe at 65 °C. Stringency washes were done with 5x SSC, 2x SSC, 1x SSC and 0.1x SSC at 65 °C.

2.4.6 PCR and sequence analysis of the AT6 mutant

Primers were designed based on the sequences of the upstream and downstream regions of *rifAT6* domain of *A. mediterranei* S699, shown in Supplemental Table S2. Chromosomal DNA of the AT6 mutant was isolated using a reported method (Kieser et al. 2000), and PCR amplification was carried out using high fidelity DNA Polymerase (Invitrogen) using conditions and the reaction mix provided with the enzyme. In addition, DMSO (3 μL) was added to the reaction mixture (100 μL). The PCR product (1.5 kb) was confirmed by agarose gel, extracted from the gel using DNA extraction kit (QIAGEN), and submitted to DNA sequencing at the Oregon State University Center for Genome Research and Biocomputing (CGRB).

2.4.7 Isolation and purification of 24-desmethylrifamycin B

Spores of the mutant strain were initially grown on a shaker in YMG medium for 3 days at 30 °C and 200 rpm. The seed culture was then used to inoculate (10%, v/v) YMG medium (10 x 100 mL) in 500 mL flasks. After incubation for 10 days under the same conditions, the cultures were centrifuged, the pooled

supernatants acidified to pH 3 with 1N HCl, and the metabolites extracted with ethyl acetate (2 x 1 L). The crude extracts of rifamycin-related compounds were subjected to silica gel chromatography using CHCl₃-MeOH/5%NH₄OH (10:1 and then 8:1) as a mobile phase. Fractions containing the products were pooled and dried using a rotary evaporator. The product obtained was further purified using HPLC [YMC-ODS-A, 250 x 10 mm, CH₃CN-HCOONH₄ (0.05 M) (60:40), flow rate 2 mL/min, 254 nm]. The product was then desalted using Sephadex LH-20 column with MeOH as eluent to give 24-desmethyrrifamycin B (20 mg) and 24-desmethyrrifamycin SV (8 mg).

24-desmethyrrifamycin B: ¹H NMR (700 MHz, D₂O, CryoProbe): δ 6.69 (s, 1H, H-3), 6.34 (d, 1H, *J* = 12 Hz, H-29), 5.98 (d, *J* = 11 Hz, 1H, H-17), 5.75 (dd, *J* = 15 Hz, 11 Hz, 1H, H-18), 5.21 (dd, *J* = 15 Hz, 10 Hz, 1H, H-19), 5.05 (m, 2H, H-25, H-28), 4.50 (d, *J* = 17 Hz, 1H, -CH₂-COOH), 4.42 (d, *J* = 17 Hz, 1H, -CH₂-COOH), 3.38 (bd, *J* = 10 Hz, 1H, H-23), 3.22 (m, 2H, H-21 and H-27), 3.22 (s, 3H, H-37), 2.11 (s, 3H, H-36), 2.08 (s, 3H, H-14), 1.98 (m, 2H, H-20 and H-26), 1.70 (s, 3H, H-13), 1.53 (m, 2H, H-22 and H-24), 1.28 (t, *J* = 12 Hz, 1H, H-24), 0.92 (d, *J* = 6.5 Hz, 3H, H-31), 0.85 (d, *J* = 7 Hz, 3H, H-32), 0.72 (d, *J* = 6.5 Hz, 3H, H-34). ¹³C NMR (175 MHz, D₂O, CryoProbe): δ_C 191.7, 176.7, 174.7, 168.1, 144.7, 142.1, 141.5, 131.5, 126.5, 126.4, 119.4, 117.8, 113.7, 112.8, 112.1, 109.6, 104.4, 101.1, 80.5, 73.9, 72.4, 71.5, 68.8, 54.9, 48.8, 41.4, 39.9, 35.9, 32.2, 21.8, 20.6, 20.5, 15.4, 9.5, 9.5, 6.9. (-)-HR-ESI-TOF-MS *m/z* 740.2939 (calcd for C₃₈H₄₆NO₁₄ [M-H]⁻: 740.2918).

24-Desmethylrifamycin SV: ^1H NMR (700 MHz, CD_3OD , CryoProbe): ^1H NMR (700 MHz, CD_3OD): δ 6.42 (s, 1H), 6.31 (bd, $J = 12$ Hz, 1H), 5.95-5.89 (m, 2H), 5.51 (s, 1H), 5.20 (bt, $J = 12$ Hz, 1H), 5.14 (bd, $J = 9$ Hz, 1H), 3.22 (s, 3H), 3.17 (t, $J = 10$ Hz, 1H), 2.13 (s, 3H), 2.12-2.11 (m, 2H), 2.01 (s, 3H), 1.96 (s, 3H), 1.67 (s, 3H), 1.54-1.49 (m, 4H), 0.93 (d, 6H), 0.78 (d, $J = 5$ Hz, 3H). HRMS (ESI-TOF) m/z (calcd for $\text{C}_{36}\text{H}_{42}\text{NO}_{12}$ $[\text{M}-\text{H}]^-$: 682.2707).

2.4.8 Conversion of 24-desmethylrifamycin B to 24-desmethylrifamycin S

24-desmethylrifamycin B (8 mg, 0.0107 mmol) was dissolved in $\text{MeOH}-\text{H}_2\text{O}$ (10:1, 5 mL) containing CuCl_2 (0.1 mM). The reaction mixture was stirred at room temperature (RT) overnight to convert 24-desmethylrifamycin B to 24-desmethylrifamycin S. The mixture was acidified to pH 3 and the product was extracted with ethyl acetate (3 x 5 mL). The extract was subjected to silica gel column using CHCl_3 - MeOH (10:1) as eluent to give 24-desmethylrifamycin S (6 mg).

^1H NMR (300 MHz, CD_3OD): 7.85 (s, 1H), 7.04 (m, 1H), 6.88 (bd, $J = 11$ Hz, 1H), 6.59 (m, 1H), 5.23 (dd, $J = 12.6$ Hz, 9.7 Hz), 4.53 (bt, $J = 8$ Hz, 1H), 4.22 (bd, $J = 10$ Hz, 1H), 3.80 (bd, $J = 10$ Hz, 1H), 3.48 (s, 3H), 2.50 (s, 3H), 2.35 (s, 3H), 2.33 (s, 3H), 2.00 (s, 3H), 1.62 (m, 3H), 1.41 (d, $J = 7$ Hz, 3H), 1.29 (d, $J = 6.8$ Hz, 3H), 0.67 (d, $J = 7$ Hz, 3H). HRMS (ESI-TOF) m/z 680.2730 (calcd for $\text{C}_{36}\text{H}_{42}\text{NO}_{12}$ $[\text{M}-\text{H}]^-$: 680.2707).

2.4.9 X-ray crystallography of 24-desmethylrifamycin S

Diffraction intensities were collected at 173(2) K on a Bruker Apex CCD diffractometer using MoK radiation = 0.71073 Å. Space group was determined based on systematic absences. Absorption corrections were applied by SADABS (Sheldrick 1998). Structures were solved by direct methods and Fourier techniques and refined on F^2 using full matrix least-squares procedures. All non-H atoms were refined with anisotropic thermal parameters. H atoms were treated in calculated positions in a rigid group model. It was found that solvent water is partially occupied in a position between molecules with an occupation factor of 0.25. H atoms in this solvent water molecule were not taken in consideration. The Flack parameter is 0.00(10). The relatively high value of R_{int} , 0.1271, is related to the fact that diffraction at high angles was very weak and intensity statistics at high angles are poor. All calculations were performed by the Bruker SHELXTL (v. 6.10) package (SHELXTL-6.10). The crystal structure data for 24-desmethylrifamycin S (Table 2.2) has been deposited at the Cambridge Crystallographic Data Centre (deposition number: CCDC 1000828).

Table 2.2. Crystal data and structure refinement for 24-desmethylrifamycin S.

Empirical formula	C ₇₂ H ₈₁ Ca N ₂ O _{24.50}	
Formula weight	1406.47	
Temperature	173(2) K	
Wavelength	0.71073 Å	
Crystal system	Orthorhombic	
Space group	C222(1)	
Unit cell dimensions	a = 14.257(7) Å	a = 90°.
	b = 20.818(11) Å	b = 90°.
	c = 25.054(13) Å	g = 90°.
Volume	7436(7) Å ³	
Z	4	
Density (calculated)	1.256 Mg/m ³	
Absorption coefficient	0.162 mm ⁻¹	
F(000)	2972	
Crystal size	0.22 x 0.22 x 0.08 mm ³	
Theta range for data collection	1.73 to 25.00°.	
Index ranges	-16<=h<=16, -24<=k<=24, -29<=l<=29	
Reflections collected	35699	
Independent reflections	6539 [R(int) = 0.1271]	
Completeness to theta = 25.00°	100.0 %	
Absorption correction	Semi-empirical from equivalents	
Max. and min. transmission	0.9872 and 0.9653	
Refinement method	Full-matrix least-squares on F ²	
Data / restraints / parameters	6539 / 0 / 452	
Goodness-of-fit on F ²	1.059	
Final R indices [I>2sigma(I)]	R1 = 0.0924, wR2 = 0.2301	
R indices (all data)	R1 = 0.1322, wR2 = 0.2576	
Absolute structure parameter	0.00(10)	
Extinction coefficient	0.0048(6)	
Largest diff. peak and hole	1.090 and -0.483 e.Å ⁻³	

2.4.10 Synthesis of 24-desmethylrifampicin

24-desmethylrifamycin S (5 mg, 0.0073 mmol) was dissolved in DMF (200 µL) and acetic acid (50 µL). After stirring the mixture at 50 °C, paraformaldehyde (3 mg) and 1,3,5-trimethyl-hexahydro-1,3,5-triazine (8 µL) were added. The reaction was stirred at 50 °C for 2 h until all starting material was converted to 3-methyl-1,3-oxazino(5,6-c)-24-desmethylrifamycin, indicated by a blue spot on TLC. Subsequently, 1-amino-4-methyl-piperazine (8 µL) was added to the mixture. The reaction was stirred at the same temperature, and monitored by

TLC until the disappearance of the blue spot and the formation of 24-desmethyrrifampicin. The mixture was diluted with cooled 2% acetic acid (1.5 mL) and extracted three times with CHCl_3 (2 mL). The organic fractions were combined and concentrated to 1 mL and further washed 3 times with Brine solution. Organic fractions were combined and dried over anhydrous sodium sulfate then dried under a rotary evaporator. Crude fractions were subjected to silica gel chromatography with CHCl_3 –MeOH in 10:1 and 8:1 ratio, as eluent. Fractions containing the product were pooled and further purified by HPLC [CH_3CN -0.05 M HCOONH_4 (60:40)] with (YMC-ODS-A, 250X10 mm ID, 5 microns particle size) column and flow rate 2 mL/min at 254 nm. Fractions containing 24-desmethyrrifampicin were dried to afford the title compound (2.5 mg, 0.0031 mmol) of reddish orange powder. ^1H NMR (500 MHz, CD_3OD): HRMS (ESI-TOF) m/z 807.3829 (calcd for $\text{C}_{42}\text{H}_{55}\text{N}_4\text{O}_{12}$ [$\text{M}-\text{H}$] $^-$: 807.3816).

2.4.11 Antibacterial assay

Antibacterial activity of rifampicin and its analogs were determined by agar diffusion assay. *Mycobacterium smegmatis* and *Staphylococcus aureus* were streaked on nutrient agar and incubated overnight at 37 °C.

Colonies were transferred to nutrient broth and incubated at 37 °C for 24 h. The growth of the cultures was measured to a proper density at 600 nm (BioRad, SmartSpec 300). The inoculum (1 mL) was mixed thoroughly with warm nutrient agar (24 mL) and poured into petri dishes. The agar plates were allowed to solidify and dry for 30 min before assay. Sterile Whatman

discs were impregnated with rifampicin and its analogs (20 μ L) at a concentration of 1 mg/mL and dried at RT. The discs were placed onto inoculated agar plates and incubated at 37 °C for 24 h. To produce a contrast background of the inhibition zone, 0.25% MTT developing dye (2 mL) was added over the plates.

Drug sensitivity assays were done by Premas Biotech, Haryana, India, using various concentrations of drugs (0.01 - 1 μ g/ml). The drug testing was done using MB BacT/ALERT System (Crump et al. 2011), which is a mycobacterial detection system that utilizes a colorimetric sensor and reflectance detector to determine the level of carbon dioxide within the bottle. The bottle contains a medium and a MB/BacT reconstitution fluid, which promotes the growth of mycobacteria. As the bacteria grow, they produce CO₂, which changes the color of the sensor located at the bottom of the bottle from green to yellow. The testing was performed with two controls: Direct growth control (DGC) and Proportionate growth control (PGC). DGC consists of 0.1 mL seed culture and 0.5 ml reconstitution fluid. PGC consists of 0.5 mL of DGC and 0.5 ml reconstitution fluid. Test bottle contains 0.5 mL seed culture, 0.5 mL reconstitution fluid, and the antibiotic. The test is considered as complete when the PGC bottle flags positive.

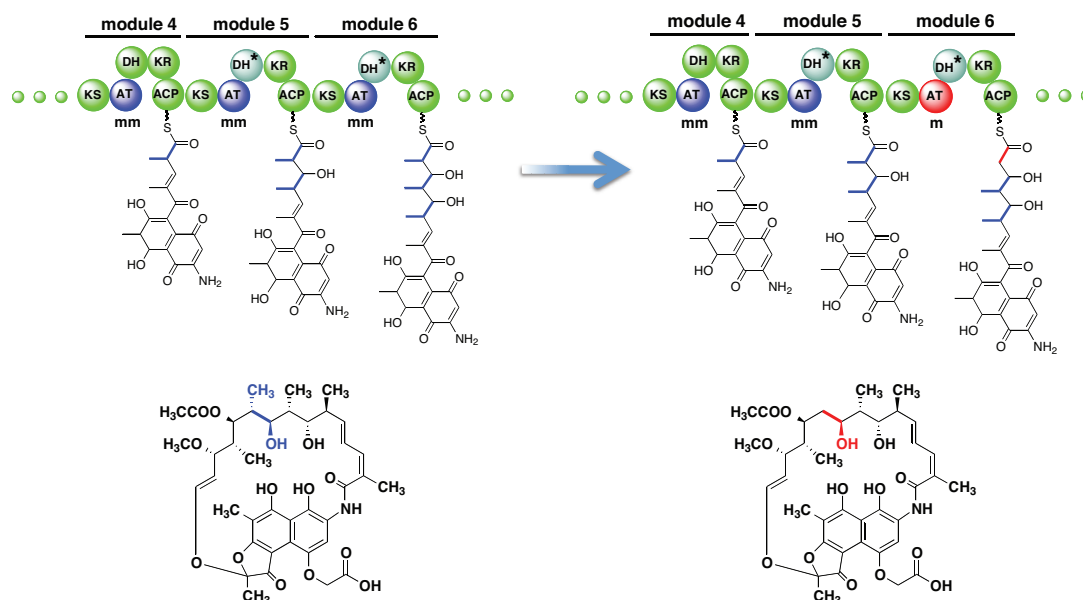
2.5 Supplemental Data

Table 2.S1. Bacterial strains and plasmids used in this study

Organism/ plasmid	Characteristics	Source or reference
<i>Amycolatopsis mediterranei</i> S699	Rifamycin B producer	Dr. G. Lancini
<i>E. coli</i> XL-1 Blue MR	<i>mcrA</i> 183 <i>mcrCB</i> -hsdSMR- <i>mrr</i> 173 <i>endA</i> 1 <i>supE</i> 44 <i>thi-recA</i> 1 <i>gyrA</i> 96 <i>relA</i> 1 <i>lac</i>	Invitrogen
<i>Staphylococcus aureus</i>	ATCC 12600	ATCC
<i>Escherichia coli</i>	ATCC 11775	ATCC
<i>M. smegmatis</i>	ATCC 14468	ATCC
<i>M. tuberculosis</i> OSDD 209	Rifampicin-sensitive <i>M. tuberculosis</i>	IGIB, India
<i>M. tuberculosis</i> OSDD 321	Rifampicin-resistant <i>M. tuberculosis</i> , which has S531L mutation in the RpoB protein	IGIB, India
<i>M. tuberculosis</i> OSDD 55	Rifampicin-resistant <i>M. tuberculosis</i> , which has H526T mutation in the RpoB protein	IGIB, India
<i>M. tuberculosis</i> OSDD 206	Rifampicin-resistant <i>M. tuberculosis</i> , which has S531L mutation in the RpoB protein	IGIB, India
<i>M. tuberculosis</i> H37Rv	Rifampicin-sensitive <i>M. tuberculosis</i>	IGIB, India
pUC 18 and pUC 19	~2.7 kb, Amp ^R for selection in <i>E. coli</i> , pBR322 origin of replication 58 bp multiple cloning site internal to a-fragment of β -galactosidase gene (<i>lacZ</i>)	Lab stock Fermentas
pIJ4026	~4.3 kb, Amp ^R for selection in <i>E. coli</i> and <i>ermE</i> for selection in <i>A. mediterranei</i> S699	M.J. Bibb, John Innes Institute
pMO2	~ 3.5 kb, Amp ^R for selection in <i>E. coli</i> , 0.85 kb <i>rapAT2</i> inserted at its <i>Sma</i> I site	Peter Leadley, University of Cambridge
pAT6A	~ 1.6 kb PCRII fragment cloned in pUC18 at its <i>Sma</i> I site	This study
pAT6B	~ 1.5 kb PCRII fragment cloned in pUC18 at its <i>Sma</i> I site	This study
pAT6C	~ 1.6 kb PCRII fragment cloned in pUC19 at its <i>Sma</i> I site	This study
pAT6D	0.85 kb <i>rapAT2</i> and ~1.5 kb PCRII fragment in pUC18	This study
pAT6E	~ 1.6 kb PCRII fragment, 0.85 kb <i>rapAT2</i> and ~1.5 kb PCRII fragment in pUC18	This study
pAT6F	~ 1.6 kb PCRII fragment, 0.85 kb <i>rapAT2</i> and ~1.5 kb PCRII fragment in pIJ4026	This study
pWE15	Amp ^R neo ^R 8.2 kb cosmid vector containing cos sites, ori, SV40 ori and an mvs with T3 and T7 promoters flanking BamHI as cloning site and EcoRI and NotI restriction sites at the either ends of mcs	Stratagene
pRIF 13	Amp ^R neo ^R , <i>rif</i> PKS insert from <i>A. mediterranei</i> S699 between EcoRI in pWE15 cosmid vector	This study
pRIF 21	Amp ^R neo ^R , <i>rif</i> PKS insert from <i>A. mediterranei</i> S699 between EcoRI in pWE15 cosmid vector	This study
pRIF 24	Amp ^R neo ^R , <i>rif</i> PKS insert from <i>A. mediterranei</i> S699 between EcoRI in pWE15 cosmid vector	This study

Table 2.S2. Primers used to amplify the flanking regions of *rifAT6*

Primer I	XbaI (41862-41892bp of <i>rifPKS</i> cluster) 5'-CTCTAGAAGGCGCTCGCCCGGCACCTGCGCGACGAAC-3'
Primer II	BalI (43513-43533bp of <i>rifPKS</i> cluster) 5'-CTGGCCAGGGAAGACCCAGACGAGCTTG-3'
Primer III	AvrII (45963- 44513bp of <i>rifPKS</i> cluster) 5'-CCCTAGGGCGGACCGGCCGGGTCGACCTGCCGA-3'
Primer IV	XbaI (45963-45989bp of <i>rifPKS</i> cluster) 5'-CTCTAGAGGTGCCAGCGATCCGGCGCCCGAGA-3'
AT6-EcoRI-F	EcoRI 5'-CCCAAGCTTCGGTGCCGTCGAACTGCT-3'
AT6-HindIII-R	HindIII 5'-CCGGAATTCAGGTGAACACCAGGCCGT-3'

**Figure 2.S1.** Domain replacement strategy for the formation of 24-desmethyrlrifamycin B.

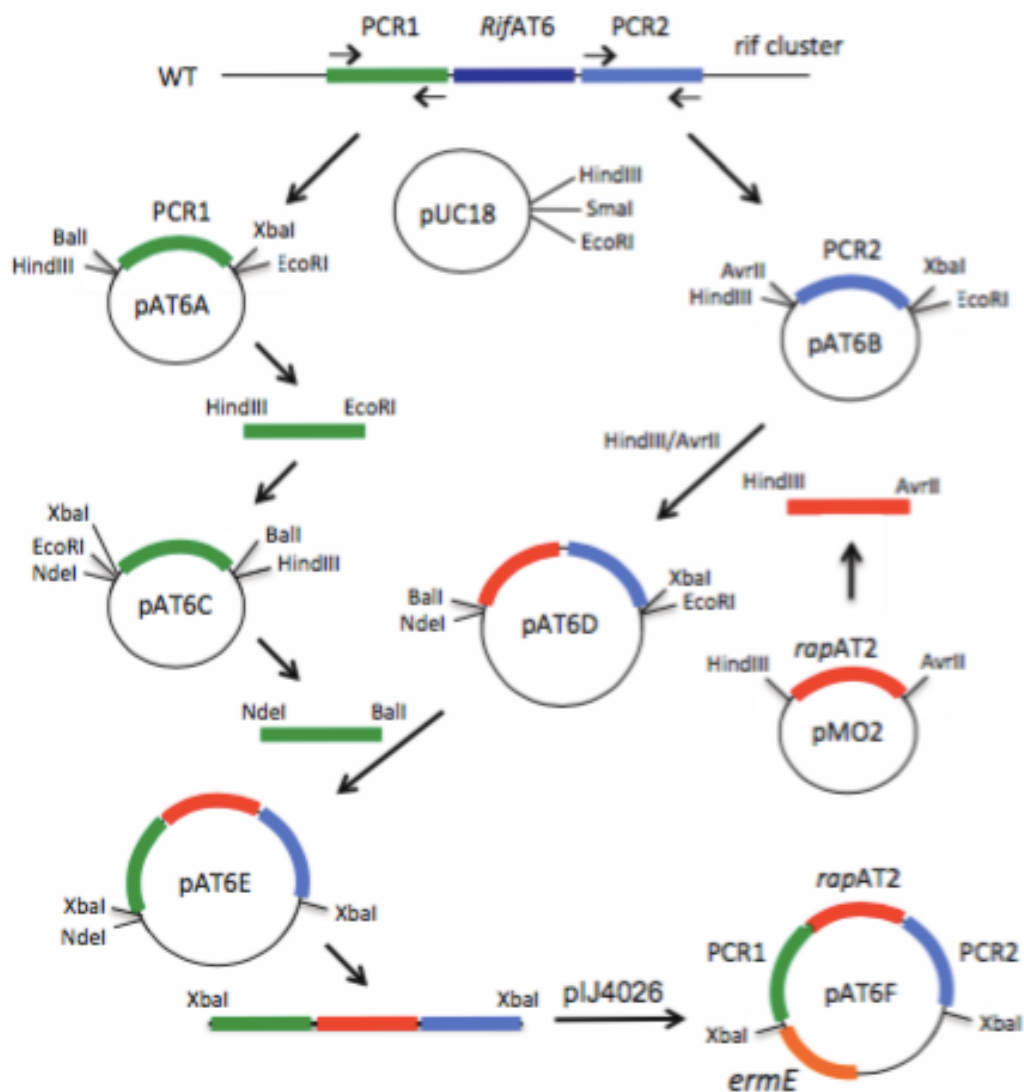


Figure 2.S2. Schematic overviews of plasmid pAT6F construction.

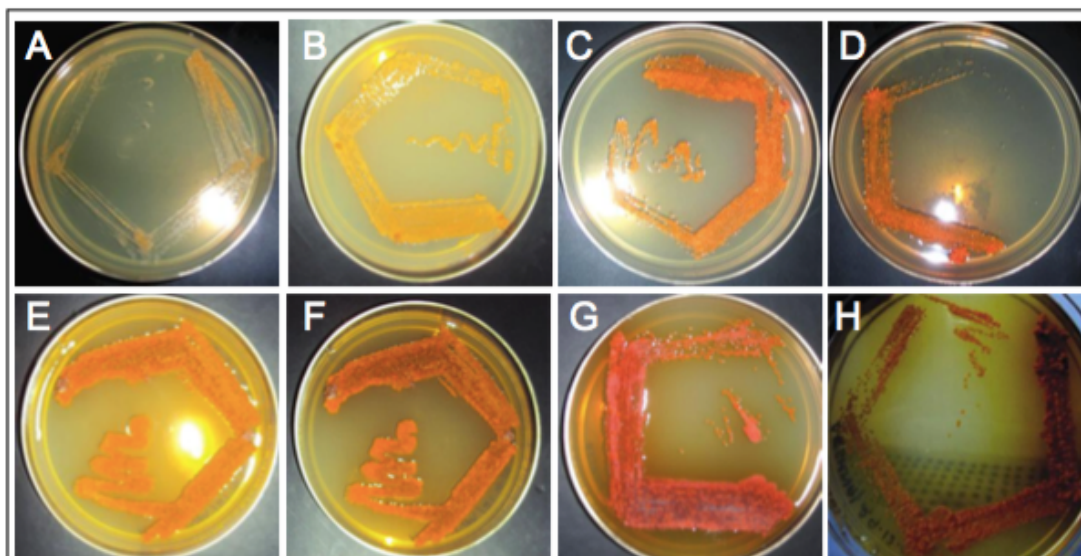


Figure 2.S3. Phenotypic appearances of single- and double-crossover mutants of *A. mediterranei* S699 on solid media. **A-D**, single cross-over clones. No pigmentation is seen around the culture of the single cross over clones, which indicates the absence of rifamycin production. **E-G**, double cross-over clones. Pigmentation is seen around the culture of double cross over clones, which indicates rifamycin production is resumed. **H**, wild-type of *A. mediterranei* S699.

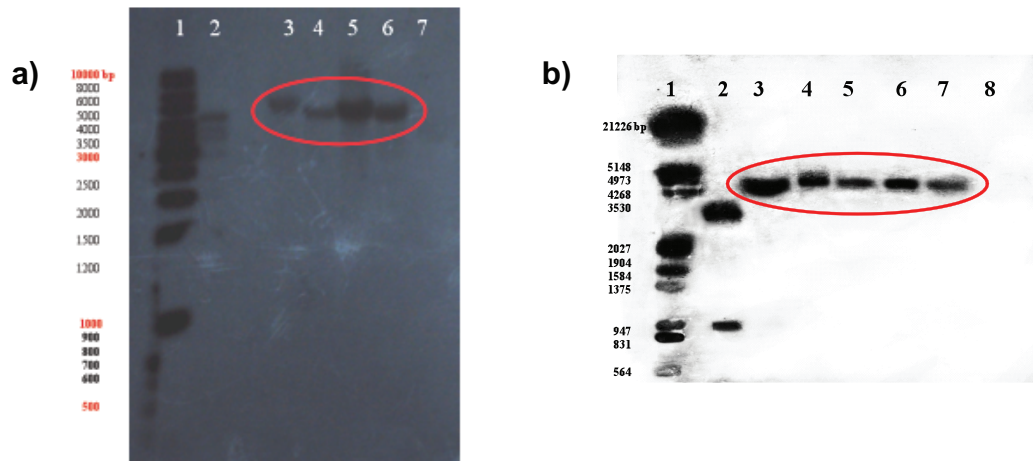


Figure 2.S4. Southern blot hybridization of single and double crossover clones. **a)** Blot of four single crossover clones' DNA digested with BamHI and probed with [α^{32} P]-labeled pIJ4026. Lane 1, DNA ladder; Lane 2, BamHI-digested pIJ4026 (positive control); Lane 3-6, BamHI-digested DNA of four S.C.O. clones; Lane 7, BamHI-digested chromosomal DNA of *A. mediterranei* S699. Signals were obtained in all four S.C.O. clones but no signal was seen in the BamHI-digested chromosomal DNA of *A. mediterranei* S699 (negative control); **b)** Double crossover clones digested with BamHI and probed with DIG-labeled *rapAT2*. Lane 1, Marker lambda DNA digested with EcoRI/HindIII, Lane 2, pMO2 digested with EcoRI and HindIII (positive control), Lane 3, S.C.O., Lane 4-7, D.C.O., Lane 8, chromosomal DNA of *A. mediterranei* S699. Positive signals are obtained in S.C.O. and all the D.C.O. clones (encircled in red). No signal is seen for *A. mediterranei* S699 (negative control).

CAGGCGCTCGCCCGGACCTGCGCGACGAACTCGGTGGTGCGGCCAGACGCCGGTGACC
 ACAGCGGCCGCGAAGGCCGACCTCGACGAGCCGATCGCCATCGTCGGGATGGCGTGCCGC
 TTGCCGGGCGGGTCGCCGGGCCGAGGACCTCTGGCGGCTGGTCGCCGAGGGCCGGGAC
 GCGGTGTCTGAGCTTCCCGACCGACCGCGGCTGGGACACCGACAGCCTGTACGACCCCGAT
 CCGGCCCGCCCGGGCAAGACCTACACCCGGCACGGCGGCTTCTGCACGAAGCCGGGCTC
 TTGCGACGCGGGCTTCTTCGGGATCTGCCACGCGAGGCGCTGCCATGGACCCGACGACG
 CGGCTGCTGCTGGAGGCTCTCGGGAGGCCATGGAAGACGCCGGGGTGACCCACTTTGCG
 CTGAAGGGCAACGAGCTCGGCGTGTTCACCGGCATGTTCCGGCAGGGTTACGTCGCTCCC
 GGGGACAGCGTGTCTACGCCGGAGCTGGAGGGTTTCGCGGGGACGGGCGGGTCTGTCGAGT
 GTCGCGTCCGGCCGCGTGTCTGACGTGTTCCGGTTCGAAGGCCGTCGCGCCGCGTACGATCGAC
 TCGGCGTGTCTGCTCTGCTGGTTCGCGATGCACCTCGCCGCGCAGTCTGCTGCGGCAGGGC
 GAGTGTCTGATGGCTTGGCCGGCGGCGCGACGGTATGGCGAACCCCGCGCATTCGTG
 GAGTTCTCGCGGACGCGGGGCTCGCCGTCGACGGTCTGCTGAAGGCCGTCGCGCCGCGCG
 GCCGACGGCACCGGCTGGGCGGAGGGCGTGGTGTGGTTCATCTCGAGCGGCTGTGGTG
 GCGCGGAAACCGGCCACCGGATCTGGCCGTGCTGCGGGCACGCGGGTCAACCAAGGAC
 GGCGCTCGAACGGCTGACCGCGCCGAACGGGCGGCTGCGACGAGCGGGTGATCCGCCGG
 GCGCTGGTGAGCGCCGGGCTGGCACCGTCCGATGTGGACGTCTGAGGCGCACGGGCACCG
 GGGACACCGCTGGGTGACCCGATCGAGGCGCAAGCTCTGCTGGCTACCTACGGCAAGGAC
 CGCGAGTCTGCGCTGTGGCTCGCTGAAAGTGAACATCGGCCACGCGCAGGCGCGC
 GCGGGGGTCCGCGGCGTCAAGATGGTCCAGGCGCTCCGGCACGAAGTCTGCGCGCG
 ACCTGTCAGCTCGACCGGCTACCCCGAGGTCGACTGGTCCGGCGGTGCCGTGCAACTG
 CTGACGGAAGCCCGCGAGTGGCCGCGCAACGGGCGCCGCGCGCGGGGCTCTCCGCG
 TTGCGCGTCAGCGGCGACGACGCGCACCTGATCTGGAGGAGGCGCCCGCGGAAGAGCCG
 GTGCCACACCCGAGGTTCCCTGGTCCCGGTGCTGGTCTCCGCGCGGAGCAGGGCGTCC
 CTGCGCGGTGAGCCCGTCTGCTCGCCGATTCGTGGCGGGTGACGCGTCTTGGCCGGT
 GTGGCCCGGGGCTGGTGACGAACCGGGCGCGCTGACCGAGCGCGCGGTGATGGTGGT
 GGCTCTCGCGAAGAACCGTGAACCTGGAAGCGCTGCGCCGCGCGCAAGACCCGCGCC
 GCGGTGGTACCGGCGCGGGGTTCCGCGGCAAGCTGCTGGGTCTTCCC
 ACCACTCGACACTCAGCGGCTTCACTGACAGGTGAGCCAGGGCACCGACAGCGGCTGCG
 CCTACTGGTACCGGTGACGATCGCGATGCCATCGACAGGCGGGCCAGTGACCGGTGCG
 CACCCAGCTCGACGAACACCGCATCTCTGAACGAGGCCACCTGCTCGCCGAACCGGACCG
 TGTCGCGGACCTGCCGACCCAGTACTCAGCGGTGATCAGCTGATCACCAGCGGCCATGG
 CGACCTGCGGCGTCCGGTAGGTCAGGCCCTTCAAGCAGCGCCCGGAACCTCTCCAGCATCG
 GTTCATACGGGCGGAATGGAACGCGTGAAGTGGTCCGACGCGCGTCCACTTCCCAGCG
 CCTCCGCGGCTGACGACGCGCGGCTCATCACCAGGAGAGAACCCGACGACGCGGCCGT
 TGACCGCGGCGATCTCCACACCTCACCAGCACGGCCGAGCCTCATCTCCGAGACCG
 GGACAGCGACCATCACCCACCCGACGACGAGCCTGCATCAGACGAGCCCGCGCGACA
 CCAAGTGCAGGCATCTCCAACGACCCACACCCGGAGAGCTATCCGGCGGCGAGCTCAC
 CGACAGAGTGACCGACCCGACCGCATCCGCGGTACACCCACGATTCCAGCAACCCGAACA
 GAGCCACCTGCAAGCGAACAGGGCGGGCTGGGCATACCCGGTCTCATTACATCGAGAT
 CGGGCACATCCAGCAGATCCACACCTGCTGATGGATCCGCGCGAAGACGGGGAACCGCG
 CGGCCAGTTCTCACCATACCCAGCAGCTGCGACCTGGCCAGCCGGCTGGGCATACCC
 GGTCTCATTACATCGAGATCGGGCACATCCAGCAGATCCACACCTGCTGATGGATCCG
 CGCGAAGACGGGGAACCGCGCGCAAGTTCTCACCATACCCAGCAGCTGCGGACCCG
 TGGCCAGGGAATACCGAG
 GCGGACCGGCGGGTGCACCTGCCGAAGTACGCTTCGACACCGGCACTACTGGCTGCG
 GCCCGCGAGTCCGCGACCGACGCGGCTTCGCTGGGCCAGGGGGCGGCGGACACCCGT
 GCTGGGCGCGTCTGTCGAGCTGCCGAGTCCGACGGCTGCTGGTTACCTCGCGGCTGTC
 CGTGCGGACGACCCGTGGCTGGCCGACACGCGGTGGTGGCGTGGTATCTCCCGG
 CTCGCGGCTGGCCGAATGGCCGTCCGGGCGGCGACGAAGCCGGGTGACCGGCCCTCGA
 CGAGCTGATTATCGAAGCTCCGCTGGTCTGTCGCCGCCAAGGCGGGTCCGCTCCAGGT
 CGCGTTGAGCGGCGGACGAGACCGGCTCGCGACGGTGGACCTTACTCCAGCGCGA
 CGCGGGCGCGGGGACGTGGACGCGGCGACGCCACCGGCGTCCGCTGACGCGCCCGCTCA
 GGAACCCGAGTTCCGACTTCCAGCCTGGCCGCCGCGGATGCCGAGCGGATCGACGTGCA
 GACCTTACACCGACCTGGCCGAGCGTGGTTACGGCTACGGGCGGCGTTCAGGGGCT
 GCAAGCGGTGTGGCGGCGGACGCGGATGTCTTCCGCGAGGTGCGCCTGCCGAGGACCT
 GCGCAAGGACGCGGGCGGTTCCGCGTCCACCGCGGTGACACACTGACCGACCGCGCGG
 CGCCACGCGCGTGGGCGGCGACGACCGCGGTGAGCCGCTGCTGGCGTTCGCGTGAACGG
 CCTGGTCTGACGCGCGCGGCGGCTCGGCCCTGCGGGTCCGCGCGAGCGGCGGCGG
 GGACACGCTGTCCGTGGCAGCGCGGACGAAACCGGCGGCTTGGTCTGACCATGGAATC
 GCTGGTCTCCCGGCGGTTTCGGCCGAGCAGCTCGGCGCGCGGCGGCGGCGGCGGCGG
 CGCGATGTTCCGCGTCTGACTGGACCGAGTGCCTGCCGTGCCCGCGCGGAATGCCGCG
 GTGGTGCGGATCGACACCGCGGACGACGTGCGGCGCTTGGCGGAGAAGGCGGACGAC
 ACCGGTGGTGGTCTGGGAAGCCGCGGGGGAGACCGGCCCTGGCCGTGAGTTCCCGGGT
 GCTCGAGATCATGACGCGCTGGCTGGCGCGCGCGCGCTTCGAGGAGGCCCGGCTGGTCTG
 GACGACCCGCGCGCGGTACCCGCGCGGTGACACACACTGACCGACCGCGCGCGGCG
 CGCGGTGGGGCGCTGGTCCGCTCCGCGCAGGCGGAACACCGGACCGGGTCTGCTGCTGCT
 GGACACCGACGCGGAATTCGCTGGGCGCGGTGCTGGCCTCCGCTGAGCGCGAGCTCGC
 GGTGCGCGGAACGAGCTTCTGCTGCCCGGCTGGCCGCGGCGGCTCTCGGACGCG
 GCCTCTGCGTTGACCGCGGACCGGACCGTGGTCTCGGCGCGCGGATCGCTGGGAC
 CT

PCR I (41862-43533 bp)

AT2

PCR II (44488-45989 bp)

Figure 2.S5. Nucleotide sequence of PCR1/rapAT2/PCR2 of pAT6F.

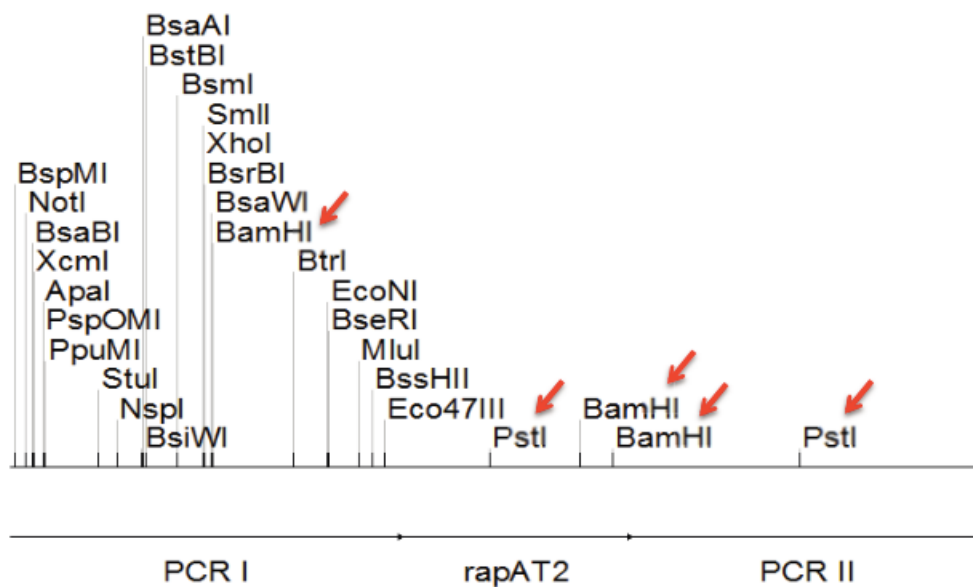


Figure 2.S6. Restriction map of hybrid DNA obtained from nucleotide sequences (Figure 2.S5) formed in the double cross over clones. Red arrows indicate the restriction sites for BamHI and PstI that were used.

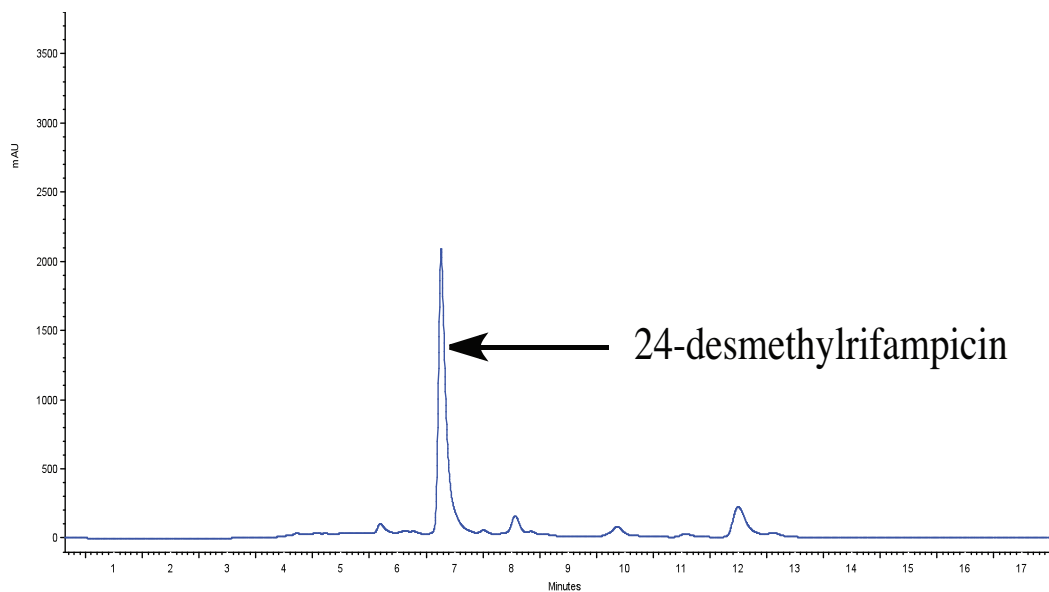


Figure 2.S7. Purification of 24-desmethyrrifampicin using HPLC. Peaks were detected at 254 nm.

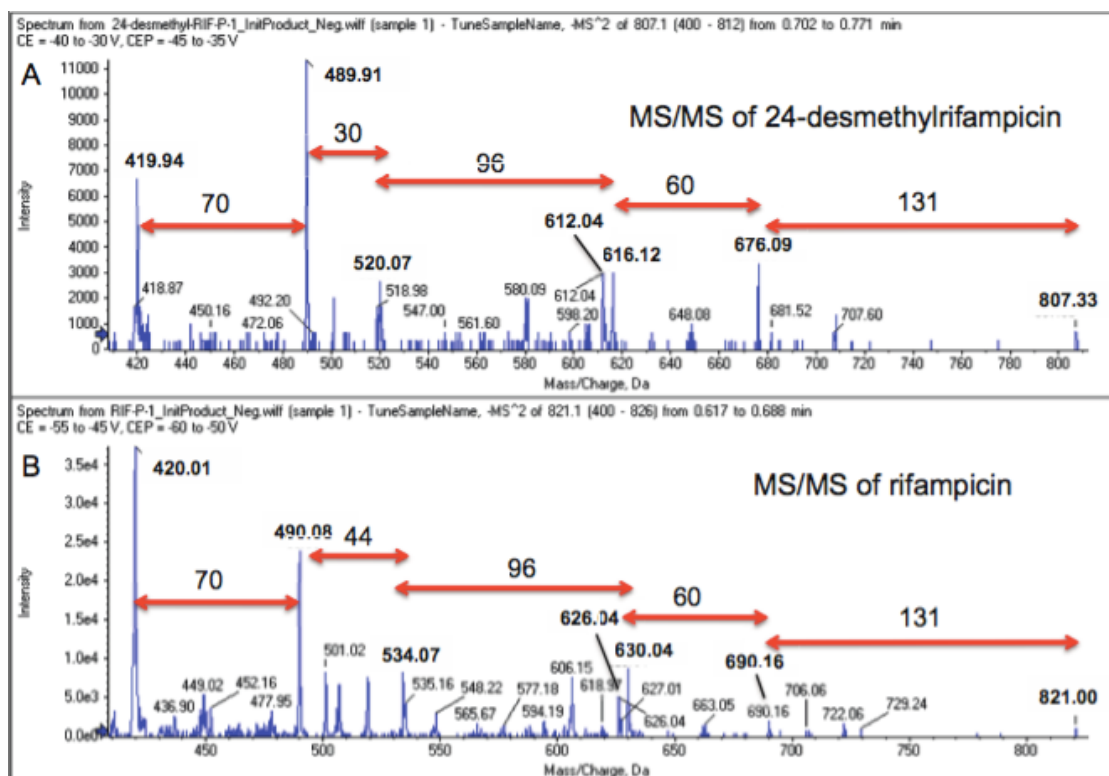


Figure 2.S8. Comparative MS/MS Analyses of rifampicin and 24-desmethylrifampicin. **A)** 24-desmethylrifampicin, **B)** rifampicin.

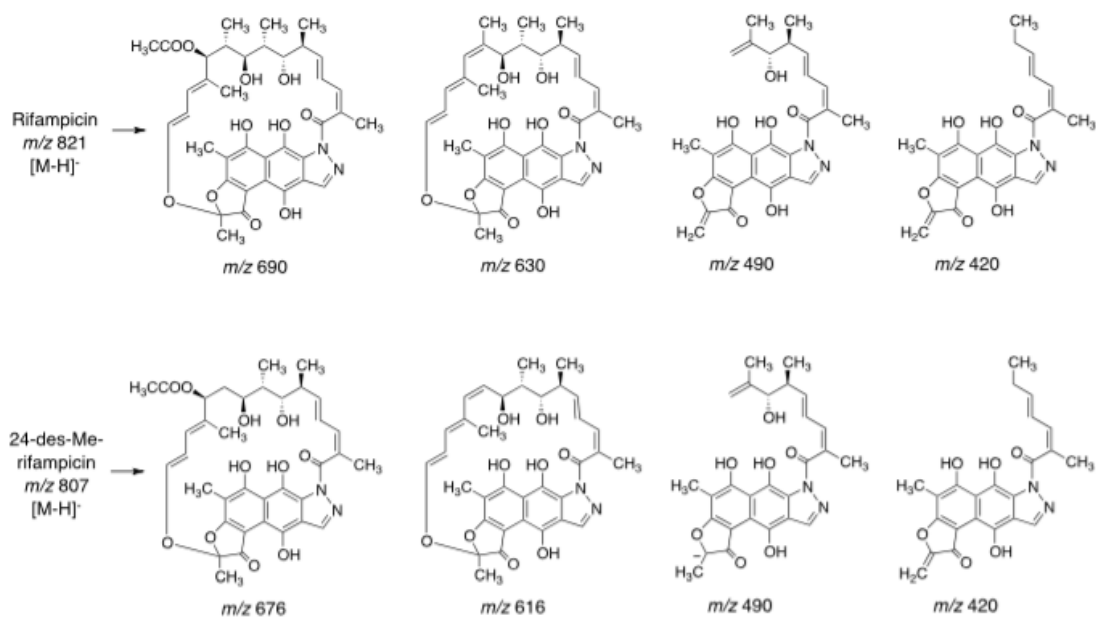


Figure 2.S9. Characteristic MS fragments of rifampicin and 24-desmethylrifampicin in ESI negative ion mode.

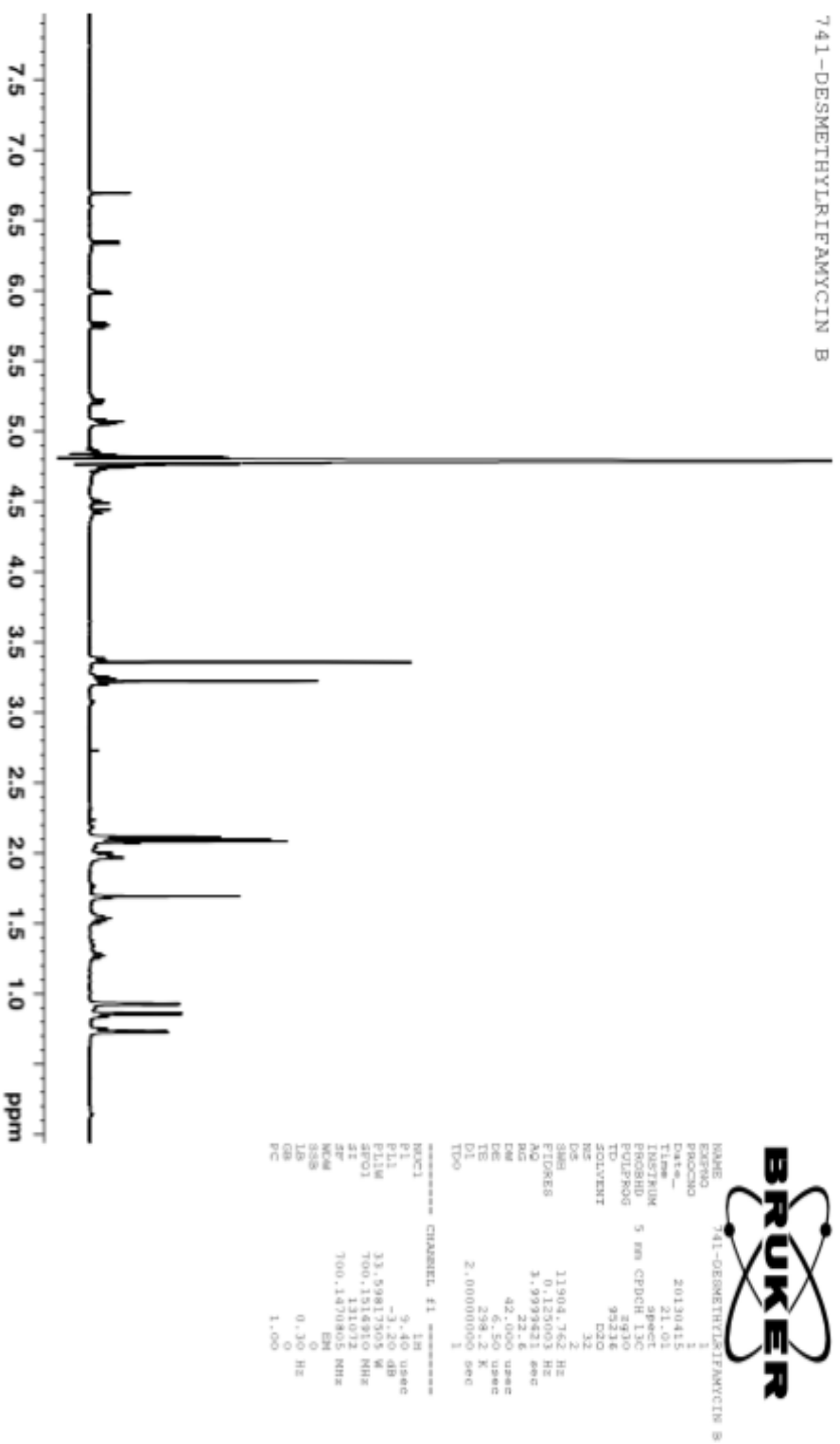


Figure 2.S10. ^1H NMR spectrum of 24-desmethytrifamycin B.

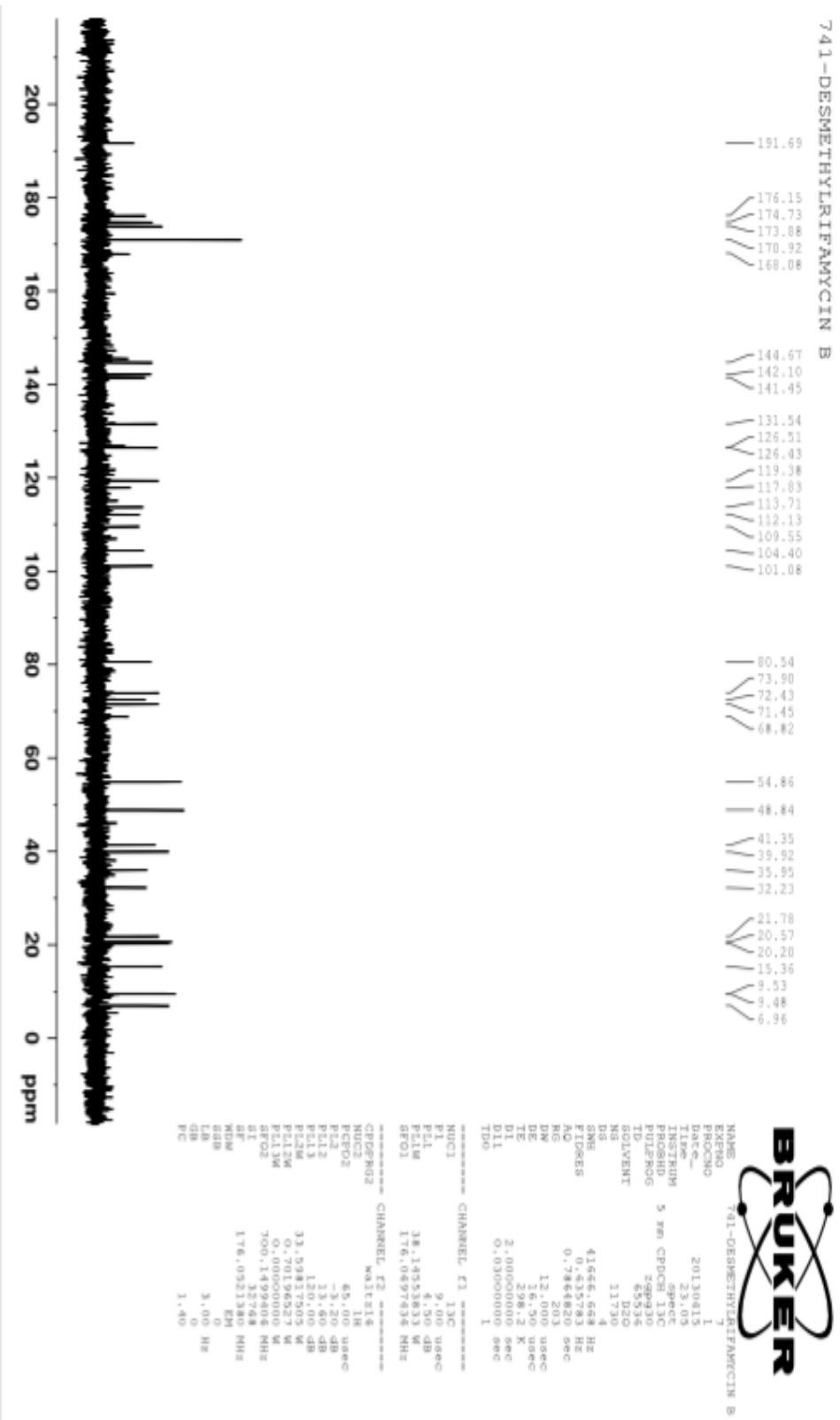


Figure 2.S11. ^{13}C NMR spectrum of 24-desmethyirifamycin B.

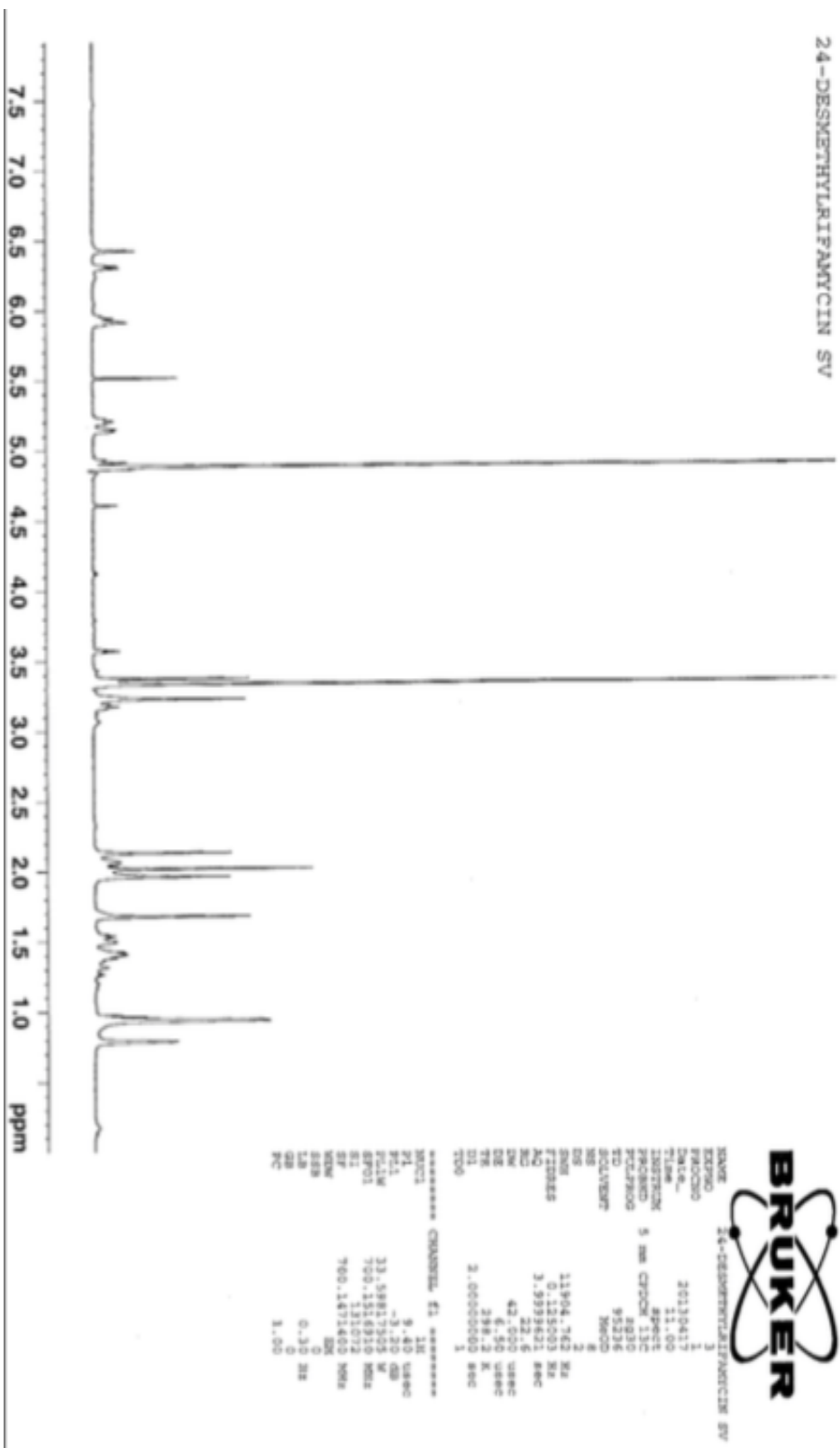


Figure 2.S12. ^1H NMR spectrum of 24-desmethytrifamycin SV.

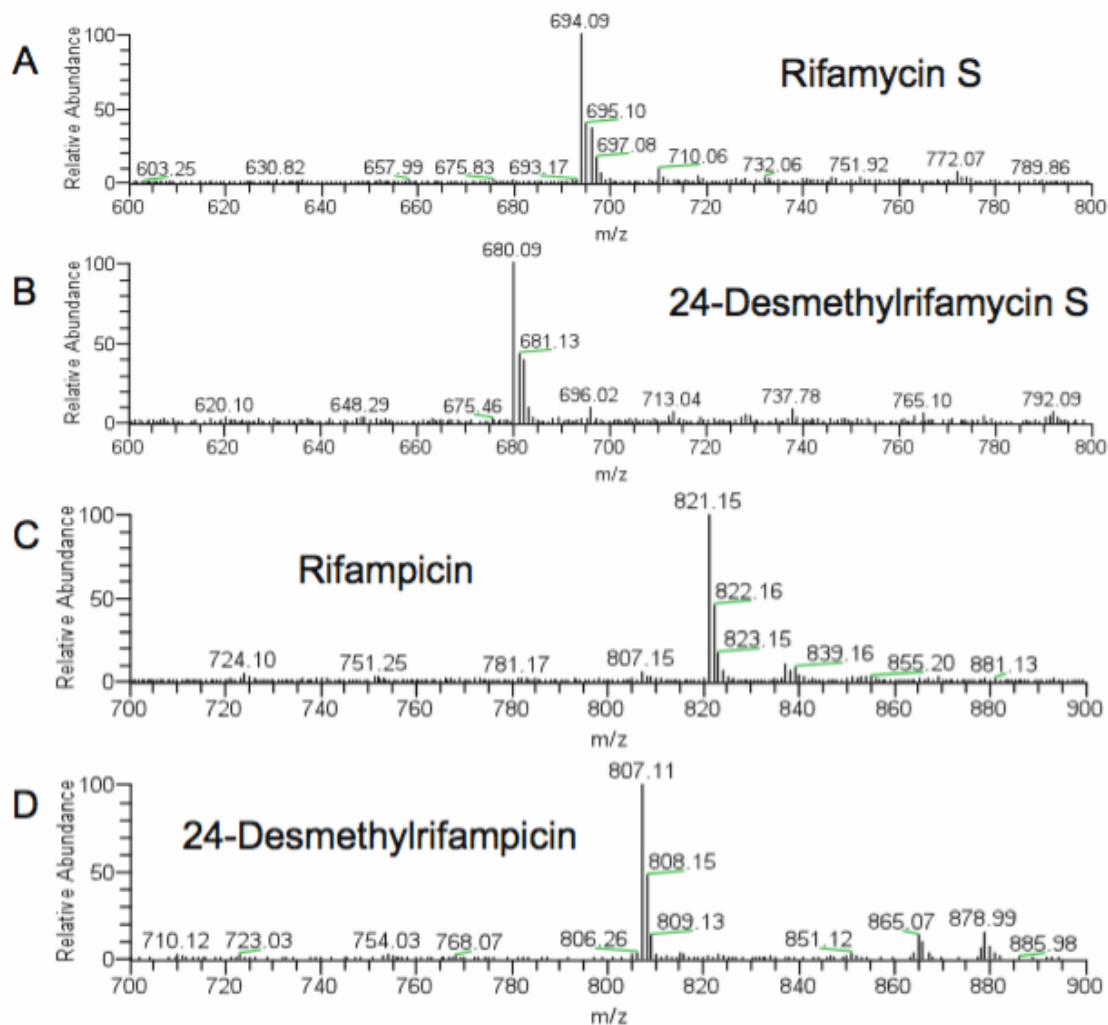


Figure 2.S13. (-)-ESI-MS spectra of rifamycin S (A), 24-desmethylrifamycin S (B), rifampicin (C), and 24-desmethylrifampicin (D).

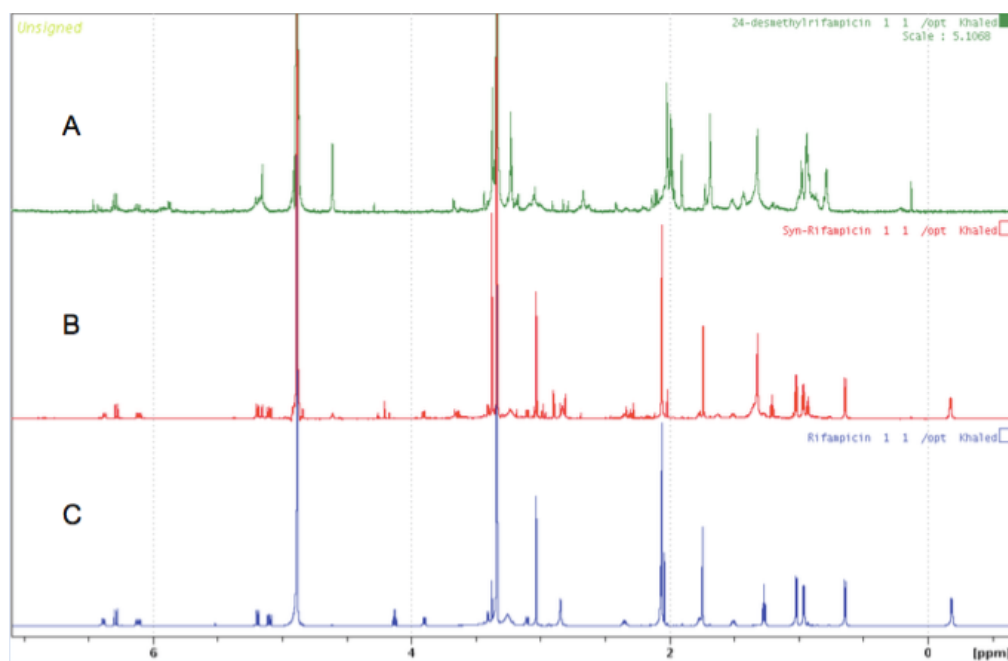


Figure 2.S14. ^1H NMR of 24-desmethylrifampicin (**A**), chemically synthesized rifampicin (**B**), and commercially available rifampicin (**C**).

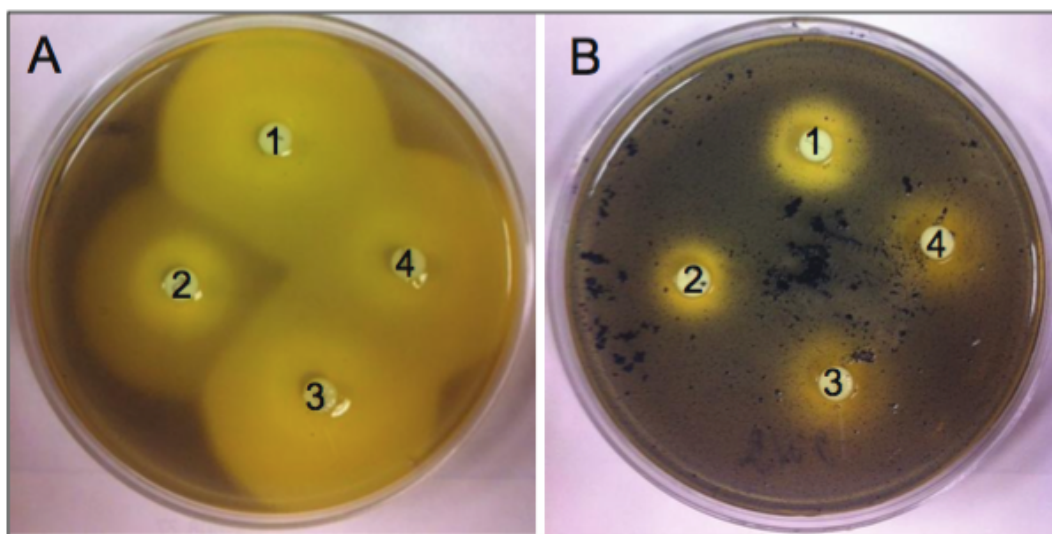


Figure 2.S15. Agar diffusion assay of rifamycin S, rifampicin, 24-desmethylrifamycin S, and 24-desmethylrifampicin against *Staphylococcus aureus* (**A**) and *Mycobacterium smegmatis* (**B**). 1, rifamycin S, 2, rifampicin, 3, 24-desmethylrifamycin S, and 4, 24-desmethylrifampicin.

2.6 References

Admiraal, S. J., C. Khosla and C. T. Walsh (2003). "A Switch for the transfer of substrate between nonribosomal peptide and polyketide modules of the rifamycin synthetase assembly line." J Am Chem Soc **125**(45): 13664-13665.

Admiraal, S. J., C. T. Walsh and C. Khosla (2001). "The loading module of rifamycin synthetase is an adenylation-thiolation didomain with substrate tolerance for substituted benzoates." Biochemistry **40**(20): 6116-6123.

Aristoff, P. A., G. A. Garcia, P. D. Kirchhoff and H. D. Hollis Showalter (2010). "Rifamycins--obstacles and opportunities." Tuberculosis (Edinb) **90**(2): 94-118.

Artsimovitch, I., M. N. Vassilyeva, D. Svetlov, V. Svetlov, A. Perederina, N. Igarashi, N. Matsugaki, S. Wakatsuki, T. H. Tahirov and D. G. Vassilyev (2005). "Allosteric modulation of the RNA polymerase catalytic reaction is an essential component of transcription control by rifamycins." Cell **122**(3): 351-363.

August, P. R., L. Tang, Y. J. Yoon, S. Ning, R. Muller, T. W. Yu, M. Taylor, D. Hoffmann, C. G. Kim, X. Zhang, C. R. Hutchinson and H. G. Floss (1998). "Biosynthesis of the ansamycin antibiotic rifamycin: deductions from the molecular analysis of the rif biosynthetic gene cluster of *Ammycolatopsis mediterranei* S699." Chem Biol **5**(2): 69-79.

Campbell, E. A., N. Korzheva, A. Mustaev, K. Murakami, S. Nair, A. Goldfarb and S. A. Darst (2001). "Structural mechanism for rifampicin inhibition of bacterial rna polymerase." Cell **104**(6): 901-912.

Crump, J. A., A. B. Morrissey, H. O. Ramadhani, B. N. Njau, V. P. Maro and L. B. Reller (2011). "Controlled comparison of BacT/Alert MB system, manual Myco/F lytic procedure, and isolator 10 system for diagnosis of *Mycobacterium tuberculosis* Bacteremia." J Clin Microbiol **49**(8): 3054-3057.

Floss, H. G. (2006). "Combinatorial biosynthesis--potential and problems." J Biotechnol **124**(1): 242-257.

Gaisser, S., G. A. Bohm, J. Cortes and P. F. Leadlay (1997). "Analysis of seven genes from the eryAI-eryK region of the erythromycin biosynthetic gene cluster in *Saccharopolyspora erythraea*." Mol Gen Genet **256**(3): 239-251.

Hartmann, G. J., P. Heinrich, M. C. Kollenda, B. Skrobranek, M. Tropschug and W. W. (1985). "Molecular mechanism of action of the antibiotic rifampicin." Angew Chem Int Ed Engl **24**: 1009-1074.

Jacobsen, J. R., A. T. Keatinge-Clay, D. E. Cane and C. Khosla (1998). "Precursor-directed biosynthesis of 12-ethyl erythromycin." Bioorg Med Chem **6**(8): 1171-1177.

Kaur, H., J. Cortes, P. Leadlay and R. Lal (2001). "Cloning and partial characterization of the putative rifamycin biosynthetic gene cluster from the actinomycete *Ammycolatopsis mediterranei* DSM 46095." Microbiol Res **156**(3): 239-246.

Khanna, M., M. Dua and R. Lal (1998). "Selection of suitable marker genes for the development of cloning vectors and electroporation in different strains of *Amycolatopsis mediterranei*." Microbiol Res **153**(3): 205-211.

Khosla, C., S. Kapur and D. E. Cane (2009). "Revisiting the modularity of modular polyketide synthases." Curr Opin Chem Biol **13**(2): 135-143.

Kieser, T., M. J. Bibb, M. J. Buttner, K. F. Chater and D. A. Hopwood (2000). Practical Streptomyces Genetics. Norwich, England, The John Innes Foundation.

Kim, C. G., T. W. Yu, C. B. Fryhle, S. Handa and H. G. Floss (1998). "3-Amino-5-hydroxybenzoic acid synthase, the terminal enzyme in the formation of the precursor of mC7N units in rifamycin and related antibiotics." J Biol Chem **273**(11): 6030-6040.

Lal, R. (1999). Cloning vector and the process for the preparation thereof. US00598560A. U. S. Patent. **US00598560A**.

Lal, R., M. Khanna, H. Kaur, N. Srivastava, K. K. Tripathi and S. Lal (1995). "Rifamycins: strain improvement program." Crit Rev Microbiol **21**(1): 19-30.

Lal, R., R. Khanna, N. Dhingra, M. Khanna and S. Lal (1998). "Development of an improved cloning vector and transformation system in *Amycolatopsis mediterranei* (*Nocardia mediterranei*)." J Antibiot (Tokyo) **51**(2): 161-169.

Lal, R., R. Khanna, H. Kaur, M. Khanna, N. Dhingra, S. Lal, K. H. Gartemann, R. Eichenlaub and P. K. Ghosh (1996). "Engineering antibiotic producers to overcome the limitations of classical strain improvement programs." Crit Rev Microbiol **22**(4): 201-255.

Lal, R., R. Kumari, H. Kaur, R. Khanna, N. Dhingra and D. Tuteja (2000). "Regulation and manipulation of the gene clusters encoding type-I PKSs." Trends Biotechnol **18**(6): 264-274.

Lal, R. and S. Lal (1994). "Recent trends in rifamycin research." Bioessays **16**(3): 211-216.

Lal, R., S. Lal, E. Grund and R. Eichenlaub (1991). "Construction of a hybrid plasmid capable of replication in *Amycolatopsis mediterranei*." Appl Environ Microbiol **57**(3): 665-671.

Lau, J., H. Fu, D. E. Cane and C. Khosla (1999). "Dissecting the role of acyltransferase domains of modular polyketide synthases in the choice and stereochemical fate of extender units." Biochemistry **38**(5): 1643-1651.

Marsili, L. and C. R. Pasqualucci (1984). Process for the preparation of 3-iminomethyl derivatives of rifamycin SV. U. S. Patent. Italy, Gruppo Lepetit S.p.A. **Re. 31,587**.

Molodtsov, V., I. N. Nawarathne, N. T. Scharf, P. D. Kirchhoff, H. D. Showalter, G. A. Garcia and K. S. Murakami (2013). "X-ray crystal structures of the *Escherichia coli* RNA polymerase in complex with benzoxazinorifamycins." J Med Chem **56**(11): 4758-4763.

Oliynyk, M., M. J. Brown, J. Cortes, J. Staunton and P. F. Leadlay (1996). "A hybrid modular polyketide synthase obtained by domain swapping." Chem Biol **3**(10): 833-839.

Prasad, B. and S. Singh (2009). "In vitro and in vivo investigation of metabolic fate of rifampicin using an optimized sample preparation approach and modern tools of liquid chromatography-mass spectrometry." J Pharm Biomed Anal **50**(3): 475-490.

Ranganathan, A., M. Timoney, M. Bycroft, J. Cortes, I. P. Thomas, B. Wilkinson, L. Kellenberger, U. Hanefeld, I. S. Galloway, J. Staunton and P. F. Leadlay (1999). "Knowledge-based design of bimodular and trimodular polyketide synthases based on domain and module swaps: a route to simple statin analogues." Chem Biol **6**(10): 731-741.

Ruan, X., A. Pereda, D. L. Stassi, D. Zeidner, R. G. Summers, M. Jackson, A. Shivakumar, S. Kakavas, M. J. Staver, S. Donadio and L. Katz (1997). "Acyltransferase domain substitutions in erythromycin polyketide synthase yield novel erythromycin derivatives." J Bacteriol **179**(20): 6416-6425.

Schupp, T., C. Toupet, N. Engel and S. Goff (1998). "Cloning and sequence analysis of the putative rifamycin polyketide synthase gene cluster from *Amycolatopsis mediterranei*." FEMS Microbiol Lett **159**(2): 201-207.

Schwecke, T., J. F. Aparicio, I. Molnar, A. Konig, L. E. Khaw, S. F. Haydock, M. Oliynyk, P. Caffrey, J. Cortes, J. B. Lester and et al. (1995). "The biosynthetic gene cluster for the polyketide immunosuppressant rapamycin." Proc Natl Acad Sci U S A **92**(17): 7839-7843.

Sheldrick, G. M. (1998). Bruker/Siemens Area Detector Absorption Correction Program. Madison, WI, Bruker AXS.

SHELXTL-6.10 "Program for Structure Solution, Refinement and Presentation." BRUKER AXS Inc., 5465 East Cheryl Parkway, Madison, WI 53711-5373 USA.

Stassi, D. L., S. J. Kakavas, K. A. Reynolds, G. Gunawardana, S. Swanson, D. Zeidner, M. Jackson, H. Liu, A. Buko and L. Katz (1998). "Ethyl-substituted erythromycin derivatives produced by directed metabolic engineering." Proc Natl Acad Sci U S A **95**(13): 7305-7309.

Staunton, J. and K. J. Weissman (2001). "Polyketide biosynthesis: a millennium review." Nat Prod Rep **18**(4): 380-416.

Stratmann, A., C. Toupet, W. Schilling, R. Traber, L. Oberer and T. Schupp (1999). "Intermediates of rifamycin polyketide synthase produced by an *Amycolatopsis mediterranei* mutant with inactivated *rifF* gene." Microbiology **145 (Pt 12)**: 3365-3375.

Tuteja, D., M. Dua, R. Khanna, N. Dhingra, M. Khanna, H. Kaur, D. M. Saxena and R. Lal (2000). "The importance of homologous recombination in the generation of large deletions in hybrid plasmids in *Amycolatopsis mediterranei*." Plasmid **43**(1): 1-11.

Verma, M., J. Kaur, M. Kumar, K. Kumari, A. Saxena, S. Anand, A. Nigam, V. Ravi, S. Raghuvanshi, P. Khurana, A. K. Tyagi, J. P. Khurana and R. Lal (2011). "Whole genome sequence of the rifamycin B-producing strain *Amycolatopsis mediterranei* S699." J Bacteriol **193**(19): 5562-5563.

Williams, D. L., L. Spring, L. Collins, L. P. Miller, L. B. Heifets, P. R. Gangadharam and T. P. Gillis (1998). "Contribution of *rpoB* mutations to

development of rifamycin cross-resistance in *Mycobacterium tuberculosis*." Antimicrob Agents Chemother **42**(7): 1853-1857.

Wilson, M. C., T. A. Gulder, T. Mahmud and B. S. Moore (2010). "Shared biosynthesis of the saliniketals and rifamycins in *Salinispora arenicola* is controlled by the sare1259-encoded cytochrome P450." J Am Chem Soc **132**(36): 12757-12765.

Xu, J., T. Mahmud and H. G. Floss (2003). "Isolation and characterization of 27-O-demethylrifamycin SV methyltransferase provides new insights into the post-PKS modification steps during the biosynthesis of the antitubercular drug rifamycin B by *Amycolatopsis mediterranei* S699." Arch Biochem Biophys **411**(2): 277-288.

Xu, J., E. Wan, C. J. Kim, H. G. Floss and T. Mahmud (2005). "Identification of Tailoring Genes Involved in the Modification of the Polyketide Backbone of Rifamycin B by *Amycolatopsis mediterranei* S699." Microbiology **151**: 2515-2528.

Xue, Q., G. Ashley, C. R. Hutchinson and D. V. Santi (1999). "A multiplasmid approach to preparing large libraries of polyketides." Proc Natl Acad Sci U S A **96**(21): 11740-11745.

Yu, T. W., Y. Shen, Y. Doi-Katayama, L. Tang, C. Park, B. S. Moore, C. Richard Hutchinson and H. G. Floss (1999). "Direct evidence that the rifamycin polyketide synthase assembles polyketide chains processively." Proc Natl Acad Sci U S A **96**(16): 9051-9056.

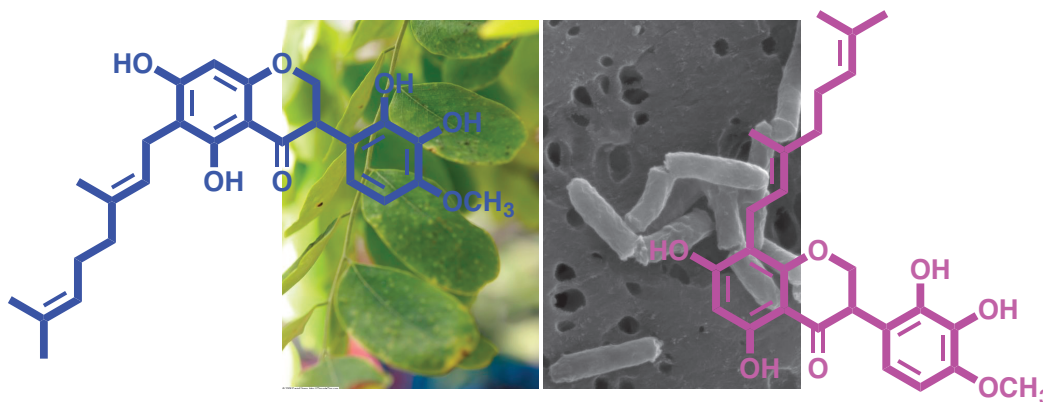
CHAPTER III

Total Synthesis of (\pm)-Isoperbergins and Correction of the Chemical Structure of Perbergin

Khaled H. Almabruk, Jeff H. Chang, and Taifo Mahmud

3.1 Abstract

Based on its reported chemical structure, perbergin, a *Rhodococcus fascians* virulence quencher from the bark of *Dalbergia perrillei*, and its isomer were synthesized in nine steps with a 13.5% yield. However, the NMR spectra of the synthetic products were inconsistent with those reported in the literature. Reevaluation of the 1D and 2D NMR spectra of the natural perbergin revealed that the geranyl moiety of perbergin is located at C-6 and has an *E*-configuration, instead of the reported C-8 geranylation with a *Z*-configuration. Interestingly, the synthetic isoperbergins demonstrated good antibacterial activity against *R. fascians*, *Mycobacterium smegmatis*, and *Staphylococcus aureus*, but not against the Gram-negative bacteria *Pseudomonas aeruginosa* and *Escherichia coli*.



Perbergin is a prenylated isoflavanone isolated from the bark of the Madagascar legume *Dalbergia pervillei* (Figure 3.1) (Rajaonson et al. 2011). This compound was identified based on its ability to protect the plant from deformations caused by the phytopathogenic actinomycete *Rhodococcus fascians*. *R. fascians* induces leaf galls and/or other deformations on a wide range of plants, resulting in significant economic losses in the nursery industry. Initially, the pathogen colonizes plants epiphytically. During infection of susceptible plant hosts, it is hypothesized that a plant metabolite triggers the bacteria to produce an autoregulatory compound that initiates a signal transduction pathway leading to the production of virulence factors (Stes et al. 2011). At a low concentration (0.2 μM), perbergin was found to function as a virulence quencher that inhibits the induction of bacterial virulence gene expression without killing the pathogen. However, at a high concentration (10 μM), it was toxic to the bacterium (Rajaonson et al. 2011).

The unique virulence quenching activity of perbergin provides new opportunities for the development of control agents for infectious diseases. Antivirulence therapy, which disarms pathogens but does not kill them, is an emerging concept to combat bacterial-mediated disease (Defoirdt 2016). During the past decade, many antivirulence strategies have been explored, including disrupting quorum sensing (bacterial cell-cell communication) (Mellbye et al. 2011), inhibiting bacterial adhesion to the host cell, and inhibiting toxin production or their secretion systems (Rasko et al. 2010). It is believed that, in contrast to traditional antibacterial agents, antivirulence

therapy may control bacterial disease without imposing selective pressure on the development of bacterial resistance (Defoirdt 2016). As part of ongoing efforts to discover new chemical entities to control bacterial diseases in humans, animals, and plants, the effects of perbergin were investigated in various pathogenic bacteria. Due to the restricted access to this natural product, it was decided to obtain the compound through chemical synthesis.

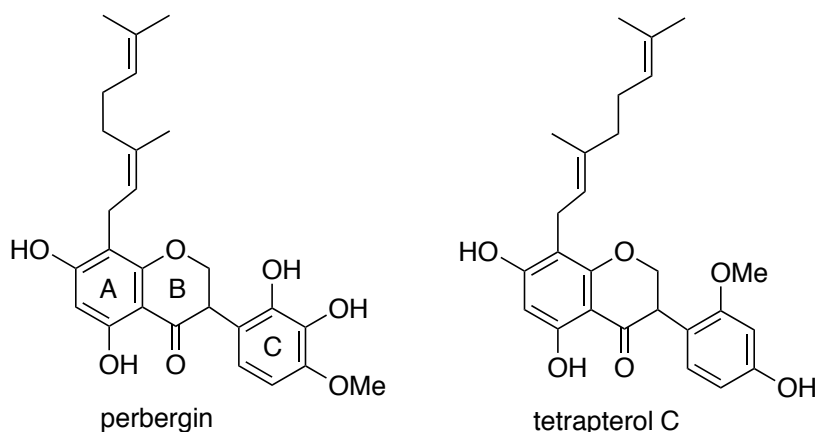
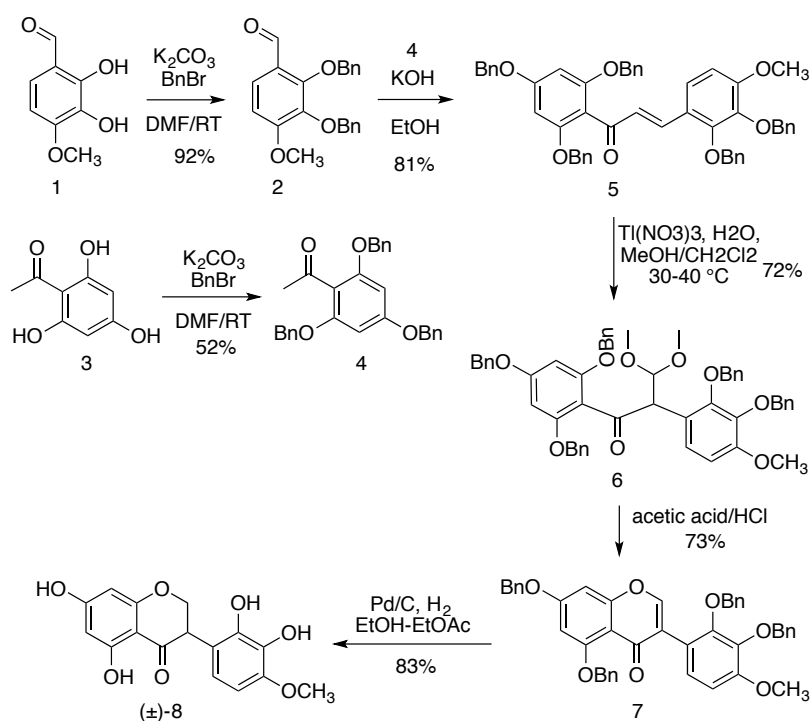


Figure 3.1. Proposed chemical structures of perbergin and tetrapterol C.

3.2 Results and Discussion

The chemical structure of perbergin has been proposed to be 8-[(2Z)-3,7-dimethylocta-2,6-dienyl]-5,7-dihydroxy-3-(2,3-dihydroxy-4-methoxyphenyl)-2,3-dihydrochromen-4-one (Rajaonson et al. 2011). It is a geranylated isoflavanone having the A and B rings similar to tetrapterol C from the roots of *Sophora tetraptera* (Figure 3.1) (linuma et al. 1995). In order to gain access to this natural product, a synthetic strategy was developed using commercially available 2,3-dihydroxy-4-methoxybenzaldehyde (**1**) and trihydroxyacetophenone (**3**) (Scheme 3.1). O-Benzoylation of **1** with BnBr

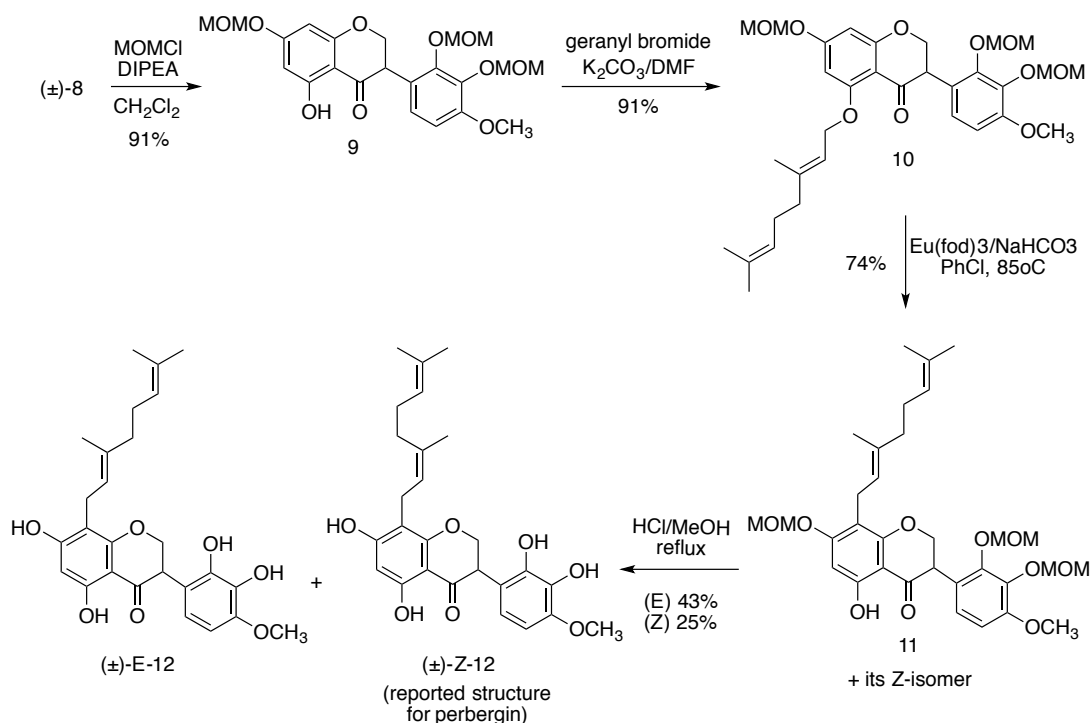
followed by coupling of the resulting aldehyde **2** with perbenzylated trihydroxyacetophenone (**4**) using 20% KOH gave chalcone **5** in 81% yield. Oxidative rearrangement of **5** to 1,2-diaryl-3,3-dimethoxypropan-1-one **6** (72%) was achieved by treating the compound with thallium (III) nitrate monohydrate in MeOH/CH₂Cl₂ (Horie et al. 1994). Treatment of **6** with concentrated acetic acid-HCl (5:1) gave isoflavonone **7** (73%) (Horie et al. 1998), which was readily converted to (±)-isoflavanone **8** (83%) through hydrogenation using 10% Pd/C as a catalyst.



Scheme 3.1. Synthetic strategy for isoflavanone (±)-**8**

Partial methoxymethyl acetal (MOM) protection of (±)-**8** using MOMCl and *N,N*-diisopropylamine gave compound **9** (90%), which was subsequently *O*-geranylated under mild conditions (K_2CO_3 , DMF, and geranyl bromide) to give

compound **10** in a good yield (91%) (Scheme 3.2). Migration of the geranyl moiety from the C-5 oxygen to C-8 was expected to take place via the para-Claisen-Cope rearrangement, involving two consecutive [3,3]-sigmatropic rearrangements (Al-Maharik et al. 2003, Poerwono et al. 2010, Mei et al. 2015). This approach has been employed in the synthesis of a number of prenylated flavonoids (Al-Maharik et al. 2003, Daskiewicz et al. 2005, Poerwono et al. 2010, Mei et al. 2015), chalcones (Vogel et al. 2008) and hydroxynaphthalenes (Torincki et al. 2012), performed under high temperature heating conditions or in the presence of a catalyst. For example, a para-substituted C-geranyl hydroxynaphthalene has been synthesized by heating O-geranyl naphth-1-yl ether in chlorobenzene at reflux for 24 h (34% yield) (Torincki et al. 2012). However, attempts to employ these conditions using 5-O-geranylated quercetin (a flavonol) as a model compound resulted in cleavage of the geranyl side chain (data not shown).



Scheme 3.2. Conversion of isoflavanone **9** to **(±)-E-12** and **(±)-Z-12**

Using a modified condition reported by Zhang and co-workers employing the europium catalyst $\text{Eu}(\text{fod})_3$ in the presence of NaHCO_3 , it was possible to convert compound **10** to isoflavanone **11** in good yield (74%) (Mei et al. 2015). The ^1H and ^{13}C NMR spectra of **11** revealed the presence of two products, which were identified as perbergin analogues with an *E*- or a *Z*-geranyl moiety. Unfortunately, attempts to separate these compounds by HPLC using a chiral-phase column were unsuccessful, prompting the subsequent reaction to be carried out using the mixture. Deprotection of **11** in MeOH under reflux in the presence of 3 N aq. HCl gave a mixture of **(±)-E-12** and **(±)-Z-12** (68%), as well as a mono-MOM-protected intermediate (20%). These products could be separated using chiral-phase HPLC (Chiralcel OD-R

column) to give pure (\pm)-**E-12** and (\pm)-**Z-12** (the reported perbergin) (Scheme 2).

Characterization of the chemical structures of both (\pm)-**E-12** and (\pm)-**Z-12** was carried out using HRMS, 1D (^1H and ^{13}C) and 2D (HSQC and HMBC) NMR, UV, and optical rotation measurement. The side chain configurations of (\pm)-**E-12** and (\pm)-**Z-12** were determined by NOESY correlations (Figure 3.2). For (\pm)-**E-12**, important correlations were observed between H-1'' (δH 3.34) and Me-8'' (δH 1.79) and between H-2'' (δH 5.21) and H-4'' (δH 2.04-2.14). On the other hand, for (\pm)-**Z-12**, correlations were observed between H-1'' (δH 3.34) and H-4'' (δH 2.22-2.25) and between H-2'' (δH 5.22) and Me-8'' (δH 1.75). Direct comparisons of the ^1H and ^{13}C NMR spectra of both compounds (measured in CDCl_3) with those reported in the literature for perbergin suggest that the geranyl moiety of perbergin has an *E*-configuration, not a *Z*-configuration (Rajaonson et al. 2011). Furthermore, it was observed also that the ^1H and ^{13}C chemical shifts of the synthetic compound [(\pm)-**E-12**], particularly those of the A ring, are somewhat different from those of the corresponding resonances of the natural product (Table 1). These discrepancies stimulated a re-evaluation of the NMR data for perbergin.

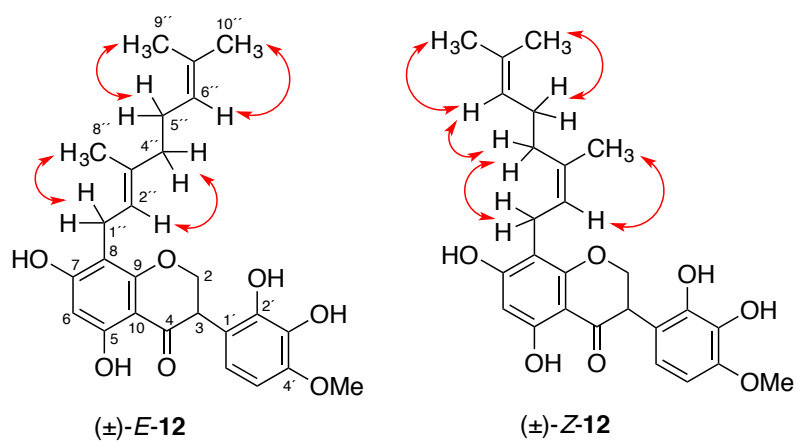


Figure 3.2. Key NOESY correlations of (±)-E-12 and (±)-Z-12

Table 3.1. ^1H (500 MHz, CDCl_3) and ^{13}C (125 MHz, CDCl_3) NMR Spectroscopic Data for Perbergin, (\pm)-*E*-12, and (\pm)-*Z*-12

No.	perbergin		(\pm)- <i>E</i> -12		(\pm)- <i>Z</i> -12	
	δ_{C}	δH (mult., J in Hz)	δ_{C}	δH (mult., J in Hz)	δ_{C}	δH (mult., J in Hz)
2a	70.1	4.54 (dd, 11.3, 5.2)	70.1	4.58 (dd, 11.3, 5.3)	70.2	4.58 (dd, 11.3, 5.3)
2b		4.69 (dd, 11.3, 8.6)		4.72 (dd, 11.3, 8.6)		4.66 (dd, 11.3, 9)
3	46.3	4.20 (dd, 8.6, 5.2)	46.1	4.20 (dd, 8.6, 5.2)	46.1	4.20 (dd, 9, 5.2)
4	197.2		197.4		197.4	
5	161.9	12.41 (s, OH)	163.0	11.98 (s, OH)	163.0	11.98 (s, OH)
6	106.9 ^a		97.4	6.01 (s)	97.1	6.01 (s)
7	164.5	6.20 (s, OH)	164.2		164.0	
8	95.6 ^a	5.97 (s) ^a	105.9		106.0	
9	161.5		160.0		160.0	
10	102.8		103.0		103.1	
1'	115.3		115.1		115.1	
2'	142.6	5.46 (s, OH)	142.6		142.6	
3'	133.6	6.32 (s, OH)	133.5		133.5	
4'	147.11		147.0		147.0	
5'	103.7	6.47 (d, 8.6)	103.6	6.48 (d, 8.6)	103.6	6.48 (d, 8.6)
6'	119.5	6.74 (d, 8.6)	119.4	6.72 (d, 8.6)	119.5	6.72 (d, 8.6)
1''	21.3	3.36 (d, 7.2)	21.6	3.34 (d, 7.2)	21.4	3.34 (d, 7.1)
2''	121.4	5.25 (t, 7.1)	121.5	5.21 (t, 7.5)	122.9	5.22 (t, 6.8)
3''	139.9		139.3		139.3	
4''	39.9	2.04-2.10 (m)	39.8	2.04-2.14 (m)	32.5	2.22-2.25 (m)
5''	26.5	2.04-2.10 (m)	26.5	2.04-2.14 (m)	26.4	2.12-2.15 (m)
6''	123.8	5.05 (t, 6.7)	123.8	5.05 (t, 6.8)	123.8	5.05 (t, 6.7)
7''	132.3		132.2		132.6	
8''	16.4	1.80 (s)	16.3	1.79 (s)	23.5	1.75 (s)
9''	25.9	1.67 (s)	25.8	1.67 (s)	25.8	1.70 (s)
10''	17.9	1.59 (s)	17.8	1.59 (s)	17.8	1.63 (s)
OMe	56.3	3.87 (s)	56.2	3.87 (s)	56.3	3.87 (s)

^aRevised chemical shifts for C-6, C-8 and H-8 of perbergin.

The 1D and 2D NMR spectra of perbergin were kindly supplied by Prof. Mondher El Jaziri of Université Libre De Bruxelles. Upon re-evaluation of these spectra, it was concluded that the geranyl moiety of perbergin is actually located at C-6, instead of C-8 as previously reported. This reassignment was made based on the HMBC spectrum of perbergin, which

showed correlations between OH-5 and C-5 (δ C 161.9), C-6 (δ C 106.9), and C-10 (δ C 102.8); between H-1'' (δ H 3.36) and C-5 [instead of C-9 (δ C 161.5)], C-6, and C-7 (δ C 164.5), and also between H-8 (δ H 5.97) and C-7, C-9 (instead of C-5), C-6, and C-10 (Figure 3.3).

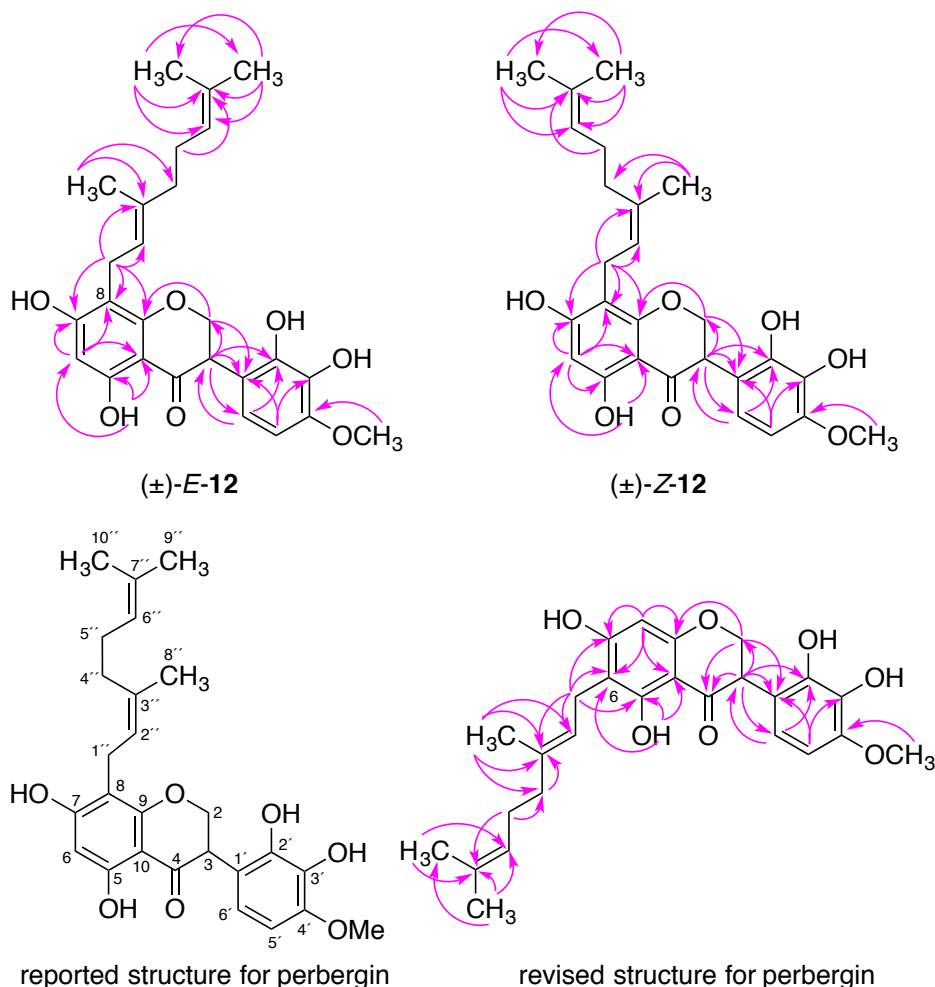


Figure 3.3. HMBC correlations of (\pm) -*E*-12, (\pm) -*Z*-12, and natural perbergin.

In addition, the chemical shift of OH-5 at 12.41 ppm for perbergin is consistent with a C-6-prenyl substitution observed in many other prenylated isoflavanones (Fukai et al. 1994, Shirataki et al. 1999). On the other hand, the

chemical shift of OH-5 in isoperbergins appears at 11.98 ppm, which is consistent with a C-8-prenyl substitution. As a result, the chemical structure of perbergin has been reassigned as 6-[(2E)-3,7-dimethylocta-2,6-dienyl]-5,7-dihydroxy-3-(2,3-dihydroxy-4-methoxyphenyl)-2,3-dihydrochromen-4-one (Figure 3.3) (Nicolaou et al. 2005).

Since perbergin at 10 μ M is toxic to *R. fascians* (Rajaonson et al. 2011), the activity of the synthetic iso-perbergins (\pm)-**E-12** and (\pm)-**Z-12** were tested against this bacterial species. The results showed that both (\pm)-**E-12** and (\pm)-**Z-12** inhibited the growth of *R. fascians* at 12.5 μ g/mL. Furthermore, as this plant pathogen is similar to mycobacteria in that they produce and use mycolic acid as components of their cell envelopes and virulence factors (Sutcliffe et al. 2010), the antibacterial activity of both (\pm)-**E-12** and (\pm)-**Z-12** were tested against *Mycobacterium smegmatis*. The non-geranylated isoflavanone (\pm)-**8** was also evaluated to determine the importance of the geranyl moiety in their antibacterial activity. While no antibacterial activity was observed for compound (\pm)-**8**, both (\pm)-**E-12** and (\pm)-**Z-12** showed good activity toward *M. smegmatis* (MIC 5 μ g/mL) (Table 3.2). These results indicate that the geranyl moiety is important for the antibacterial activity of (\pm)-**E-12** and (\pm)-**Z-12**. Despite not being a mycolic acid-containing bacterium, compounds (\pm)-**E-12** and (\pm)-**Z-12** are also active against *Staphylococcus aureus* (MIC 5 μ g/mL). However, they were not active toward the Gram-negative bacteria *Pseudomonas aeruginosa* and *Escherichia coli* (Table 3.2).

Table 3. 2. Antibacterial Activity of (±)-*E*-12, (±)-*Z*-12, and the (±)-Isoflavanone 8^a

compound	MIC (μg/mL)				
	<i>R.f.</i>	<i>M.s.</i>	<i>S.a.</i>	<i>P.a.</i>	<i>E.c.</i>
(±)- <i>E</i> -12	12.5	5	5	>50	>50
(±)- <i>Z</i> -12	12.5	5	5	>50	>50
(±)-8	>50	>50	>50	>50	>50
apramycin	50	2.5	30	50	>50
ampicillin	20	>50	>50	<5	<5

^aKey to bacteria used: *R.f.*, *Rhodococcus fascians*; *M.s.*, *Mycobacterium smegmatis*; *S.a.*, *Staphylococcus aureus*; *P.a.*, *Pseudomonas aeruginosa*; *E.c.*, *Escherichia coli*.

In conclusion, using the reported chemical structure for perbergin as a synthetic target, compounds (±)-*E*-12 and (±)-*Z*-12 were synthesized in nine steps from commercially available 2,3-dihydroxy-4-methoxybenzylaldehyde and trihydroxyacetophenone. However, discrepancies in the NMR data for the natural and synthetic materials and re-evaluation of the 1D and 2D NMR spectra of the natural perbergin revealed that the geranyl moiety of this important virulence quencher is actually located at C-6 and has an *E*-configuration, instead of the reported C-8 geranylation with a *Z*-configuration. Nevertheless, the synthetic isoperbergins demonstrated good antibacterial activity against the Gram-positive bacteria, *R. fascians*, *M. smegmatis*, and *S. aureus*. Further developments of prenylated flavonoids may lead to new antibacterial agents to control bacterial diseases in humans, animals, and plants.

3.3 Experimental Section

3.3.1 General Experimental Procedures

Optical rotations were measured on a Jasco P-1010 polarimeter (100 mm or 10 mm cells were used) at the sodium D line. Ultraviolet (UV) absorptions were measured on an Eppendorf BioSpectrometer kinetic instrument using an Eppendorf μ Cuvette G1.0 microliter measuring cell. Circular Dichroism (CD) spectra were recorded on a Jasco J-815 Circular Dichroism spectropolarimeter. Proton NMR spectra were recorded on a Bruker 500 MHz spectrometer. Proton chemical shifts are reported in ppm (δ) relative to the residual solvent signals as the internal standard (CDCl_3 : δ_{H} 7.26; $(\text{CD}_3)_2\text{CO}$: δ_{H} 2.05). Multiplicities in the spectra are described as follows: s = singlet, bs = broad singlet, d = doublet, bd = broad doublet, t = triplet, bt = broad triplet, q = quartet, m = multiplet; coupling constants are reported in Hz. Carbon NMR spectra were recorded on a Bruker 500 (125 MHz) spectrometer with complete proton decoupling. Carbon chemical shifts are reported in ppm (δ) relative to the residual solvent signal as the internal standard (CDCl_3 : δ_{C} 77.16; $(\text{CD}_3)_2\text{CO}$: δ_{C} 29.84, and 206.26). High-resolution ESI mass spectrometry was performed in positive ion mode on a 6230 TOF mass spectrometer (Agilent Technologies, Santa Clara, CA). Analytical thin-layer chromatography (TLC) was performed using silica plates (60 Å) with a fluorescent indicator (254 nm). The compounds were visualized with a UV lamp and ceric ammonium molybdate (CAM) solution. Chromatographic purification of products was performed on silica gel (60 Å, 72–230 mesh)

columns. HPLC was performed using a Shimadzu dual LC-20AD solvent delivery system with a Shimadzu SPD-M20A UV/vis photodiode array detector. All chemicals and solvents were purchased either from Sigma Aldrich, Alfa Aesar, or Tokyo Chemical Industry (TCI). All reactions were performed under an argon or nitrogen atmosphere employing oven-dried glassware.

3.3.2 Synthesis of 2,3-Bis(benzyloxy)-4-methoxybenzaldehyde (2)

To a solution of 2,3-dihydroxy-4-methoxybenzaldehyde (500 mg, 2.97 mmol) in DMF (15 mL) was added K_2CO_3 (1440 mg, 10.4 mmol) and the reaction was stirred for 30 min at room temperature, then benzyl bromide (1240 μ L, 10.4 mmol) was added to the solution. After 14 h, the reaction was quenched with saturated solution of NH_4Cl , and extracted with ethyl acetate twice (50 mL each). The organic layer was collected and washed three times with brine solution and then dried over anhydrous Na_2SO_4 . The organic layer was evaporated to dryness and then subjected to silica gel column using hexanes-EtOAc (8:2) then (7:3). Fractions containing the product were pooled and dried under vacuum to give the title compound (950 mg, 92%).

Compound **2**: yellowish oil; 1H NMR (500 MHz, acetone- d_6) δ 10.09 (1H, s), 7.53 (1H, d, J = 8.5 Hz), 7.41-7.35 (10H, m), 6.99 (1H, d, J = 8.5 Hz), 5.25 (2H, s), 5.11 (2H, s), 3.99 (3H, s); ^{13}C NMR (125 MHz, acetone- d_6) δ 188.6, 160.5, 156.4, 141.8, 138.5, 137.8, 129.6 (2C), 129.3 (2C), 129.2 (2C), 129.1, 129.1(2C), 128.8, 127.4, 124.5, 109.1, 77.3, 75.8, 56.7; (+)-HRTOFESIMS m/z 349.1443 $[M+H]^+$ (calcd for $C_{22}H_{21}O_4$, 349.1440).

3.3.3 Synthesis of 1-(2,4,6-Tris(benzyloxy)phenyl)ethan-1-one (4)

To a solution of 2,4,6-trihydroxyacetophenone (**3**, 500 mg, 2.97 mmol) in DMF (15 mL) was added K₂CO₃ (1850 mg, 13.4 mmol) and the reaction was stirred for 30 min at room temperature, then benzyl bromide (1415 μ L, 11.9 mmol) was added to the solution. After 14 h, the reaction was quenched with a saturated solution of NH₄Cl then extracted with ethyl acetate twice (50 mL each). The organic layer was washed three times with brine solution and then dried over anhydrous Na₂SO₄. The organic layer was evaporated to dryness and then subjected to silica gel column using hexanes-EtOAc (8:2) then (7:3). Fractions containing the product were pooled and dried to give the title compound (680 mg, 52%).

Compound **4**: colorless oil; ¹H NMR (500 MHz, CDCl₃) δ 7.41-7.38 (15H, m), 6.24 (2H, s), 5.04 (4H, s), 4.99 (2H, s), 2.47 (3H, s); ¹³C NMR (125 MHz, CDCl₃) δ 201.4, 161.1, 157.2, 136.5 (2C), 136.4, 128.7(2C), 128.6 (3C), 128.2, 127.9 (2C), 127.5 (2C), 127.1(6C), 115.3, 93.5 (2C), 70.7(2C), 70.3, 32.6; (+)-HRTOFESIMS m/z 439.1908 [M+H]⁺ (calcd for C₂₉H₂₇O₄, 439.1909).

3.3.4 Synthesis of (E)-3-(2,3-Bis(benzyloxy)-4-methoxyphenyl)-1-(2,4,6-tris(benzyloxy)phenyl)prop-2-en-1-one (5)

To a solution of **2** (400 mg, 1.14 mmol) and **4** (503 mg, 1.14 mmol) in EtOH (9 mL) was added 20% aq. KOH (3 mL) and the reaction mixture was stirred at room temperature for 48 h. The reaction was cooled to 0 °C, quenched with 10% aq. HCl (10 mL), then diluted with ddH₂O (50 mL). The aqueous solution was extracted with CHCl₃ (70 mL) twice. The organic layer was dried over

anhydrous Na_2SO_4 . The organic solvent was evaporated to dryness in vacuo and subjected to silica gel column chromatography using hexanes-EtOAc (8:2) then (7:3). Fractions containing the product were pooled and dried to give the title compound (710 mg, 81%).

Compound **5**: yellow oil; ^1H NMR (500 MHz, acetone- d_6) δ 7.73 (1H, d, J = 16.5 Hz), 7.55 (1H, d, J = 8.8 Hz) 7.52-7.18 (24H, m), 7.13 (2H, m), 6.95 (1H, d, J = 8.8 Hz), 6.89 (1H, d, J = 16.5 Hz), 6.75 (1H, d, J = 8.8 Hz), 6.52 (2H, s), 5.15 (2H, s), 5.08 (4H, s), 5.05 (2H, s), 4.87 (2H, s), 3.94 (3H, s); ^{13}C NMR (125 MHz, acetone- d_6) δ 194.5, 162.0, 158.4 (2C), 156.9, 152.7, 142.6, 140.3, 138.8, 138.1 (2C), 138.0, 137.9, 129.4 (2C), 129.3 (2C), 129.2 (3C), 129.2 (3C), 129.1(2C), 129.0 (2C), 128.8, 128.8, 128.7, 128.7(2C), 128.5 (2C), 128.1 (4C), 123.5, 122.9, 113.8, 109.6, 94.5 (2C), 76.7, 75.8, 70.9(2C), 70.9, 56.6; (+)-HRTOFESIMS m/z 769.3174 $[\text{M}+\text{H}]^+$ (calcd for $\text{C}_{51}\text{H}_{45}\text{O}_7$, 769.3165).

3.3.5 Synthesis of 2-(2,3-Bis(benzyloxy)-4-methoxyphenyl)-3,3-dimethoxy-1-(2,4,6-tris(benzyloxy)phenyl)propan-1-one (6)

To a solution of **5** (500 mg, 0.65 mmol) in MeOH- CH_2Cl_2 (9:1) (6.50 mL) was added $\text{Ti}(\text{NO}_3)_3 \cdot 3\text{H}_2\text{O}$ (578 mg, 1.30 mmol). The reaction mixture was stirred at 30-40 °C for 4 h. Upon a complete conversion of the starting material to the product, the reaction was brought to 0 °C then 10% solution Na_2SO_3 (5 mL) and 2% aq. HCl (2 mL) were added. The reaction was stirred for another 30 min at the same temperature. The reaction was diluted with dd H_2O (50 mL), extracted with CHCl_3 (60 mL) twice, washed with brine solution twice, and dried over anhydrous Na_2SO_4 . The organic solvent was evaporated to

dryness then subjected to silica gel column chromatography using hexanes-EtOAc (10:2) then (7:3). Fractions containing the product were pooled and dried to give the title compound (390 mg, 72%).

Compound **6**: yellowish oil; ^1H NMR (500 MHz, acetone- d_6) δ 7.39-7.23 (25H, m), 6.96 (1H, d, J = 8.8 Hz), 6.45 (1H, d, J = 8.8 Hz), 6.27 (2H, s), 5.32 (1H, d, J = 8.5 Hz), 5.16 (1H, d, J = 8.5 Hz), 5.04 (2H, s), 4.90 (1H, d, J = 8.5 Hz), 4.92 (2H, s), 4.82 (2H, q, J = 12 Hz), 4.31 (1H, d, J = 8.5 Hz), 3.73 (3H, s), 3.31 (3H, s), 3.08 (3H, s); ^{13}C NMR (125 MHz, acetone- d_6) δ 197.5, 161.3, 157.4 (2C), 153.0, 151.4, 141.3, 138.3, 138.0, 137.1(2C), 136.9, 128.4(2C), 128.2 (2C), 128.1(4C), 128.1 (2C), 128.0 (2C), 127.8, 127.7 (2C), 127.6, 127.4 (2C), 127.3, 127.1 (2C), 127.0 (4C), 125.0, 120.6, 113.9, 107.5, 104.5, 93.0 (2C), 74.7, 74.3, 69.9, 69.8 (2C), 55.3, 54.3, 53.9, 51.2; (+)-HRTOFESIMS m/z 853.3358 (calcd for $\text{C}_{53}\text{H}_{50}\text{NaO}_9$, 853.3353).

3.3.6 Synthesis of 5,7-Bis(benzyloxy)-3-(2,3-bis(benzyloxy)-4-methoxyphenyl)-4*H*-chromen-4-one (**7**)

To a solution of **6** (350 mg, 0.42 mmol) in AcOH (20 mL) was added a mixture of AcOH-12 N HCl (5:1) (20 mL). The mixture was stirred for 5 min then left to stand at room temperature for 1 h at which time the reaction mixture was cooled down and ddH₂O (50 mL) was added. The mixture was brought to 60 °C for 30 min then extracted with CHCl₃ (100 mL) twice. The CHCl₃ layer was washed three times with brine solution and then dried over anhydrous Na₂SO₄. The organic layer was evaporated to dryness then subjected to silica gel column chromatography using hexanes-EtOAc (10:2) then (7:3). Fractions

containing the product were pooled and dried to give the title compound (208 mg, 73%).

Compound **7**: yellowish oil; ^1H NMR (500 MHz, acetone- d_6) δ 8.59 (1H, s), 7.47-7.12 (20H, m), 6.78 (1H, d, J = 8.5 Hz), 6.59 (1H, d, J = 8.5 Hz), 6.30 (2H, s), 5.17-5.05 (2H, m), 4.79 (2H, s), 4.90 (2H, s), 4.82 (2H, s), 3.81 (3H, s); ^{13}C NMR (125 MHz, acetone- d_6) δ 187.5, 162.3, 158.2, 154.2, 151.8, 142.4, 139.0, 138.4, 138.0 (2C), 137.7, 129.3, 129.3 (2C), 129.2 (3C), 129.2, 129.1, 129.0, 128.9, 128.8 (2C), 128.7, 128.6 (3C), 128.5, 128.4, 128.4, 127.6 (3C), 123.0, 115.8, 109.9, 108.3, 93.8 (2C), 75.7, 75.6, 70.7 (2C), 56.3; (+)-HRTOFESIMS m/z 677.2534 (calcd for $\text{C}_{44}\text{H}_{37}\text{O}_7$, 677.2536).

3.3.7 Synthesis of (\pm)-3-(2,3-Dihydroxy-4-methoxyphenyl)-5,7-dihydroxychroman-4-one ((\pm)-**8**)

rifamyinCompound **7** (90 mg, 0.133 mmol) was dissolved in EtOH-EtOAc (1:1) (5 mL) then Pd/C 10% (40 mg) was added. The mixture was degassed under vacuum, and then hydrogen gas was applied. The reaction mixture was stirred for 3 h, during which TLC was used to monitor the reaction. Upon completion, the mixture was passed through a celite column and the pass-through solution was dried and subjected to silica gel column chromatography using CHCl_3 -MeOH (9:1) as eluent. Fractions containing the product were pooled and dried to afford the title compound (35 mg, 83%).

Compound (\pm)-**8**: Brownish fluffy powder, $[\alpha]_D^{22}$ 0 (c = 1, MeOH); ^1H NMR (500 MHz, acetone- d_6) δ 12.37 (1H, s, OH), 6.59 (1H, d, J = 8.5 Hz), 6.48 (1H, d, J = 8.5 Hz), 5.96 (1H, d, J = 2 Hz), 5.95 (1H, d, J = 2 Hz), 4.64 (1H, t,

$J = 11$ Hz), 4.48 (1H, dd, $J = 11, 5.5$ Hz), 4.28 (1H, dd, $J = 10.5, 5.5$ Hz), 3.80 (3H, s); ^{13}C NMR (125 MHz, acetone- d_6) δ 198.0, 167.3, 165.4, 164.5, 148.6, 144.5, 134.5, 120.8, 116.1, 104.0, 103.5, 96.8, 95.7, 70.9, 56.3, 47.6; (+)-HRTOFESIMS m/z 319.0813 (calcd for $\text{C}_{16}\text{H}_{15}\text{O}_7$, 319.0818).

3.3.8 Synthesis of 5-Hydroxy-3-(4-methoxy-2,3-bis(methoxymethoxy)phenyl)-7-(methoxymethoxy)chroman-4-one (9)

Compound (\pm)-**8** (25 mg, 0.078 mmol) was dissolved in CH_2Cl_2 (1.5 mL) then *N,N*-diisopropylethylamine (82 μL , 0.46 mmol) was added to the mixture at 0 °C. The reaction mixture was left stirring at room temperature for 30 min, and subsequently MOMCl (22 μL , 0.273 mmol) was added. The reaction was stirred at 0 °C for 2 h, then left to come to rt. The reaction was quenched with potassium phosphate buffer pH 7.0, diluted with ddH₂O (8 mL), and extracted with EtOAc (10 mL) twice. The organic layer was washed with brine solution twice, dried over anhydrous Na_2SO_4 , and the solvent was removed in vacuo. The crude material was subjected to silica gel column chromatography using hexanes-EtOAc (7:3) then (6:4). Fractions containing the product were pooled and dried to afford the title compound (32 mg, 91%).

Compound **9**: Colorless solid, ^1H NMR (500 MHz, CDCl_3) δ 12.11 (1H, s, OH), 6.82 (1H, d, $J = 8.6$ Hz), 6.70 (1H, d, $J = 8.6$ Hz), 6.20 (1H, d, $J = 2$ Hz), 6.14 (1H, d, $J = 2$ Hz), 5.18 (2H, s), 5.14 (2H, s), 5.11 (2H, d, $J = 2$ Hz), 4.53-4.48 (3H, m), 3.84 (3H, s), 3.59 (3H, s), 3.50 (3H, s), 3.48 (3H, s); ^{13}C NMR (125 MHz, CDCl_3) δ 197.6, 165.3, 164.3, 163.2, 153.5, 150.0, 138.6, 124.3, 121.1,

106.1, 104.3, 99.9, 98.7, 97.0, 95.5, 94.0, 71.2, 57.8, 57.5, 56.5, 56.0, 45.8;
 (+)-HRTOFESIMS m/z 451.1604 (calcd for $C_{22}H_{27}O_{10}$, 451.1604).

3.3.9 Synthesis of (*E*)-5-((3,7-Dimethylocta-2,6-dien-1-yl)oxy)-3-(4-methoxy-2,3-bis(methoxymethoxy)phenyl)-7-(methoxymethoxy)chroman-4-one (10**)**

To a solution of **9** (15 mg, 0.033 mmol) in DMF (0.35 mL) was added K_2CO_3 (9 mg, 0.066 mmol), and the reaction mixture was stirred for 30 min at room temperature. Subsequently, geranyl bromide (9.2 μ L, 0.04 mmol) was added to the reaction mixture and stirred for another 3 h until complete consumption of the starting material as judged by TLC. The reaction was then quenched with potassium phosphate buffer pH 7.0 and extracted with EtOAc twice. The EtOAc layer was dried over anhydrous Na_2SO_4 then the organic solvent was dried in vacuo. The extract was subjected to silica gel column chromatography using hexanes-EtOAc (7:3) as mobile phase. Fractions containing the product were pooled and dried under vacuum to give the title compound (18 mg, 91%).

Compound **10**: Colorless solid; 1H NMR (500 MHz, $CDCl_3$) δ 6.82 (1H, d, J = 8.6 Hz), 6.66 (1H, d, J = 8.6 Hz), 6.25 (1H, d, J = 2 Hz), 6.19 (1H, d, J = 2 Hz), 5.51 (1H, t, J = 6 Hz), 5.20-5.17 (3H, m), 5.13-5.04 (4H, m), 4.61 (1H, t-like m), 5.50 (1H, m), 4.42 (1H, m), 3.81 (3H, s), 3.58 (3H, s), 3.52 (3H, s), 3.49 (3H, s), 2.10-2.01 (4H, m), 1.70 (3H, s), 1.65 (3H, s), 1.58 (3H, s); ^{13}C NMR (125 MHz, $CDCl_3$) δ 190.0, 164.9, 163.1, 161.9, 152.9, 149.8, 140.4, 138.6, 131.7, 124.5, 123.9, 122.5, 119.4, 108.1, 107.6, 99.9, 98.7, 95.1,

95.04, 94.1, 71.3, 66.3, 57.8, 57.4, 56.5, 56.0, 46.8, 39.5, 26.3, 25.7, 17.7, 16.8; (+)-HRTOFESIMS m/z 609.2672 (calcd for $C_{32}H_{42}NaO_{10}$, 609.2672).

3.3.10 Synthesis of (*E*)- and (*Z*)-8-(3,7-Dimethylocta-2,6-dien-1-yl)-5-hydroxy-3-(4-methoxy-2,3-bis(methoxymethoxy)phenyl)-7-(methoxymethoxy)chroman-4-one (11)

To a solution of **10** (11 mg, 0.018 mmol) in chlorobenzene (300 μ L) was added $Eu(fod)_3$ (2 mg, 0.0018 mmol) and $NaHCO_3$ (1.57 mg, 0.018 mmol). The mixture was stirred at 85 $^{\circ}C$ for 24 h then the reaction mixture was filtered over celite and the solvent was evaporated in vacuo. The residue was subjected to silica gel column chromatography using hexanes-EtOAc (8:2) as a mobile phase. Fractions containing the product were pooled to give a mixture of (*E*)- and (*Z*)-**11** (7.9 mg, 74%).

Compounds (*E*)- and (*Z*)-**11**: Yellowish oil; 1H NMR (500 MHz, $CDCl_3$) δ 12.15 (1H, s, OH), 6.82 (1H, d, J = 8.6 Hz), 6.82 (1H, d, J = 8.6 Hz), 6.69 (2H, d, J = 8.6 Hz), 6.28 (2H, s), 5.22 (2H, s), 5.22 (2H, s), 5.18 (2H, s), 5.18 (2H, s), 5.17-5.15 (m), 5.13-5.10 (m), 5.07 (t-like m), 4.58-4.41 (m), 3.83 (s), 3.59 (s, MOM-CH₃), 3.50 (s, MOM-CH₃), 3.50 (s, MOM-CH₃), 3.47 (s, MOM-CH₃), 3.47 (s, MOM-CH₃), 3.26 (4H, d, J = 7 Hz), 2.21-1.923 (8H, m), 1.74 (3H, s), 1.69 (3H, s), 1.67(3H, s), 1.65 (3H, s), 1.63 (3H, s), 1.57 (3H, s); ^{13}C NMR (125 MHz, $CDCl_3$) δ 198.0, 162.9, 162.5, 159.6, 153.4, 150.0, 138.6, 135.0, 131.3, 124.5, 124.3, 124.3, 123.1, 122.4, 121.4, 109.5, 108.1, 104.1, 99.9, 98.7, 94.9, 93.9, 71.2, 57.8, 57.5, 56.4, 56.4, 56.0, 45.7, 39.8, 30.9, 26.7,

25.7, 25.70, 23.5, 21.6, 21.4, 17.7, 16.0; (+)-HRTOFESIMS m/z 609.2673 (calcd for $C_{32}H_{42}NaO_{10}$, 609.2672).

3.3.11 Synthesis of (±)-Z-12 and (±)-E-12

To a solution of **11** (3 mg, 0.0051 mmol) in MeOH (200 μ L) was added 3 N aq. HCl (60 μ L). The reaction was heated under reflux for 1.5 h and quenched with saturated solution of NH_4HCO_3 . The solution was concentrated down to half its volume and lyophilized. The dry residue was re-dissolved in acetonitrile (200 μ L) and centrifuged at 14000 rpm to remove any insoluble debris. The products were purified using chiral HPLC (Chiralcel OD-R column, 250 x 4.6 mm), acetonitrile-ammonium acetate (pH 4.5) gradient (50% acetonitrile for 10 min, then 100% acetonitrile by 25 min, then 50% at 30 min), flow rate 1 mL/min. Peaks at retention times of 17.6 min and 19.2 min were collected and dried to give (±)-Z-**12** (0.6 mg, 25%) and (±)-E-**12** (1 mg, 43%), respectively. Two inseparable peaks around 21 min were collected to give 7-O-MOM protected (±)-Z-**12** and (±)-E-**12** (0.5 mg, 20%).

Compounds (±)-E-**12**: Brown solid; $[\alpha]^{21.8}_D 0$ (c 0.04, MeOH); UV (50% aq. MeOH) λ_{max} (log ϵ) 205 (4.85), 295 (4.27), 334 (3.69) nm; 1H NMR and ^{13}C NMR data are provided in Table 1; (+)-HRTOFESIMS m/z 455.2068 (calcd for $C_{26}H_{31}O_7$, 455.2072).

Compounds (±)-Z-**12**: Brown solid; UV (50% aq. MeOH) λ_{max} (log ϵ) 205 (4.93), 295 (4.37), 335 (3.74) nm; 1H NMR and ^{13}C NMR data are provided in Table 1; (+)-HRTOFESIMS m/z 455.2075 (calcd for $C_{26}H_{31}O_7$, 455.2072).

3.3.12 Antibacterial Activity Assay

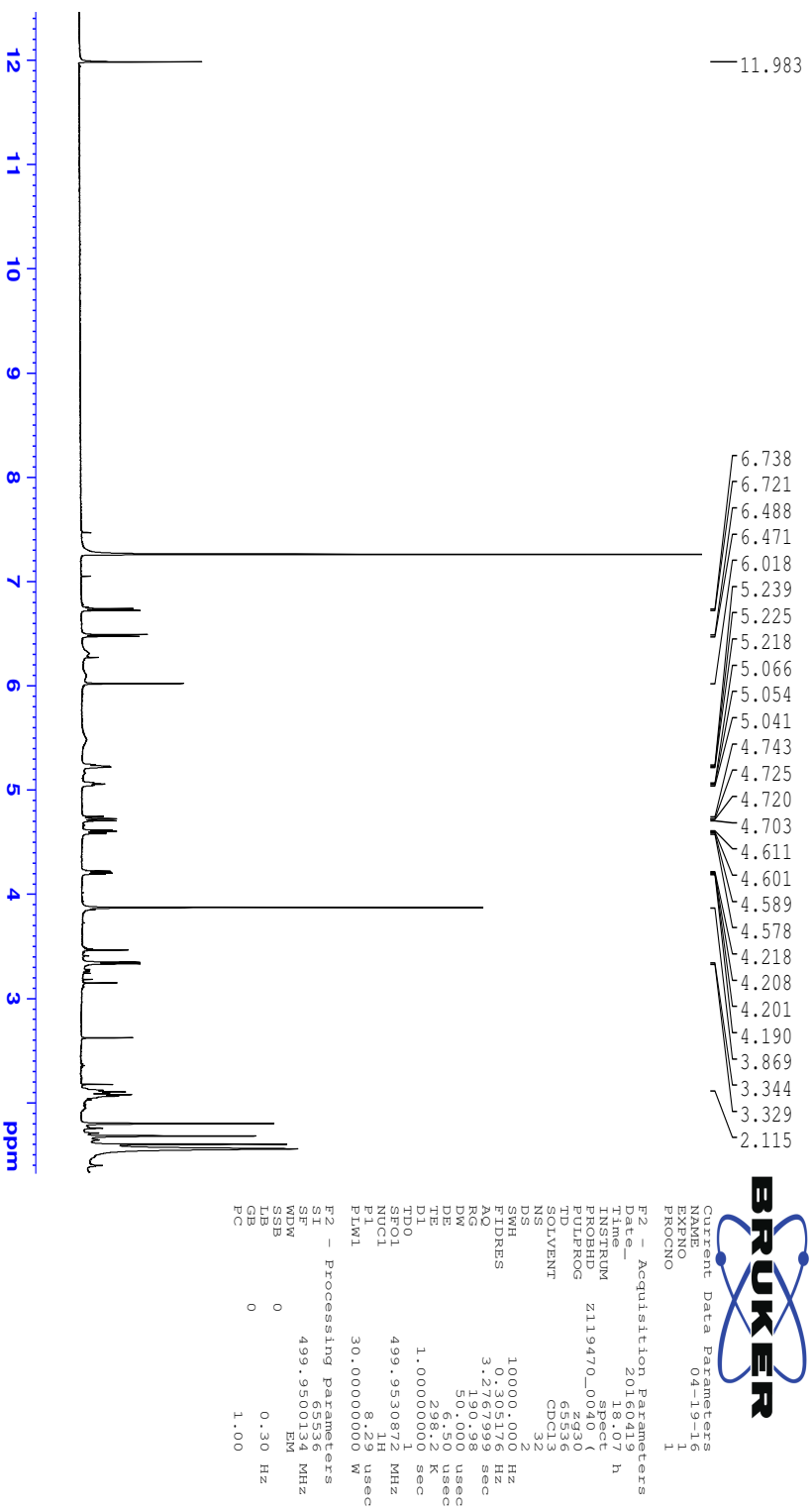
Antibacterial activity was determined by a microdilution assay. *R. fascians*, *M. smegmatis*, *S. aureus*, *P. aeruginosa*, and *E. coli* were streaked on nutrient agar (Difco) and grown overnight at 37 °C. Colonies were transferred to nutrient broth and incubated at 37 °C for 24 h. Turbidity of the inoculum was measured to OD₆₀₀ 0.15 (BioRad, SmartSpec 3000). Each strain (90 µL) was loaded onto a 96-well plate; then 10 µL of the samples (dissolved in MeOH or DMSO) was added. The final concentrations of the samples were 50, 25, 12.5, 5, 2.5, and 1.25 µg/mL, and every concentration was evaluated in triplicate. Plates were incubated at 37 °C for 24 h except for *M. smegmatis*, which was kept at 30 °C for 48 h. MTT (50 µL) developing dye was added to each well, and the minimum inhibitory concentrations were determined.

3.4 Acknowledgment

The authors thank Mondher El Jaziri and Billo Diallo for sharing the NMR spectra for perbergin. It was brought to our attention that a corrigendum will be submitted to *Environmental Microbiology* in response to the structure of perbergin reported herein. The authors also thank Benjamin Philmus for high-resolution mass spectrometry data acquisition, Mostafa Abugrain for technical assistance with anti-*Rhodococcus* assay, and Philip J. Proteau for critical reading of this manuscript. The picture of *Dalbergia pervillei* leaf used in the Table of Content graphic was taken by David Stang and adapted from the Useful Tropical Plants Database (<http://tropical.theferns.info>), and the photograph of *Rhodococcus fascians* was taken by Teresa Sawyer at the

OSU Electron Microscopy Facility and kindly provided by Melodie Putnam. This work is supported by the National Institute of Food and Agriculture, U.S. Department of Agriculture award 2014-51181-22384 to T.M. and J.H.C. Any opinion, findings, and conclusions or recommendations expressed in this material are those of the author(s) and do not necessarily reflect the views of the U.S. Department of Agriculture.

3.5 Supplemental Data

Figure 3.S1. ^1H NMR spectrum of (\pm)-E-12 (500 MHz, CDCl_3).

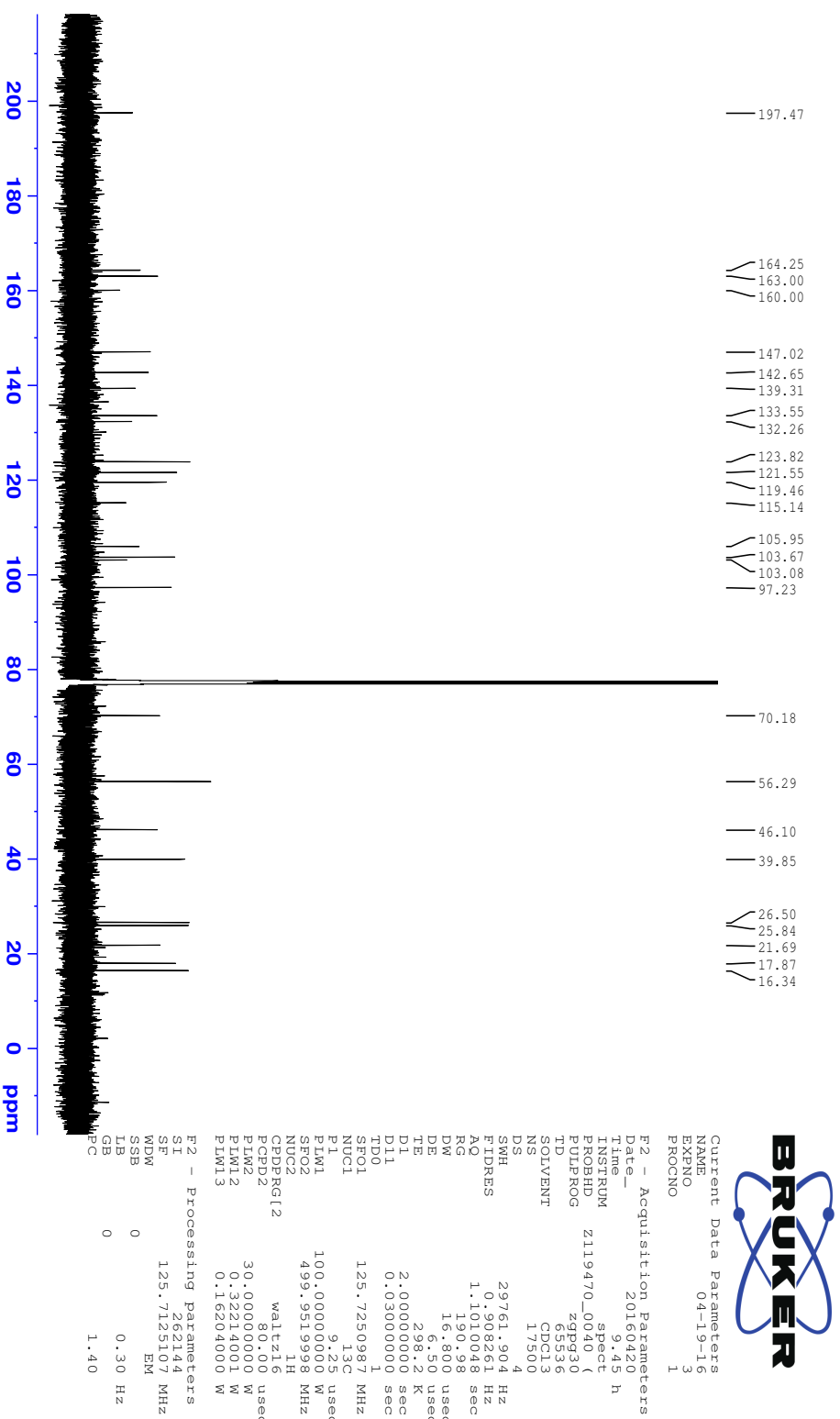
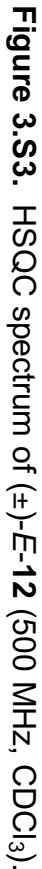


Figure 3.S2. ^{13}C NMR spectrum of (±)-E-12 (125 MHz, CDCl_3).



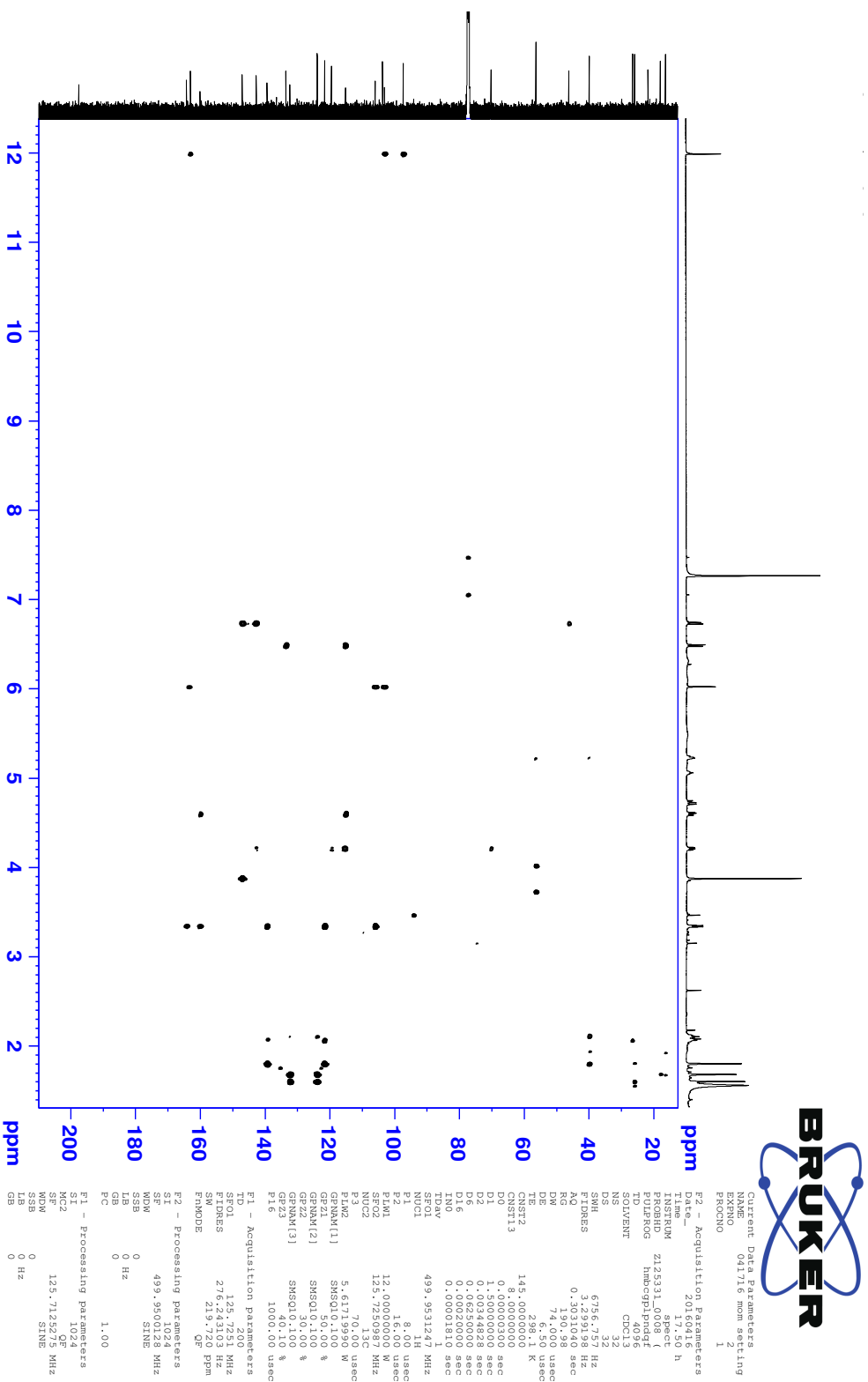


Figure 3.S4. HMBC spectrum of (±)-E-12 (500 MHz, CDCl₃).

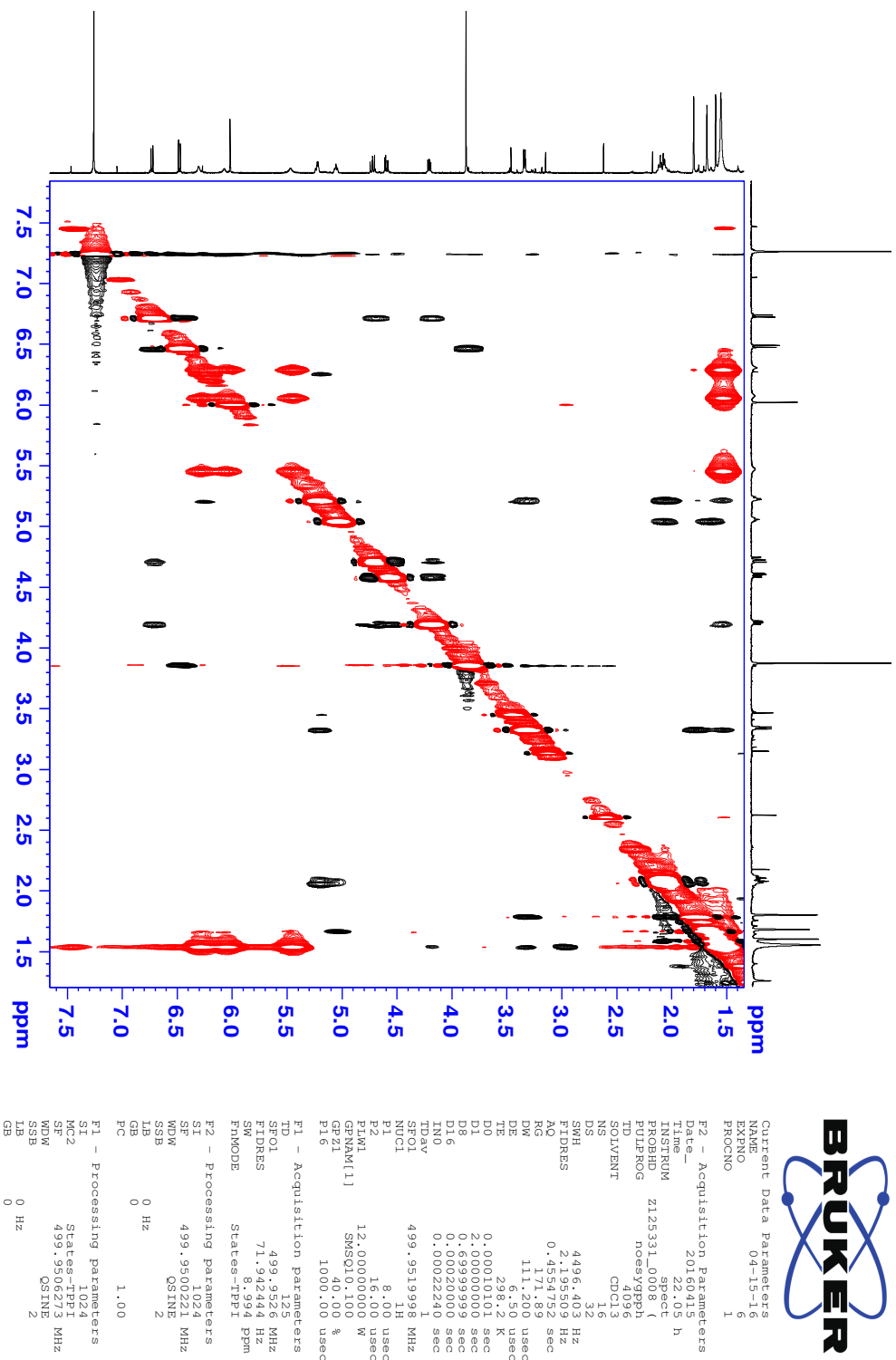


Figure 3.S5. NOESY spectrum of (±)-**E-12** (500 MHz, CDCl₃).

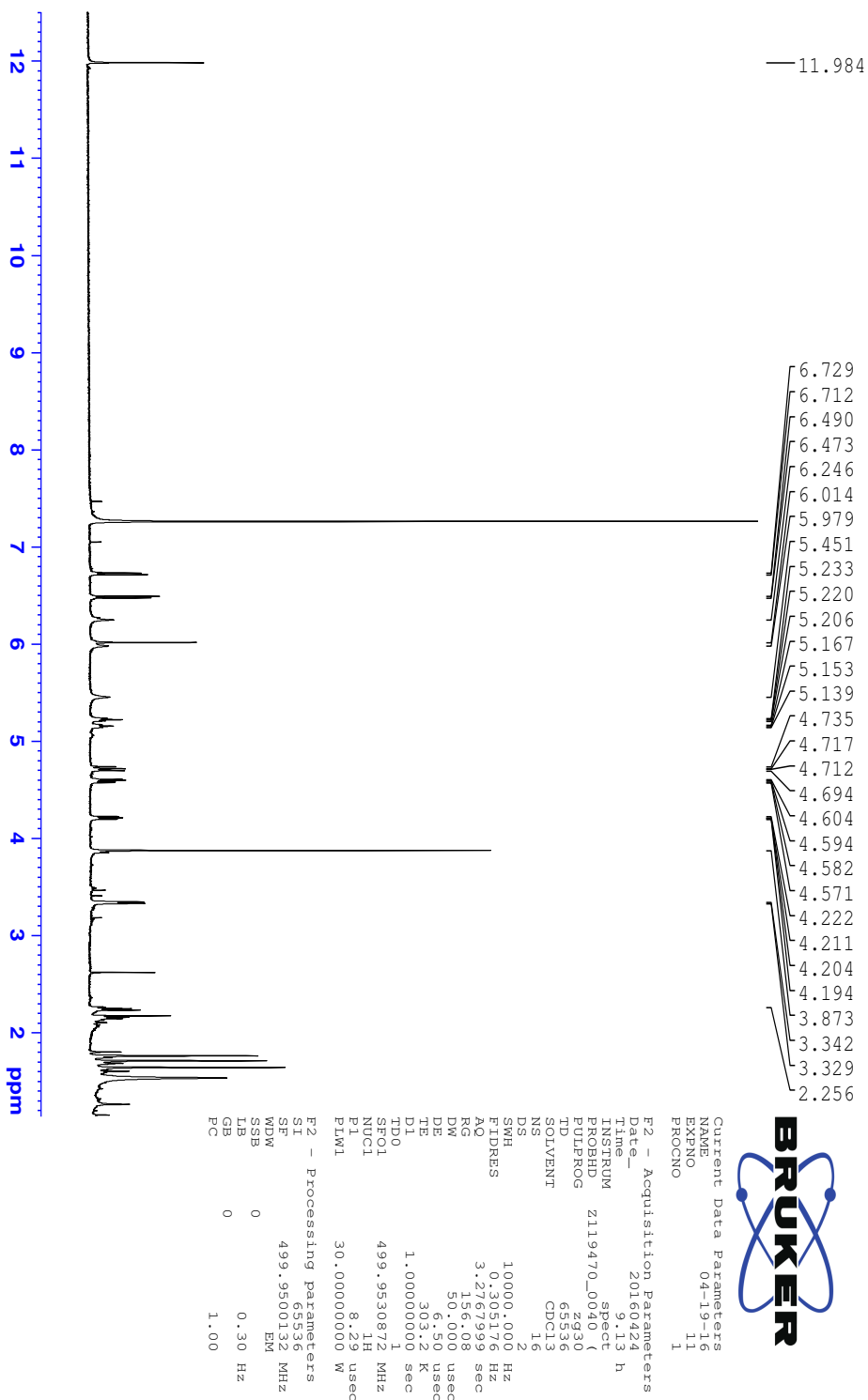


Figure 3.S6. ¹H NMR spectrum of (±)-Z-12 (500 MHz, CDCl₃).

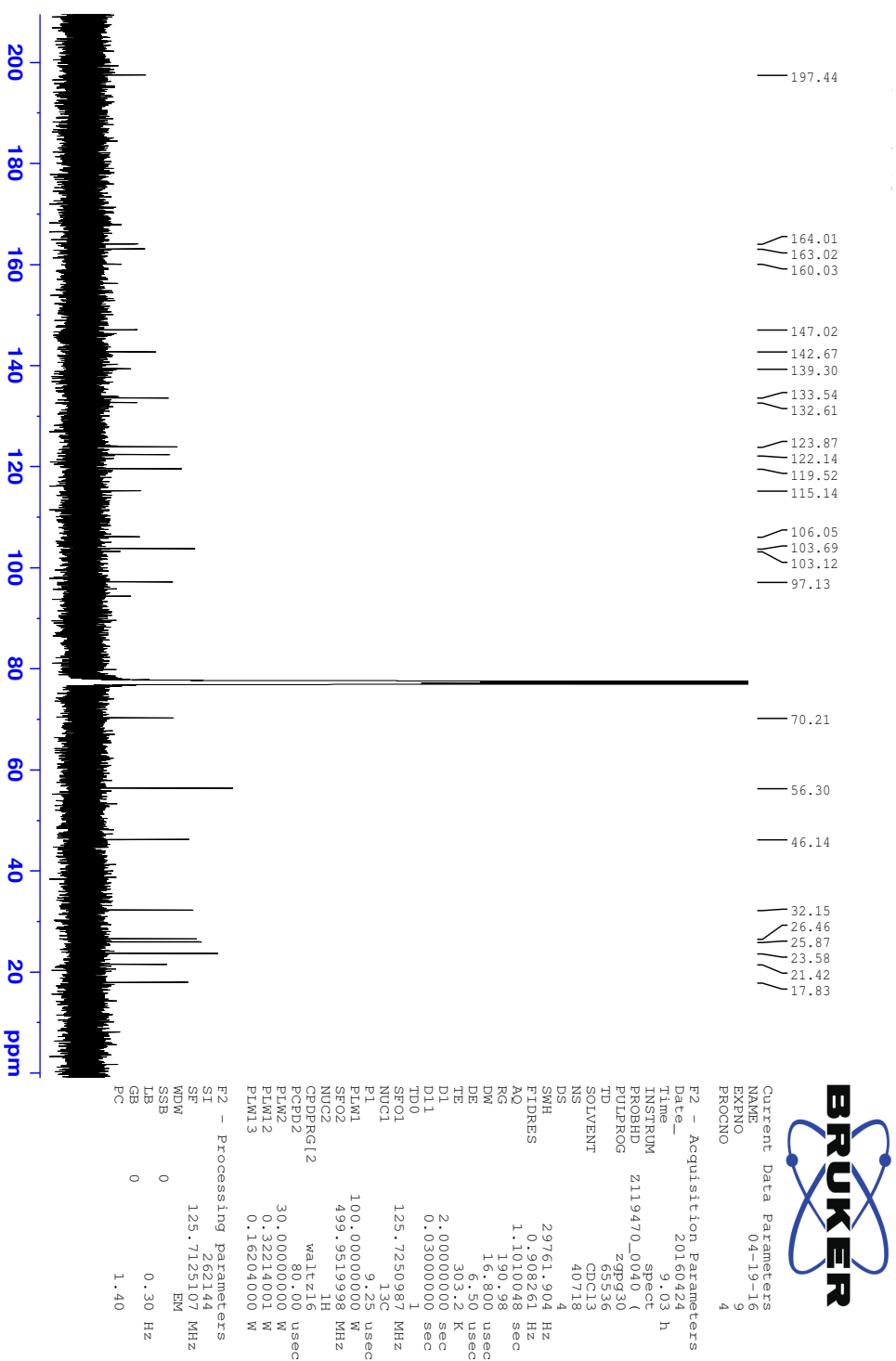


Figure 3.S7. ^{13}C NMR spectrum of (±)-Z-12 (125 MHz, CDCl_3).

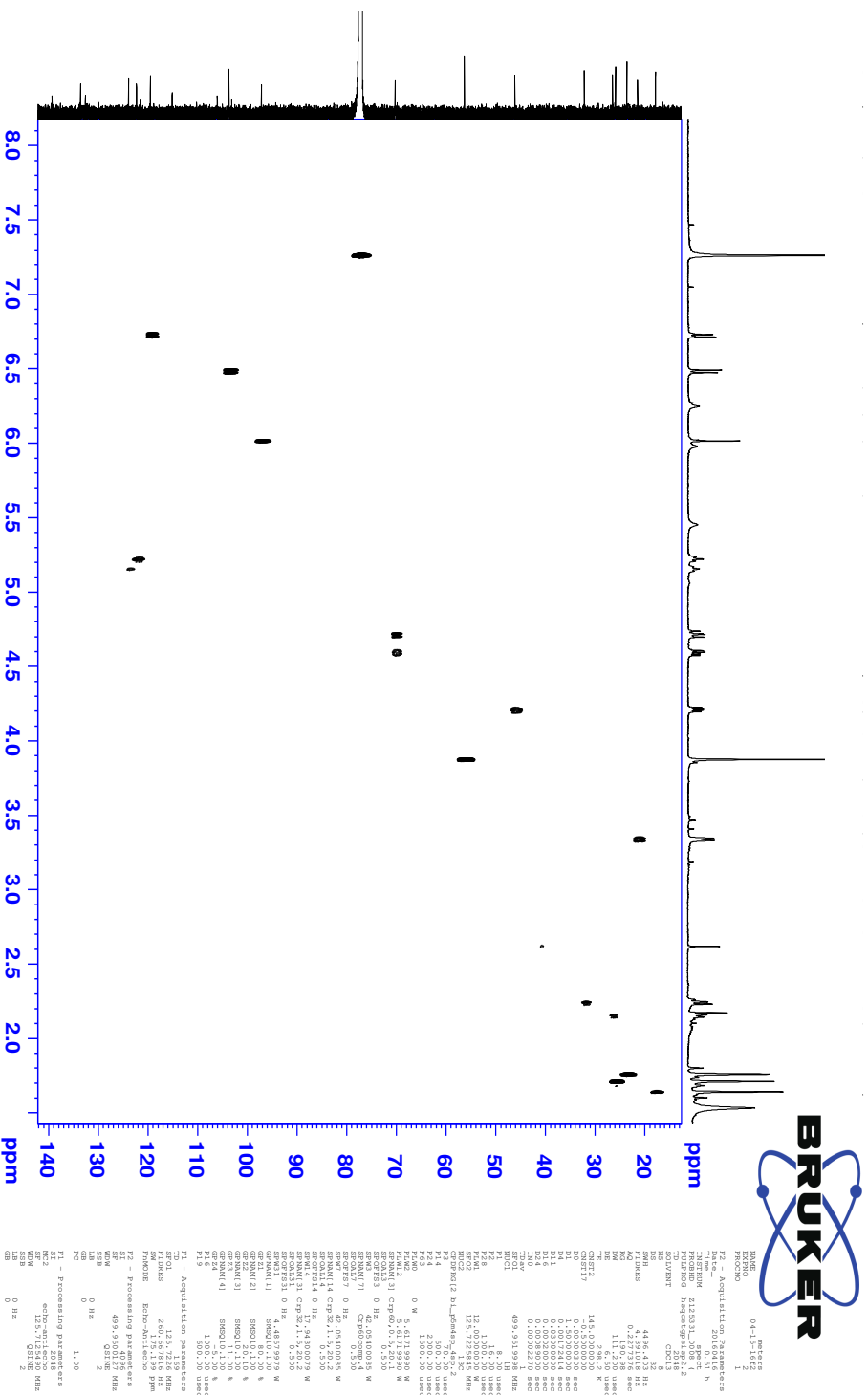


Figure 3.S8. HSQC spectrum of (±)-Z-12 (500 MHz, CDCl₃).

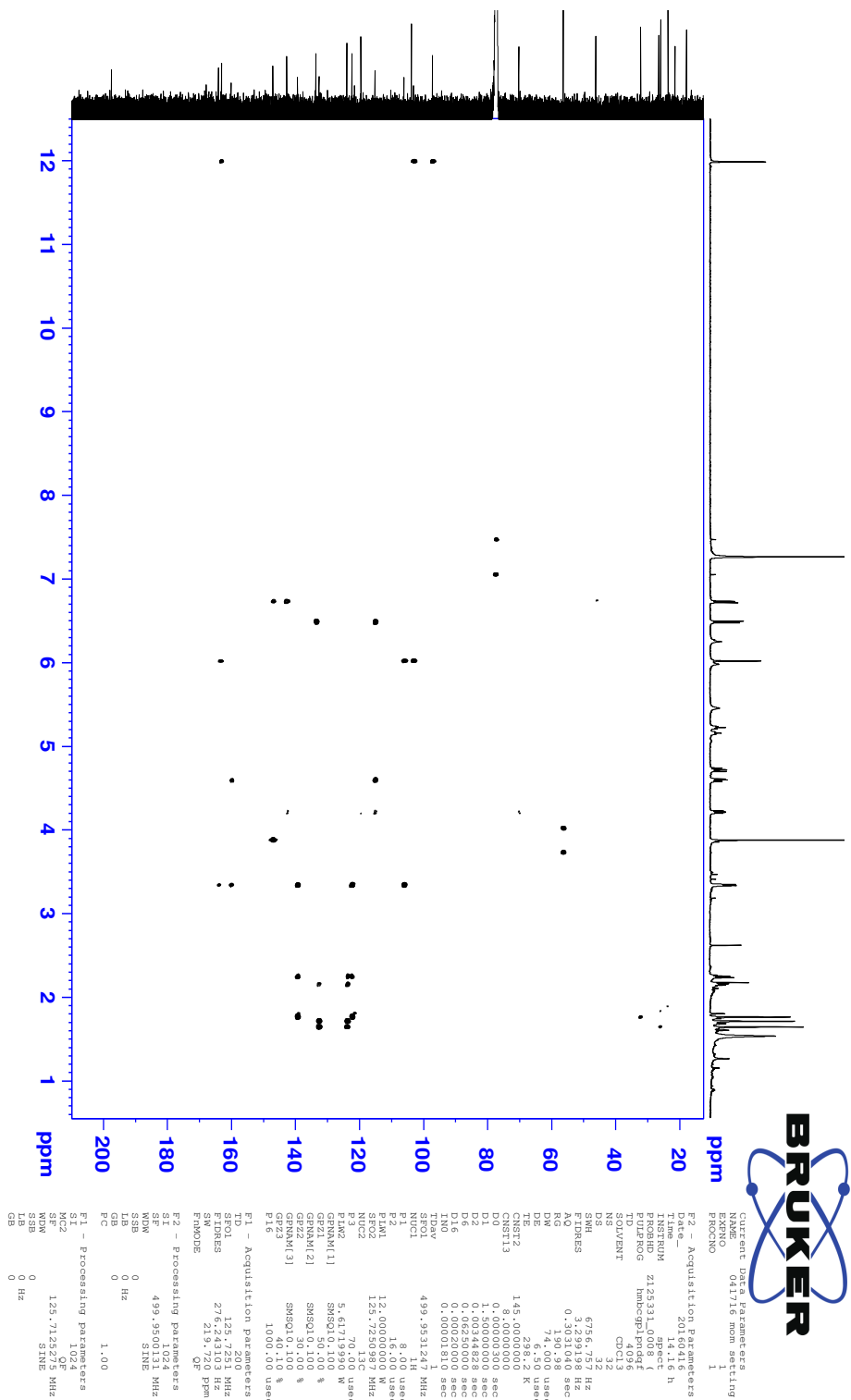


Figure 3.S9. HMBC spectrum of (\pm)-Z-12 (500 MHz, CDCl₃).

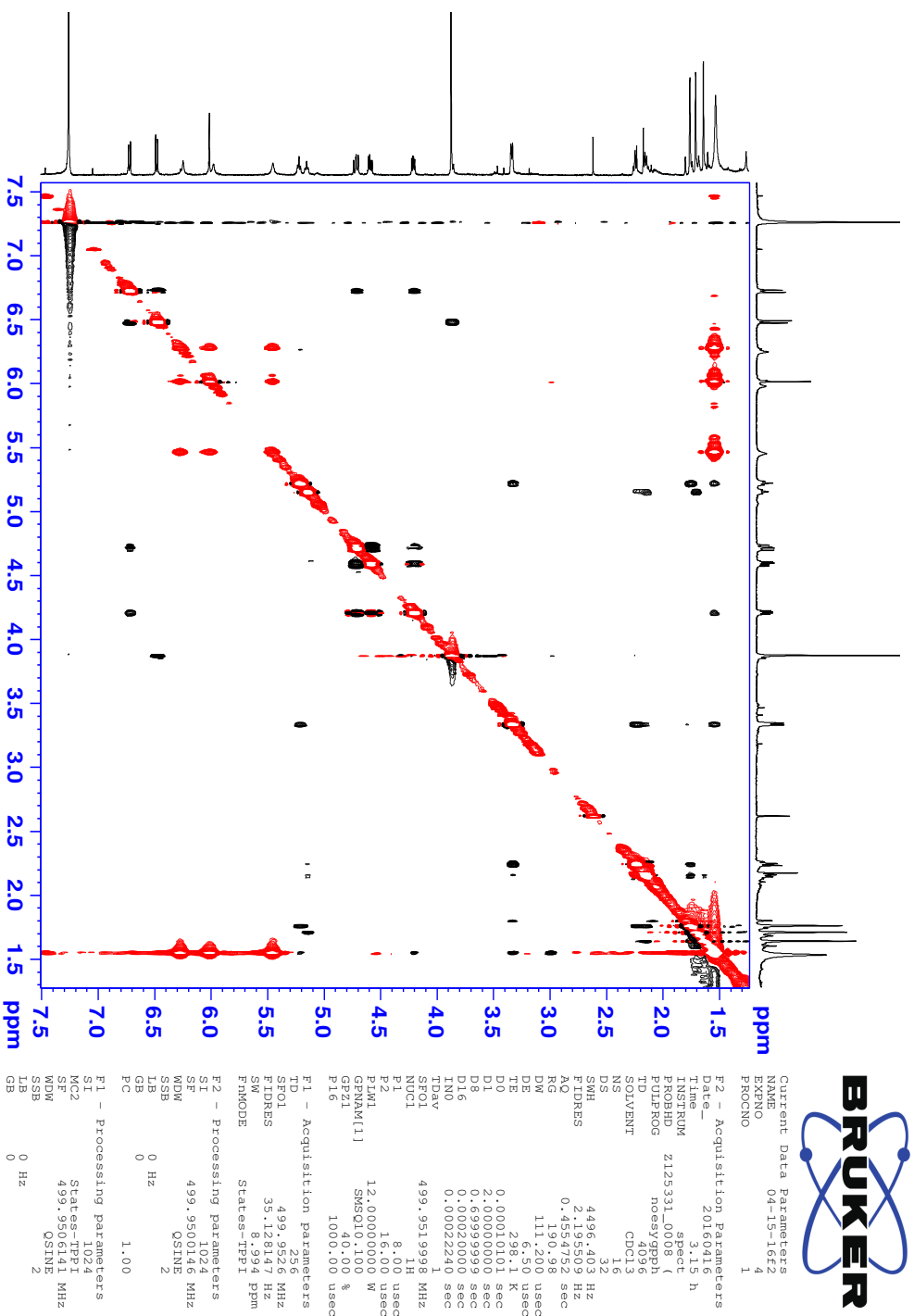


Figure 3.S10. NOESY spectrum of (±)-Z-12 (500 MHz, CDCl₃)

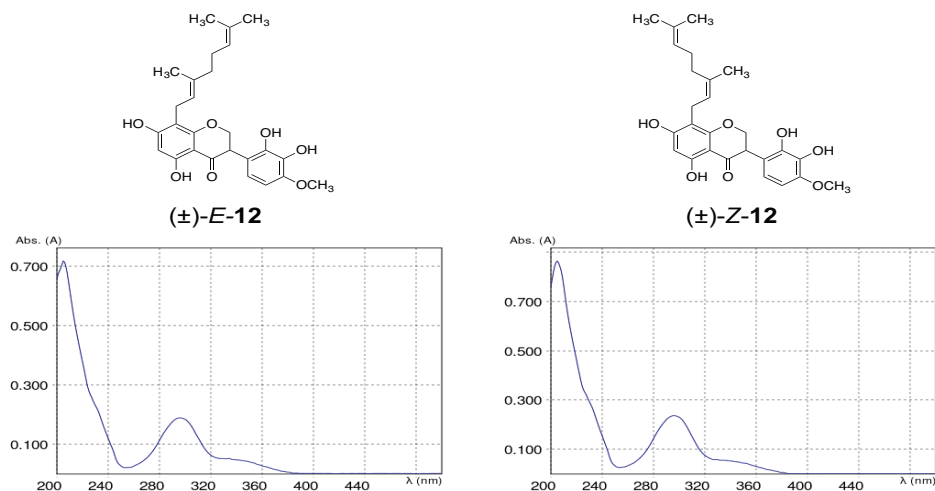


Figure 3.S11. UV spectra of **(±)-E-12** and **(±)-Z-12**.

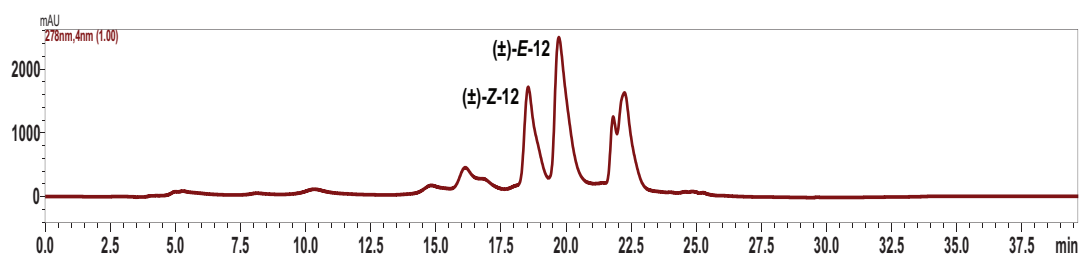


Figure 3.S12. Chiral HPLC traces of **(±)-E-12** and **(±)-Z-12**.

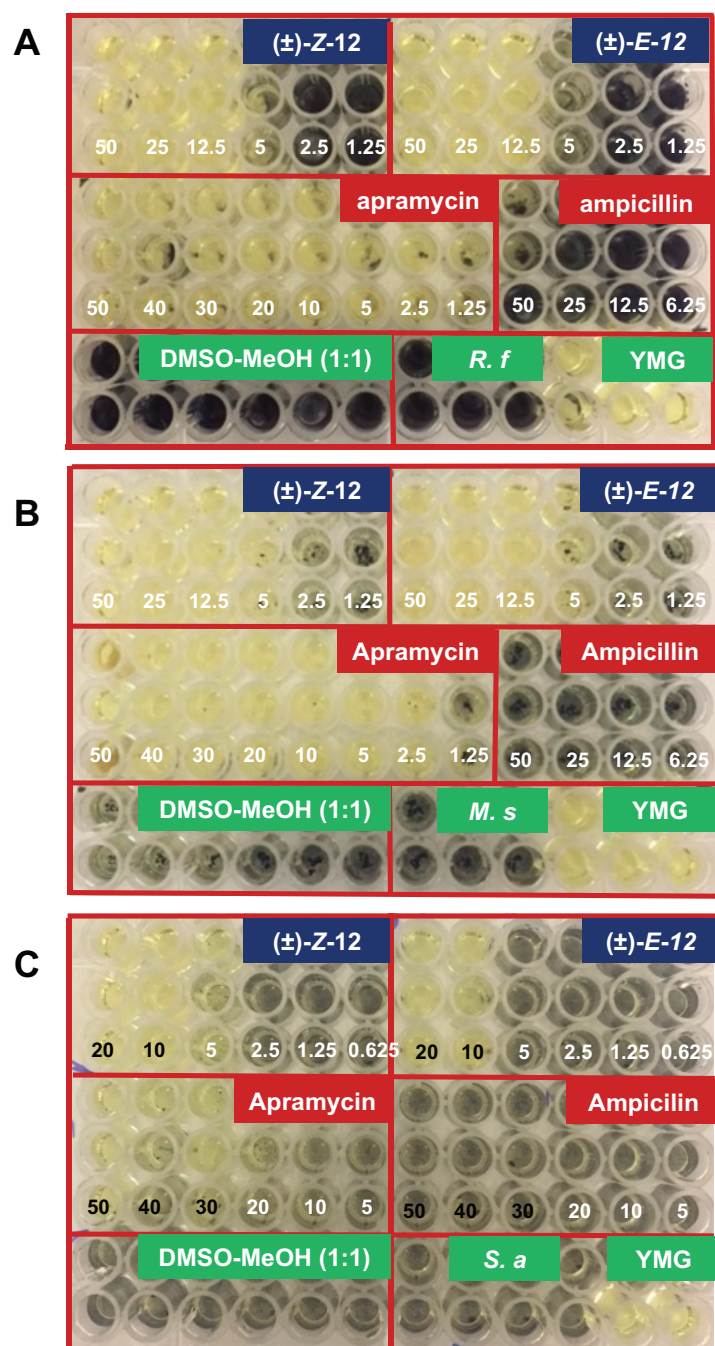


Figure 3.S13. Antibacterial assay of (\pm) -E-12 and (\pm) -Z-12 against *R. fascians* (A), *M. smegmatis* (B), and *S. aureus* (C).

3.7 References

- Al-Maharik, N. and N. P. Botting (2003). "Synthesis of lupiwighteone via a para-Claisen-Cope rearrangement." *Tetrahedron* **59**: 4177-4181.
- Daskiewicz, J. B., F. Depeint, L. Viornery, C. Bayet, G. Comte-Sarrazin, G. Comte, J. M. Gee, I. T. Johnson, K. Ndjoko, K. Hostettmann and D. Barron (2005). "Effects of flavonoids on cell proliferation and caspase activation in a human colonic cell line HT29: an SAR study." *J Med Chem* **48**(8): 2790-2804.
- Defoirdt, T. (2016). "Specific Antivirulence Activity, A New Concept for Reliable Screening of Virulence Inhibitors." *Trends Biotechnol* **34**(7): 527-529.
- Fukai, T., L. Tantai and T. Nomura (1994). "¹H NMR chemical shift of the isoflavanone 5-hydroxyl proton as a characterization of 6- or 8-prenyl group." *Heterocycles* **37**(3): 1819-1826.
- Horie, T., Y. Kawamura, C. Sakai, A. Akita and M. Kuramoto (1994). "Oxidative Rearrangement of Chalcones without a Hydroxy Group by Thallium(iii) Nitrate in Methanol." *Journal of the Chemical Society-Perkin Transactions 1*(6): 753-759.
- Horie, T., K. Shibata, K. Yamashita, K. Fujii, M. Tsukayama and Y. Ohtsuru (1998). "Studies of the selective O-alkylation and dealkylation of flavonoids. XXIV. A convenient method for synthesizing 6- and 8-methoxylated 5,7-dihydroxyisoflavones." *Chemical & Pharmaceutical Bulletin* **46**(2): 222-230.
- Iinuma, M., M. Ohyama, Y. Kawasaki and T. Tanaka (1995). "Flavonoid compounds in roots of *Sophora tetraptera*." *Phytochemistry* **39**(3): 667-672.
- Mei, Q., C. Wang, Z. Zhao, W. Yuan and G. Zhang (2015). "Synthesis of icariin from kaempferol through regioselective methylation and para-Claisen-Cope rearrangement." *Beilstein J Org Chem* **11**: 1220-1225.
- Mellbye, B. and M. Schuster (2011). "The sociomicrobiology of antivirulence drug resistance: a proof of concept." *mBio* **2**(5): e00131-00111.
- Nicolaou, K. C. and S. A. Snyder (2005). "Chasing molecules that were never there: misassigned natural products and the role of chemical synthesis in modern structure elucidation." *Angew Chem Int Ed Engl* **44**(7): 1012-1044.
- Poerwono, H., S. Sasaki, Y. Hattori and K. Higashiyama (2010). "Efficient microwave-assisted prenylation of pinostrobin and biological evaluation of its derivatives as antitumor agents." *Bioorg Med Chem Lett* **20**(7): 2086-2089.
- Rajaonson, S., O. M. Vandeputte, D. Vereecke, M. Kiendrebeogo, E. Ralambofetra, C. Stevigny, P. Duez, C. Rabemanantsoa, A. Mol, B. Diallo, M. Baucher and M. El Jaziri (2011). "Virulence quenching with a prenylated isoflavanone renders the Malagasy legume *Dalbergia pervillei* resistant to *Rhodococcus fascians*." *Environ Microbiol* **13**(5): 1236-1252.
- Rasko, D. A. and V. Sperandio (2010). "Anti-virulence strategies to combat bacteria-mediated disease." *Nat Rev Drug Discov* **9**(2): 117-128.
- Shirataki, Y., S. Matsuoka, M. Komatsu, M. Ohyama, T. Tanaka and M. Iinuma (1999). "Four isoflavanones from roots of *Sophora tetraptera*." *Phytochemistry* **50**: 695-701.

Stes, E., O. M. Vandeputte, M. El Jaziri, M. Holsters and D. Vereecke (2011). "A successful bacterial coup d'etat: how *Rhodococcus fascians* redirects plant development." Annu Rev Phytopathol **49**: 69-86.

Sutcliffe, I. C., A. K. Brown and L. G. Dover (2010). The Rhodococcal Cell Envelope: Composition, Organisation, and Biosynthesis. Berlin Heidelberg, Springer-Verlag.

Torincsi, M., P. Kolonits, J. Fekete and L. Novak (2012). "Rearrangement of Aryl Geranyl Ethers." Synthetic Communications **42**(21): 3187-3199.

Vogel, S. and J. Heilmann (2008). "Synthesis, cytotoxicity, and antioxidative activity of minor prenylated chalcones from *Humulus lupulus*." J Nat Prod **71**(7): 1237-1241.

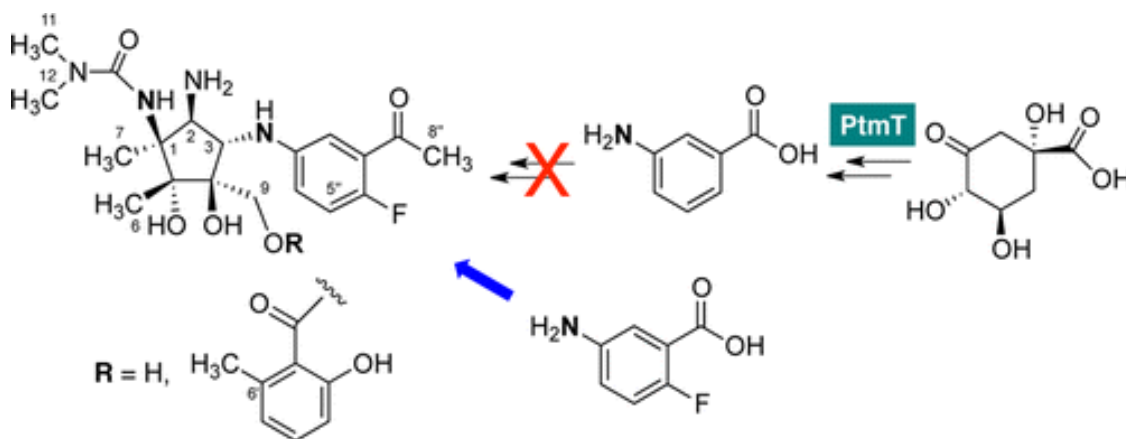
CHAPTER IV

Mutasynthesis of Fluorinated Pactamycin Analogues and Their Antimalarial Activity

Khaled H. Almabruk, Wanli Lu, Yuexin Li, Mostafa Abugreen, Jane X. Kelly,
and Taifo Mahmud

4.1 Abstract

A mutasynthetic strategy has been used to generate fluorinated TM-025 and TM-026, two biosynthetically engineered pactamycin analogues produced by *Streptomyces pactum* ATCC 27456. The fluorinated compounds maintain excellent activity and selectivity toward chloroquine-sensitive and multidrug-resistant strains of malarial parasites as the parent compounds. The results also provide insights into the biosynthesis of 3-aminobenzoic acid in *S. pactum*.



4.2 Introduction

Pactamycin, a bacterial-derived natural product discovered by Upjohn Company in the early 1960s, has been known to have broad-spectrum growth inhibitory activity against bacteria (Bhuyan 1962), mammalian cells (White 1962), viruses (Taber et al. 1971), and protozoa (Otoguro et al. 2010). This broad-spectrum activity is primarily due to its strong binding to a conserved region within the ribosome of most organisms that leads to non-selective inhibition of protein synthesis (Brodersen et al. 2000, Dinos et al. 2004). Consequently, its wide-ranging cytotoxicity, coupled with stability issues and the difficulties to generate analogues of pactamycin through organic synthesis, have hampered its further development. As one of the most complex aminocyclitol natural products, pactamycin had presented great synthetic challenges; although, through seminal work of Hanessian and co-workers, recently, this densely functionalized aminocyclitol antibiotic has finally surrendered to total synthesis (Hanessian et al. 2011, Hanessian et al. 2012). In addition, a number of synthetic methodologies to access the aminocyclopentitol moiety of pactamycin have also been reported (Knapp et al. 2007, Malinowski et al. 2012). Nevertheless, long synthetic routes and low overall yields remain major limitations of the synthetic approach to generate pactamycin analogues for clinical uses.

Recently, using biosynthetic engineering technology, we were able to generate a number of mutant strains of *Streptomyces pactum* ATCC 27456

that produce novel analogues of pactamycin with improved chemical and biological properties (Figure 4.4) (Ito et al. 2009, Lu et al. 2011). One of the mutants, in which *ptmH* (a gene that encodes a radical SAM-dependent protein) was inactivated (Figure 4.1A), produces two novel analogues of pactamycin, TM-025 and TM-026.

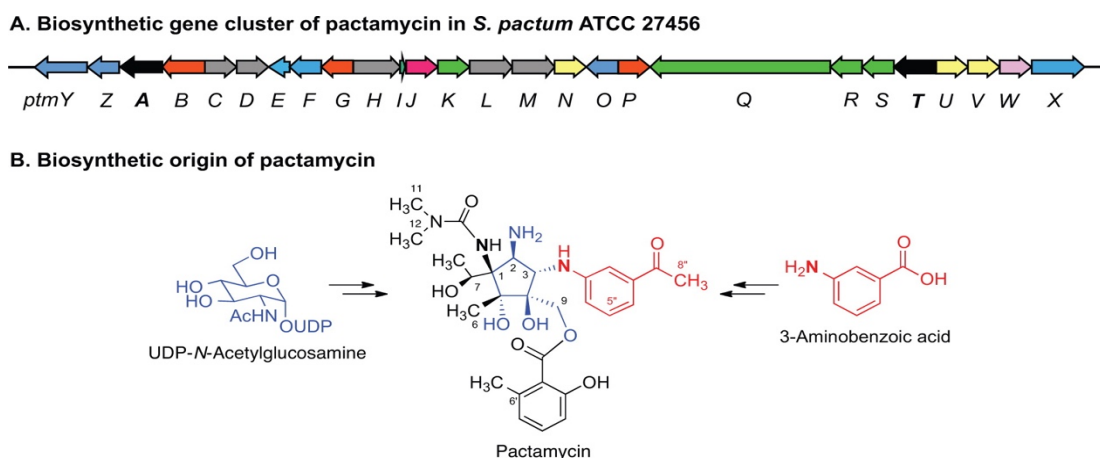


Figure 4.1. Identification of genes responsible for the production of pactamycin precursor.

These new analogues are chemically more stable and are produced in 10 to 20-fold higher yield than pactamycin. More significantly, they showed potent antimalarial activity at low nanomolar concentrations, but in contrast to pactamycin have no significant antibacterial activity and reduced cytotoxicity against human colorectal HCT-116 cells (Lu et al. 2011).

To further improve the pharmacological properties of these analogues, we explored the application of mutasynthetic approach to generate fluorinated derivatives of TM-025 and TM-026 by blocking the synthesis of 3-aminobenzoic acid (the precursor of pactamycin) in *S. pactum* and performing precursor-directed structure modifications. Fluorinated compounds are rare in

nature; however, fluorine atom has been widely used in medicinal chemistry to improve drug properties. An estimated 15-20% of new pharmaceutical leads contains fluorine atom in their structures (Chan et al. 2012).

In this paper, we describe the identification and inactivation of genes responsible for the formation of 3-aminobenzoic acid in *S. pactum*, chemical complementation experiments, synthesis of fluorinated compounds and precursor-directed biosynthesis of pactamycin analogues, and investigation of their biological activities.

4.3 Results and Discussion

To generate fluorinated TM-025 and TM-026 and other analogues of pactamycin we decided to explore the application of mutasynthesis approach. Previously, Rinehart and co-workers demonstrated that feeding of *S. pactum* var. *pactum* with 3-amino-4-fluorobenzoic acid resulted in the production of a fluorinated pactamycin analogue (Adams et al. 1994). The product was reported to have a comparable biological activity as pactamycin, but the production yield appeared to be inferior, as the fluorinated precursor has to compete with the natural one in the cells. Therefore, we set out to engineer a mutant strain of *S. pactum* that lacks the ability to produce the precursor 3-aminobenzoic acid.

Based on isotope incorporation studies using ^{13}C -labeled glucose, it has been proposed that 3-aminobenzoic acid is derived from an intermediate of the shikimate pathway (either dehydroquininate or dehydroshikimate) involving a

transamination reaction (Rinehart et al. 1981). However, no genetic and biochemical data were available to support that notion. Our recent investigations of the pactamycin biosynthetic gene cluster revealed the presence of two genes, *ptmA* and *ptmT*, that encode PLP-dependent aminotransferases, in the cluster. However, it is unclear if any of these genes is involved in 3-aminobenzoic acid formation. To investigate the role of the aminotransferase genes in pactamycin biosynthesis, we carried out in-frame deletion of *ptmA* and *ptmT* individually from the *S. pactum* genome and analyzed the metabolic profiles of the resulting mutants.

The mutants were constructed by cloning two 1 kb PCR fragments upstream and downstream of the *ptmA* and *ptmT* genes, respectively, and separately cloned into the plasmid pTMN002 (Lu et al. 2011). The products pTMW034 (for *ptmA*) and pTMW037 (for *ptmT*) were individually introduced into *S. pactum* by conjugation. Apramycin resistant strains representing single crossover mutants were obtained and subsequently grown on nonselective mannitol-soy flour agar containing MgSO₄ to allow the formation of double crossover recombinants. Apramycin sensitive colonies were counter-selected by replica plating onto MS-Mg agar with and without apramycin, and the resulting double-crossover candidate strains were confirmed by PCR amplification.

HPLC (Figure 4.2) and MS analyses of the extracts of those mutants showed that both mutants lack the ability to produce pactamycin or its intermediates. While the results suggest that both *ptmA* and *ptmT* are critical for pactamycin

biosynthesis it was not clear if *ptmA* or *ptmT* is involved in the formation of 3-aminobenzoic acid.

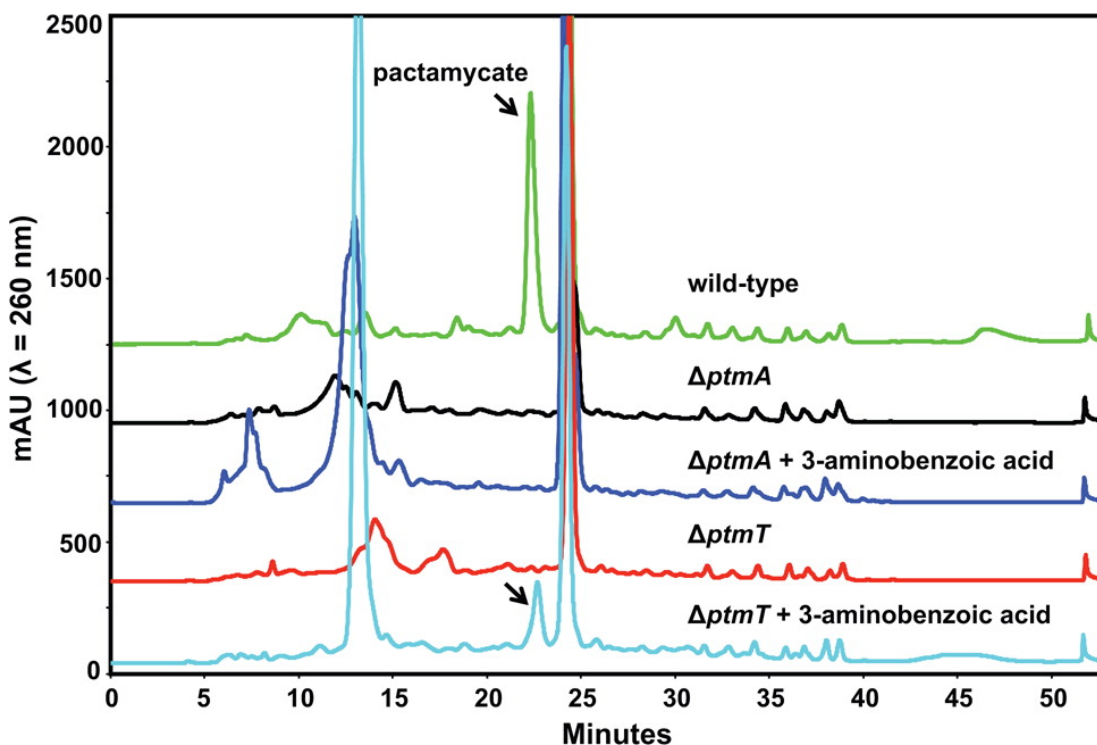


Figure 4.2. HPLC analysis of EtOAc extracts of the wild-type and the mutant strains of *S. pactum*

To investigate if any of the genes is involved in the formation of 3-aminobenzoic acid, we carried out chemical complementation experiments with 3-aminobenzoic acid. The compounds were pulse-fed to the cultures of $\Delta ptmA$ and $\Delta ptmT$ mutants and the products were harvested and analyzed by HPLC and MS. The results showed that feeding $\Delta ptmT$ mutant with 3-aminobenzoic acid did rescue the production of pactamycin, whereas that of $\Delta ptmA$ mutant did not (Figure 4.2). The results convincingly indicated that *ptmT*, not *ptmA*, is involved in the formation of 3-aminobenzoic acid. To

confirm this incorporation results, we subsequently fed the mutant with [1- ^{13}C]-3-aminobenzoic acid, and MS analysis of the EtOAc extract of the culture broths revealed the incorporation of ^{13}C in the final products, confirming the direct involvement of 3-aminobenzoic acid in pactamycin biosynthesis and PtmT is a dedicated enzyme for 3-aminobenzoic acid biosynthesis.

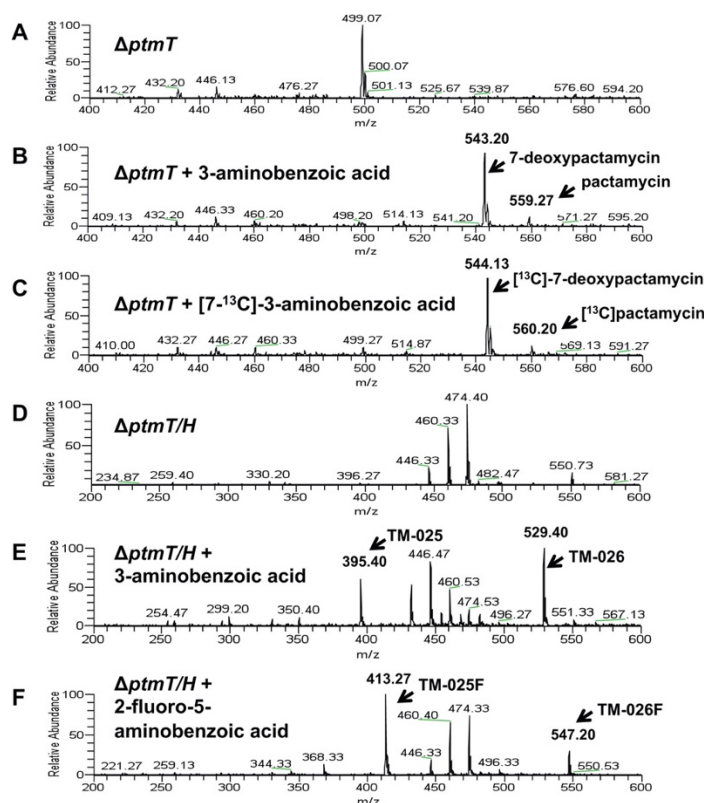


Figure 4.3. Mass spectral data for EtOAc (A–C) and *n*-BuOH (D–F) extracts of *S. pactum* mutants with and without chemical complementations

To produce fluorinated TM-025 and TM-026 as well as other possible analogues by mutasynthesis approach, we generated a $\Delta ptmT/H$ double mutant strain. This mutant strain was obtained by introducing the *ptmT* knockout plasmid pTMW037 into $\Delta ptmH$ mutant, which produces TM-025 and TM-026, by conjugation. The product of this double-mutation ($\Delta ptmT/H$

mutant) was cultured in the production medium and confirmed for its lack of TM-025 and TM-026 production. We then fed $\Delta ptmT/H$ mutant with 3-aminobenzoic acid and analyzed its metabolites. As expected, this chemical complementation experiment resulted in the recovery of TM-025 and TM-026 production, which confirmed the full functionality of the biosynthetic machinery in this mutant except for those genes that have been inactivated.

To explore the possibility of producing pactamycin analogues with different amino position of aminoacetophenone, we fed $\Delta ptmT/H$ mutant with 2-, 3-, and 4-aminobenzoic acids, individually. The compounds (50 μ mol) were pulse-fed at 16, 28, 40, 52, 64 h and the products were isolated using EtOAc and analyzed by MS. The results showed that only feeding experiments with 3-aminobenzoic acid gave the expected products TM-025 and TM-026, whereas 2- and 4-aminobenzoic acids did not give any corresponding products, suggesting substrate rigidity of some of the enzymes in the pathway.

To explore the possibility of generating fluorinated TM-025 and TM-026 by mutasynthesis, we fed $\Delta ptmT/H$ mutant with 2-fluoro-5-aminobenzoic acid and 5-fluoro-4-methyl-3-aminobenzoic acid. Both compounds were chemically prepared from commercially available 2-fluoro-5-nitrobenzoic acid and 5-fluoro-4-methyl-3-nitrobenzoic acid by catalytic hydrogenation of the latter compounds. The compounds were pulse-fed to the $\Delta ptmT/H$ mutant and the products were extracted with EtOAc and analyzed by MS and NMR. Fortunately, feeding experiments with 2-fluoro-5-aminobenzoic acid give rise

to fluorinated analogues of TM-025 and TM-026, designated as TM-025F and TM-026F. TM-025F and TM-026F gave quasi-molecular ions m/z 413 and 547, respectively, 18 atom mass unit (amu) higher than those of TM-025 and TM-026 (Figure 4.3E-F). Further confirmation of these products was carried out by comparing their MS/MS fragmentation patterns with those of TM-025 and TM-026 (Figure 4.S4) and by NMR analyses. Despite that 2-fluoro-5-nitrobenzoic acid was incorporated in relatively high yields, giving rise to 4-5 mg/L of each TM-025F and TM-026F, feeding experiments with 5-fluoro-4-methyl-3-aminobenzoic acid did not give any new products.

To test the antimalarial activity of TM-025F and TM-026F, the compounds were subjected to an in vitro antimalarial activity assay. The compounds, along with TM-025, TM-026, and pactamycin were tested against chloroquine sensitive (D6) and multidrug-resistant (Dd2 and 7G8) strains of *Plasmodium falciparum*. The results showed that TM-025F and TM-026F maintain strong activity against malarial parasites with IC_{50} in low nM concentrations (Table 4.1). The results also revealed that fluorine atom substitution in the aminoacetophenone moiety of TM-025 and TM-026 does not significantly affect their antimalarial activity in vitro.

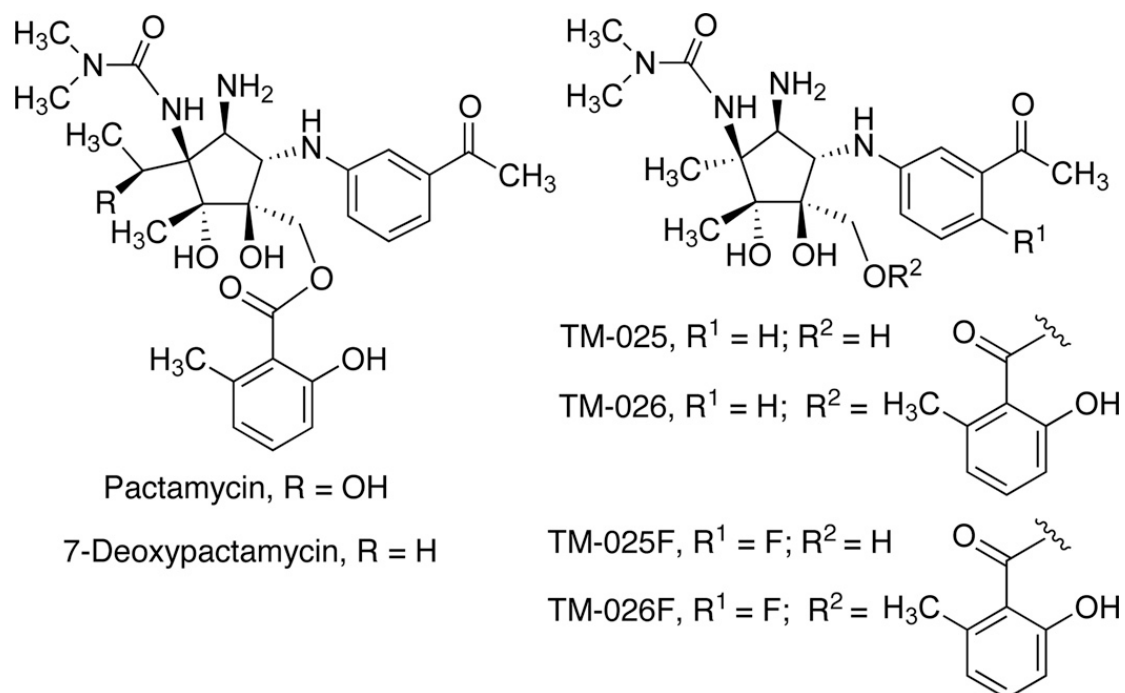


Figure 4.4. Chemical structures of pactamycin analogs.

Table 4.1. Antimalarial Activity of Pactamycin Analogues

Compounds	IC ₅₀ (nM)		
	D6	Dd2	7G8
Pactamycin	4.9	3.9	4.2
TM-025	9.8	13.9	9.3
TM-026	14.5	18.5	11.8
TM-025F	12.3	16.8	12.4
TM-026F	26.5	39.1	24.9
Chloroquine	8.4	95	78.8

D6, chloroquine-sensitive *P. falciparum*; Dd2 and 7G8, multidrug-resistant *P. falciparum*.

To examine if the fluorinated analogues retain the target selectivity of TM-025 and TM-026, we carried out antibacterial activity tests against both Gram-positive (*Mycobacterium smegmatis*, *Staphylococcus aureus*, *Bacillus subtilis*) and Gram-negative (*Pseudomonas aeruginosa* and *E. coli*) bacteria in an agar diffusion assay. Similar to TM-025 and TM-026, neither TM-025F nor TM-026F showed any significant activity against bacteria at the concentrations used (Figure 4.S13), suggesting their higher affinity against plasmodial cells than bacteria.

In conclusion, we have used an efficient mutasynthetic strategy to generate fluorinated TM-025 and TM-026, two promising pactamycin analogues, in *S. pactum*. Similar to the parent compounds, the fluorinated analogues maintain excellent activity and selectivity toward chloroquine-sensitive and multidrug-resistant strains of *P. falciparum*. The results also provide insight into the biosynthesis of 3-aminobenzoic acid, which is relatively obscure, as well as substrate preferences of some of the enzymes in the pathway.

4.4 Experimental Section

4.4.1 Bacterial strains and plasmids

Pactamycin producing *S. pactum* ATCC 27456 was purchased from American Type Culture Collection (ATCC). *Escherichia coli* DH10B was used as a host strain for the construction of recombinant plasmids. *E. coli* ET12567 was used as donor strain in conjugation experiments. pJET1.2 (Fermentas) and pGEM-T (Promega) were used as cloning vectors. pTMN002 is a pJTU1278+ derivative containing an oriT transfer element required for conjugation (Ito et al. 2009, He et al. 2010). All bacterial strains and plasmids used in this study are listed in Table 4.S1.

4.4.2 General DNA manipulations

Genomic DNA of *S. pactum* ATCC 27456 was prepared by standard protocol (Kieser et al. 2000) or using the DNeasy Tissue Kit (QIAGEN). DNA fragments were recovered from an agarose gel by using the QIAquick Gel Extraction Kit (QIAGEN). Restriction endonucleases were purchased from Invitrogen or Promega. Preparation of plasmid DNA was done by using a QIAprep Spin Miniprep Kit (QIAGEN). All other DNA manipulations were performed according to standard protocols (Kieser et al. 2000, Sambrook et al. 2001). PCR was performed in 30 cycles by using a Mastercycler gradient thermocycler (Eppendorf) and Platinum *Taq* DNA polymerase (Invitrogen) or Platinum *Pfx* DNA polymerase (Invitrogen). Oligodeoxyribonucleotides for PCR primers were synthesized by Sigma-Genosys, and are shown in Table 4.S2. The nucleotide sequences of the gene fragments were determined at

the Center for Genome Research and Biocomputing (CGRB) Core Laboratories, Oregon State University.

4.4.3 Construction of *ptmA* and *ptmT* knock-out plasmids

For the construction of *ptmA* knock-out plasmid, two 1 kb PCR fragments upstream and downstream of the *ptmA* gene were generated with primers *ptmA*-F1/*ptmA*-R1 and *ptmA*-F2/*ptmA*-R2 (see Table 4.S2), respectively, and separately cloned into pJET1.2 cloning vector for DNA sequencing. HindIII and EcoRI digested upstream DNA fragment, EcoRI and XbaI digested downstream DNA fragment, and HindIII and XbaI digested pTMN002 were ligated to create pTMW034, which was introduced into *S. pactum* by conjugation with the *E. coli* donor strain ET12567 (pUZ8002). Apramycin resistant strains representing single crossover mutants were obtained and subsequently grown on nonselective mannitol-soy flour agar containing magnesium sulfate (10 mM, MS-Mg) to allow the formation of double crossover recombinants. Apramycin sensitive colonies were counterselected by replica plating onto MS-Mg agar with and without apramycin (50 $\mu\text{g mL}^{-1}$). The resulting double-crossover candidate strains were confirmed by PCR amplification with external primers (*ptmA*-P1 and *ptmA*-P2, Table 2) flanking the targeted *ptmA* gene. The resulting PCR fragment from putative double crossover mutants was subcloned into pGEM-T Easy vector and sequenced to confirm that part of *ptmA* has been removed from the genomic DNA. A similar approach was used for the construction of *ptmT* knock-out plasmid pTMW037, except that the PCR fragments upstream and downstream of the

ptmT gene were generated with primers *ptmT*-F1/*ptmT*-R1 and *ptmT*-F2/*ptmT*-R2, respectively. pTMW037 was introduced into *S. pactum* wild type strain or $\Delta ptmH$ strain, separately, to generate *S. pactum* $\Delta ptmT$ or *S. pactum* $\Delta ptmT/H$ mutant strains.

4.4.4 Feeding experiments with 3-aminobenzoic acid and [7-¹³C]-3-aminobenzoic acid

The $\Delta ptmA$ and $\Delta ptmT$ mutants were streaked on BTT agar [glucose (1%), yeast extract (0.1%), beef extract (0.1%), casein hydrolysate (0.2%), agar (1.5%), pH 7.4] and incubated at 30 °C for 3 days. Spores of the $\Delta ptmA$ and $\Delta ptmT$ mutants were individually grown in two Erlenmeyer flasks (125 mL) containing seed medium [glucose (1%), yeast extract (0.1%), beef extract (0.1%), casein hydrolysate (0.2%), pH 7.4] (50 mL) for 3 days at 28°C and 200 rpm. Each of these seed cultures (10 mL each) was used to inoculate six Erlenmeyer flasks (500 mL) containing modified Bennett medium (100 mL). After incubation for 16 h under the same conditions, the cultures were grouped into two groups; the first group was fed with 3-aminobenzoic acid (5 mM, 200 µL) and the second group was fed with [7-¹³C]-3-aminobenzoic acid (5 mM, 200 µL). 3-aminobenzoic acid was purchased from Aldrich and [7-¹³C]-3-aminobenzoic acid was a gift from Prof. Heinz G. Floss. The feeding was repeated every 12 h for 2 days. After five days of incubation, the cultures were centrifuged and the pH was adjusted to 7.5 using NaOH solution (1 M). The metabolites of each group were extracted with *n*-BuOH (3 x 300 mL). The organic solvent was evaporated using rotary evaporator and the products were analyzed by MS.

4.4.5 Feeding experiments with 2-, 3-, and 4-aminobenzoic acids

The *ptmT/H* mutant was streaked on BTT agar [glucose (1%), yeast extract (0.1%), beef extract (0.1%), casein hydrolysate (0.2%), agar (1.5%), pH 7.4] at 30 °C for 3 days. Spores of the $\Delta ptmT/H$ mutant were initially grown in three Erlenmeyer flasks (125 mL) containing seed medium [glucose (1%), yeast extract (0.1%), beef extract (0.1%), casein hydrolysate (0.2%), pH 7.4] (50 mL) for 3 days at 28°C and 200 rpm. This seed culture (10 mL each) was used to inoculate nine Erlenmeyer flasks (500 mL) containing modified Bennett medium (100 mL). After incubation for 16 h under the same conditions, the cultures were grouped into three groups; the first group was fed with 2-aminobenzoic acid (5 mM, 200 μ L), the second group was fed with 3-aminobenzoic acid (5 mM, 200 μ L) and the third group was fed with 4-aminobenzoic acid. 2- and 3-aminobenzoic acids were purchased from Aldrich and 4-aminobenzoic acid was chemically synthesized from 4-aminomethylbenzoate by refluxing the compound with 3 N NaOH for 1 h. The feeding was repeated every 12 h for 2 days. After five days of incubation, the cultures were centrifuged and the supernatants of each group were pooled and the pH was adjusted to 7.5 using NaOH solution (1 M). The metabolites of each group were extracted with BuOH (3 x 300 mL). The organic solvent was evaporated using rotary evaporator and the products were analyzed by MS.

4.4.6 Synthesis of 2-fluoro-5-aminobenzoic acid

2-Fluoro-5-nitrobenzoic acid (100 mg, 0.5405 mmol) was dissolved in EtOH-6N HCl (1:1, 1 mL) and then Pd/C (10%, 15 mg) was added and the mixture was stirred under hydrogen pressure for 3 h. The reaction was monitored by TLC (visualized by ninhydrin) until the starting material has converted completely to the product. The mixture was passed through celite and the eluted solution was evaporated to dryness and subjected to Sephadex LH-20. Fractions containing the product were pooled and dried to afford the title compound (80 mg). ^1H NMR (300 MHz, CD_3OD) δ : 7.89 (m, 3-H, 1H), 7.62 (m, 4-H, 1H), 7.36 (t, $J = 9$ Hz, 6-H, 1H). ^{13}C NMR (75 MHz, CD_3OD) δ_{C} : 165.42, 164.45, 160.91, 130.24, (d, $J_{\text{C-F}}=9.6$ Hz, 1C), 127.85 (d, $J_{\text{C-F}}=1.5$ Hz, 1C), 121.86 (d, $J_{\text{C-F}}=11$ Hz, 1C), 119.91 (d, $J_{\text{C-F}}=19$ Hz, 1C). LRMS (EI+) m/z 155 [M^+]. HRMS (EI+) m/z 155.03811 (calcd for $\text{C}_7\text{H}_6\text{FNO}_2$ [M^+]: 155.03825).

4.4.7 Synthesis of 3-amino-4-methyl-5-fluorobenzoic acid

3-Nitro-4-methyl-5-fluorobenzoic acid (30 mg, 0.150 mmol) was dissolved in EtOH-6N HCl (1:1, 1 mL) and then Pd/C (10%, 10 mg) was added and the mixture was stirred under hydrogen pressure for 3 h. The reaction was monitored by TLC until the starting material has converted completely to the product. The mixture was passed through celite and the eluted solution was evaporated to dryness and subjected to Sephadex LH-20. Fractions containing the product were pooled and dried to afford the title compound (22 mg). ^1H NMR (300 MHz, CD_3OD) δ : 7.41 (d, J = 10 Hz, 6-H, 1H), 6.60 (d, J = 6 Hz, 2-H, 1H), 2.27 (d, J = 1.4 Hz, 4- CH_3 , 3H). ^{13}C NMR (75 MHz, CD_3OD) δ_{C} : 168.37, 163.68, 160.41, 134.76 (d, $J_{\text{C-F}}$ =19 Hz, 1C), 131.223, 129.19 (d, $J_{\text{C-F}}$ =5 Hz, 1C), 124.59 (d, $J_{\text{C-F}}$ =7.5 Hz, 1C), 120.13 (d, $J_{\text{C-F}}$ = 3 Hz, 1C), 15.51 (d, $J_{\text{C-F}}$ = 3 Hz, 1C). LRMS (TOF MS ES-) m/z : 186.0 $[\text{M-H}]^-$. HRMS (TOF MS ES-) m/z : 168.0455 (calcd for $\text{C}_8\text{H}_7\text{FNO}_2$ $[\text{M-H}]^-$: 168.0461).

4.4.8 Feeding experiments with 2-fluoro-5-aminobenzoic acid and 3-amino-4-methyl-5-fluorobenzoic acid

The procedure for feeding experiments with 2-fluoro-5-aminobenzoic acid and 3-amino-4-methyl-5-fluorobenzoic acid is similar to that for 2-, 3-, and 4-aminobenzoic acids.

4.4.9 Isolation of TM-025F and TM-026F

Five days culture broths (500 mL) of the $\Delta\text{ptmT/H}$ mutant fed with 2-fluoro-5-aminobenzoic acid (5 mM, 5 mL) were centrifuged and the supernatant was adjusted to pH 7.5. The metabolites were extracted three times with EtOAc

(500 mL each) and 2 times with BuOH (500 mL each). The organic solutions were dried over anhydrous Na_2SO_4 and the solvents were dried in vacuo to afford crude EtOAc extract (90.2 mg) and BuOH extract (280 mg). The EtOAc extract was subjected to silica gel column and eluted with 100% CHCl_3 followed by CHCl_3 -MeOH (9:1) and CHCl_3 -MeOH (8:2). Fractions containing TM026F were pooled and the organic solvent was dried under rotary evaporator to give pure TM026F (4 mg/L). Yellowish powder, ^1H NMR (500 MHz, CD_3OD) δ : 7.15 (t, J = 8 Hz, 1H, H-4'), 7.07 (m, 1H, H-4''), 6.86 (m, 1H, H-3''), 6.70 (dd, J = 11 Hz, J = 9 Hz, 1H, H-6''), 6.62 (d, J = 8 Hz, 1H, H-5'), 6.58 (d, J = 7.5 Hz, 1H, H-3'), 4.32 (d, J = 12 Hz, 1H), 4.05 (d, J = 9 Hz, 1H), 3.65 (d, J = 9 Hz, 1H), 3.60 (d, J = 6.5 Hz, 1H), 2.97 (s, 6H, $\text{N}(\text{CH}_3)_2$), 2.41 (d, J = 5 Hz, 3H, COCH_3), 2.25 (s, 3H), 1.63 (s, 3H, 7- CH_3), 1.40 (s, 3H, 6- CH_3). ^{13}C NMR (175 MHz, CryoProbe, CD_3OD) δ_{C} : 197.82, 170.75, 160.57, 159.75, 156.26 (d, $J_{\text{C-F}}$ = 243 Hz, 1C), 145.60, 141.16, 133.53, 125.67 (d, $J_{\text{C-F}}$ = 12 Hz, 1C), 123.32, 120.73 (d, $J_{\text{C-F}}$ = 7 Hz, 1C), 117.93 (d, $J_{\text{C-F}}$ = 24 Hz, 1C), 117.07, 115.29, 112.70, 83.99, 82.92, 67.00, 66.55, 65.87, 65.72, 36.74 (2C), 31.44 (d, $J_{\text{C-F}}$ = 8.7 Hz, 1C), 22.27, 16.15, 14.89. LRMS (TOF MS ES+) m/z 547.3 $[\text{M}+\text{H}]^+$. HRMS (TOF MS ES+) m/z 547.2560 (calcd for $\text{C}_{27}\text{H}_{35}\text{FN}_4\text{O}_7$ $[\text{M}+\text{H}]^+$: 547.2568).

The BuOH extract was first dissolved in MeOH and then three volumes of CHCl_3 was added. The mixture was loaded onto a silica gel column and let stand for 10 min. Subsequently, the metabolite was eluted with CHCl_3 -MeOH (10:1) and the ratio was change incrementally to CHCl_3 -MeOH (6:4).

Fractions containing the product were pooled and dried to give TM-025F (4.5 mg/L). Yellowish powder, ^1H NMR (300 MHz, CD_3OD) δ : 7.16 (bd, $J = 5.1$ Hz, 1H, H-4''), 7.00 (m, 2H, H-2'', H-6''), 4.05 (d, $J = 11.4$ Hz, 1H, 8-Ha), 3.98 (bd, $J = 7.5$ Hz, 1H, 3-H), 3.6 (m, 1 H, 2-H), 3.45 (d, $J = 11.4$ Hz, 1H, H-8b), 2.96 (s, 6H, $\text{N}(\text{CH}_3)_2$), 2.56 (d, $J = 4.5$ Hz, COCH_3), 1.61 (s, 3H, 7- CH_3), 1.41 (s, 3H, 6- CH_3). ^{13}C NMR (75 MHz, CD_3OD) δ_{C} : 198.61, 160.43, 154.41, 145.91, 126.48 (d), 120.46 (d), 118.09, 117.75, 113.17, 83.28, 82.55, 66.67, 66.24, 64.87, 63.15, 36.54, 31.10 (d), 16.58, 14.57. LRMS (TOF MS ES+) m/z 413.2 $[\text{M}+\text{H}]^+$. HRMS (TOF MS ES+) m/z 413.2195 (calcd for $\text{C}_{19}\text{H}_{29}\text{FN}_4\text{O}_5$ $[\text{M}+\text{H}]^+$: 413.2200).

4.4.10 *In vitro* Antimalarial Activity Assay

P. falciparum strains D6, Dd2, and 7G8 were cultured in human erythrocytes at 2% hematocrit in RPMI 1640 containing 0.5% Albumax, 45 $\mu\text{g/L}$ hypoxanthine, and 50 $\mu\text{g/L}$ gentamicin, as previously described (Kelly et al. 2007) *In vitro* antimalarial activity was determined by the malaria SYBR Green I-based fluorescence (MSF) assay described previously (Smilkstein et al. 2004) with slight modification (Kelly et al. 2007). Stock solutions of each test drug were prepared in sterile distilled water at a concentration of 10 mM. The drug solutions were serially diluted with culture medium and distributed to asynchronous parasite cultures on 96-well plates in quadruplicate in a total volume of 100 μL to achieve 0.2% parasitemia with a 2% hematocrit in a total volume of 100 μL . Automated pipetting and dilution were carried out with a programmable Precision 2000 robotic station (Bio-Tek, Winooski, VT). The

plates were then incubated for 72 h at 37 °C. After incubation, 100 µL of lysis buffer with 0.2 µl/ml SYBR Green I (54, 66) was added to each well. The plates were incubated at room temperature for an hour in the dark and then placed in a 96-well fluorescence plate reader (Spectramax Gemini-EM; Molecular Diagnostics) with excitation and emission wavelengths at 497 nm and 520 nm, respectively, for measurement of fluorescence. The 50% inhibitory concentration (IC₅₀) was determined by nonlinear regression analysis of logistic dose-response curves (GraphPad Prism software).

4.4.11 Antibacterial Activity Assay

Antibacterial activity of pactamycin and its analogues was determined by an agar diffusion assay. *M. smegmatis*, *S. aureus*, *B. subtilis*, *P. aeruginosa*, and *E. coli* were streaked on nutrient agar (Difco) and grown overnight at 37 °C. Colonies were transferred to nutrient broth and incubated at 37 °C for 24 h. Turbidity of the inoculum was measured to a proper density at 600 nm (BioRad, SmartSpec 3000). For plate preparation, inoculum (500 µL) was mixed thoroughly with warm nutrient agar (50 mL) and poured to 25 mL square plates. The agar plates were allowed to solidify and dry for 30 min before assay. Sterile blank paper disks (Becton-Dickinson) were impregnated with pactamycin and its analogues (20 µL) at various concentrations and dried at room temperature. The disks were placed onto inoculated agar plates and incubated at 37 °C for 24 h. In order to produce a contrast background of the inhibition zone, 0.25% MTT developing dye (1 mL) was added over the plates.

4.5 Supplemental Data

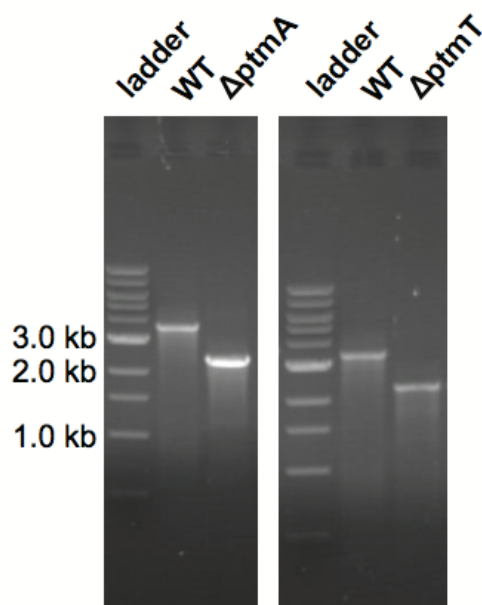
Table 4.S1. Strains and plasmids used in this study.

Strains	Relevant genotype/comments	Source/Ref
<i>Escherichia coli</i> DH10B	<i>F mcrA Δ(mrr-hsdRMS-mcrBC)φ80lacZΔM15 ΔlacX74 recA1 endA1 araD139 Δ(ara, leu)7697 galU galK λ⁻ rspL nupG</i>	GibcoBRL
<i>E. coli</i> ET12567(pUZ8002)	<i>dam dcm hsdS</i> , pUZ8002	⁷
<i>Streptomyces pactum</i> ATCC 27456	Wild-type pactamycin producing strain	ATCC
<i>S. pactum</i> Δ <i>ptmH</i>	<i>ptmH</i> disruption mutant	⁸
<i>S. pactum</i> Δ <i>ptmA</i>	<i>ptmA</i> disruption mutant	This study
<i>S. pactum</i> Δ <i>ptmT</i>	<i>ptmT</i> disruption mutant	This study
<i>S. pactum</i> Δ <i>ptmH-ptmT</i>	<i>ptmH</i> and <i>ptmT</i> double mutant	This study
Plasmids		
pJET1.2	pMBI-based PCR product cloning vector; T7 promoter; <i>bla</i> .	Fermentas
pGEM-T	High copy number PCR cloning vector containing T7 and SP6 RNA polymerase promoters flanking a multiple cloning region within the alpha-peptide coding region of the enzyme beta-galactosidase; <i>bla</i> .	Promega
pJTU1278+	pHZ1358 derivative containing <i>lacZ</i> and MCS	¹
pTMN002	pJTU1278+ derivative containing a 1 kb <i>aac(3)/IV</i> apramycin resistance cassette	²
pTMW032	1 kb DNA fragment containing downstream PCR product of <i>ptmA</i> gene in pJET1.2	This study
pTMW033	1 kb DNA fragment containing upstream PCR product of <i>ptmA</i> gene in pJET1.2	This study
pTMW034	Two 1 kb PCR fragments upstream and downstream of the <i>ptmA</i> gene in pTMN002	This study
pTMW035	1 kb DNA fragment containing downstream PCR product of <i>ptmT</i> gene in pJET1.2	This study
pTMW036	1 kb DNA fragment containing upstream PCR product of <i>ptmT</i> gene in pJET1.2	This study
pTMW037	Two 1 kb PCR fragments upstream and downstream of the <i>ptmT</i> gene in pTMN002	This study
TIP3	Fosmid clone containing part of the <i>ptm</i> cluster	²
5A7	Fosmid clone containing part of the <i>ptm</i> cluster	²
24H11	Fosmid clone containing part of the <i>ptm</i> cluster	²

Table 4.S2. Primers used in this study

Primer	Sequence ^(a)
<i>ptmA</i> -F1	5'- CCC <u>AAGCTT</u> GCTGCTCGCCTTCGTGGA -3'
<i>ptmA</i> -R1	5'- CCG <u>GAATTC</u> CCAGGGCTCGTACCGCATC -3'
<i>ptmA</i> -F2	5'- CCG <u>GAATTC</u> ATCGTCGCCACCCTCCGCTCG -3'
<i>ptmA</i> -R2	5'- TGCT <u>TCTAGAC</u> CGGCGTGACGGGCGTCGTT -3'
<i>ptmA</i> -P1	5'- CGACCACTCGCTGGGCTTCA -3'
<i>ptmA</i> -P2	5'- GACGATGTCCGCCGACCATT -3'
<i>ptmT</i> -F1	5'- CCC <u>AAGCTT</u> CTCTGGCCCGTGATGAATCCG -3'
<i>ptmT</i> -R1	5'- CCG <u>GAATTC</u> GTTGGCACCCACTGAGAACCTC -3'
<i>ptmT</i> -F2	5'- CCG <u>GAATTC</u> CAGCGGTCCCTGGTCGGA -3'
<i>ptmT</i> -R2	5'- TGCT <u>TCTAGAT</u> CGCATCGGCCCTCGTCG -3'
<i>ptmT</i> -P1	5'- CAGCCGCACGCAGGTCAGTT -3'
<i>ptmT</i> -P2	5'- GACGTTGATGCAGGTGGACAGC -3'

^(a) nucleotides underlined refer to restriction sites

**Figure 4.S1.** Gel electrophoreses of PCR products that confirm $\Delta ptmA$ and $\Delta ptmT$ mutant strains of *S. pactum*.

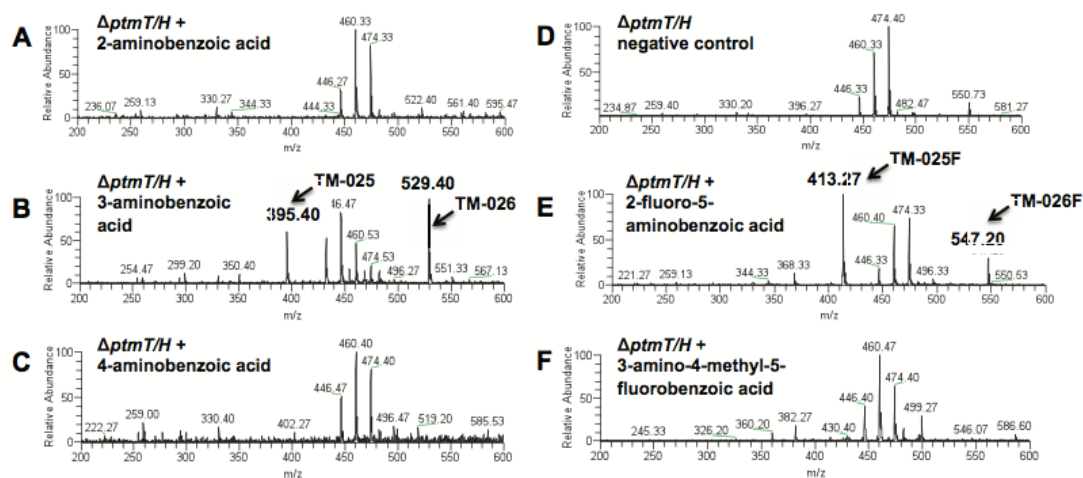


Figure 4.S2. MS data for *n*-BuOH extracts from $\Delta ptmT/H$ cultures complemented with external precursors.

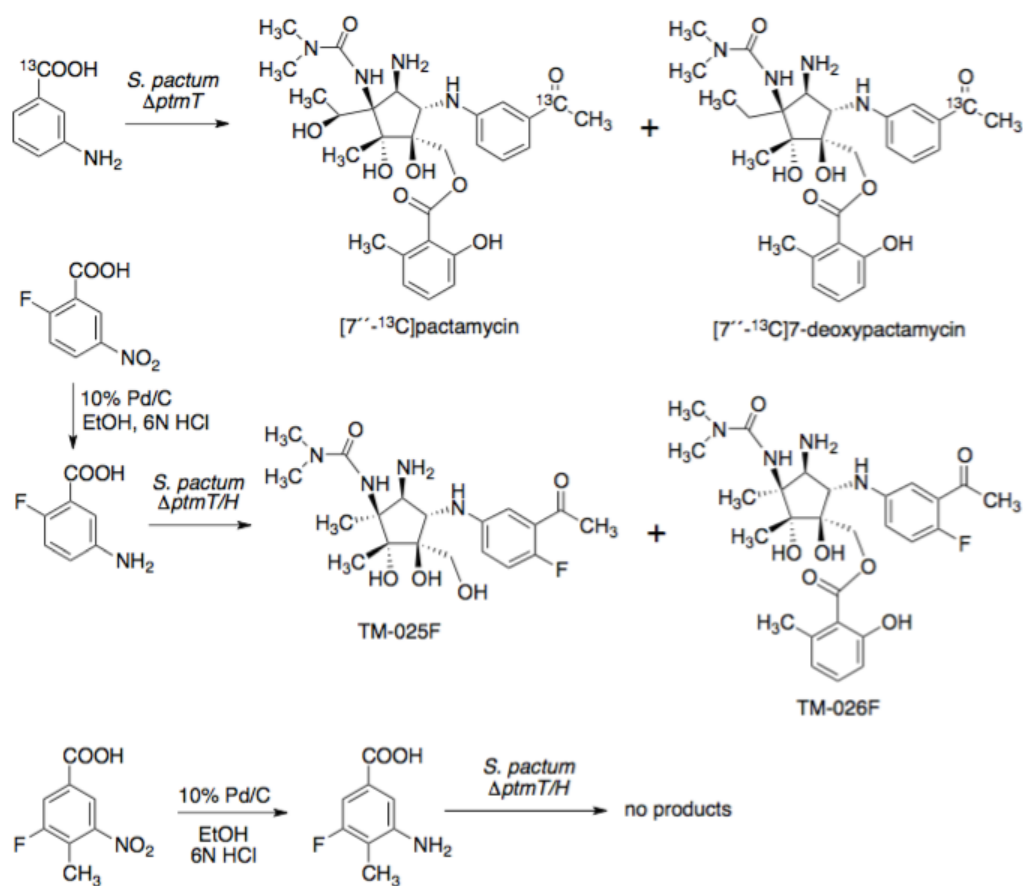


Figure 4.S3. Preparation of fluorinated precursors and chemical complementation experiments with $\Delta ptmT/H$ mutants.

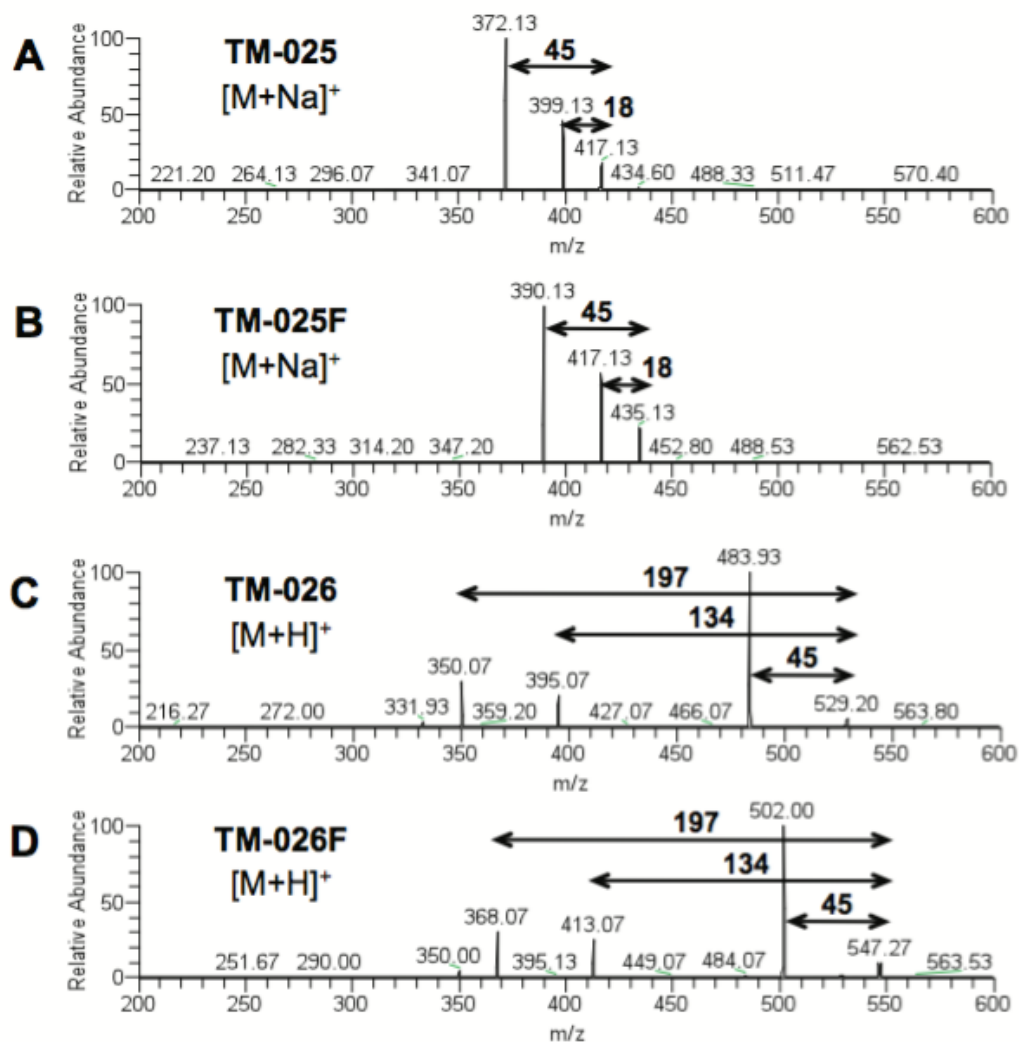


Figure 4.S4. MS/MS analysis of TM-025, TM-026, and their fluorinated analogs.

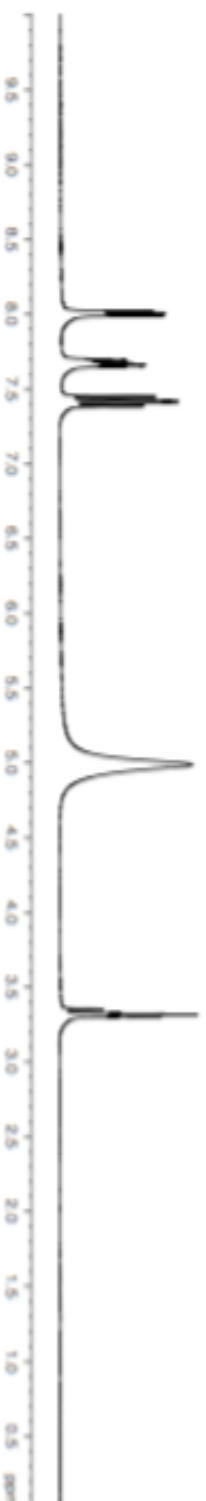


Figure 4.S5. ^1H NMR spectrum of 2-fluoro-5-aminobenzoic acid.

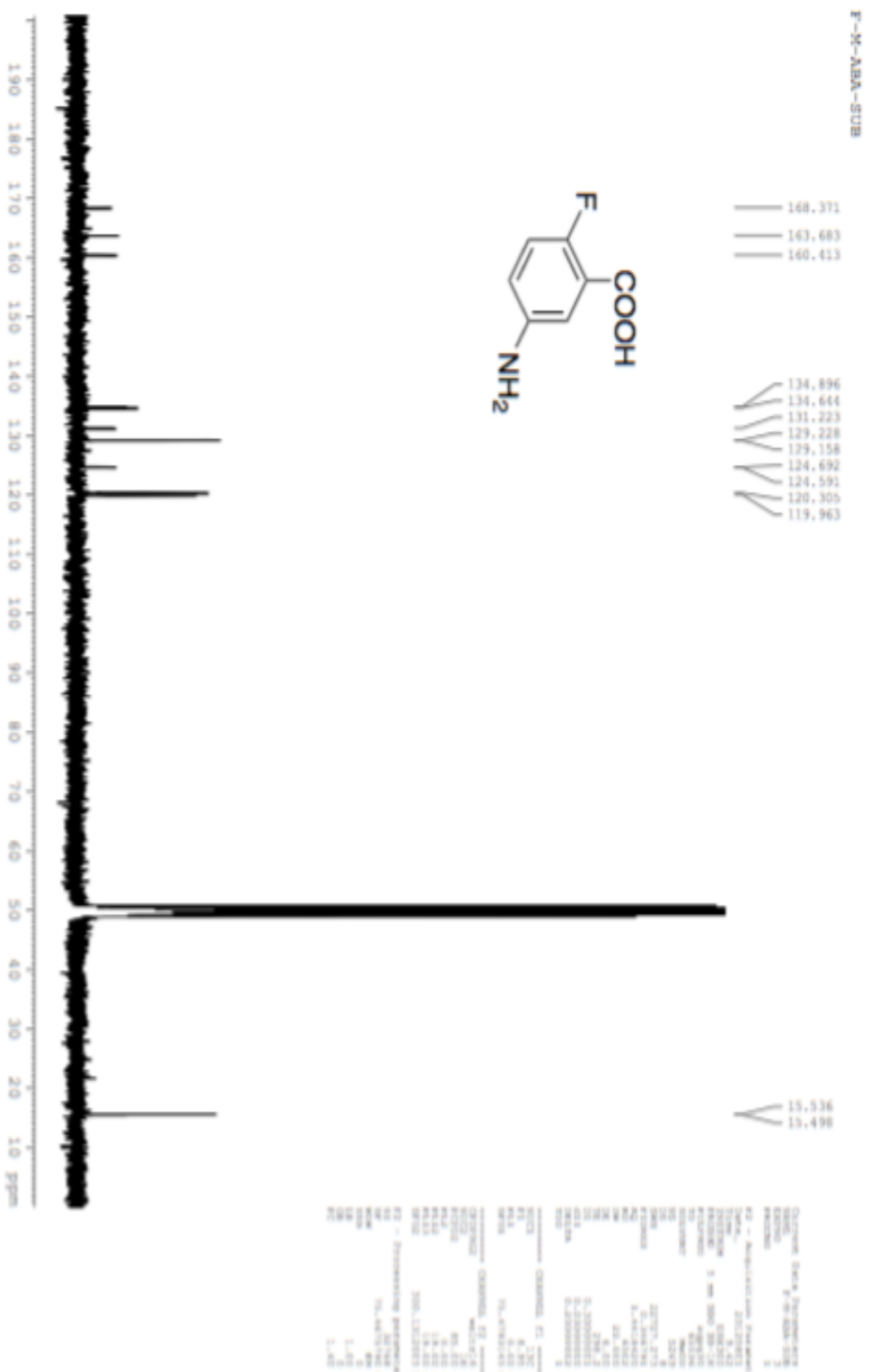


Figure 4.S6. ^{13}C NMR spectrum of 2-fluoro-5-aminobenzoic acid.

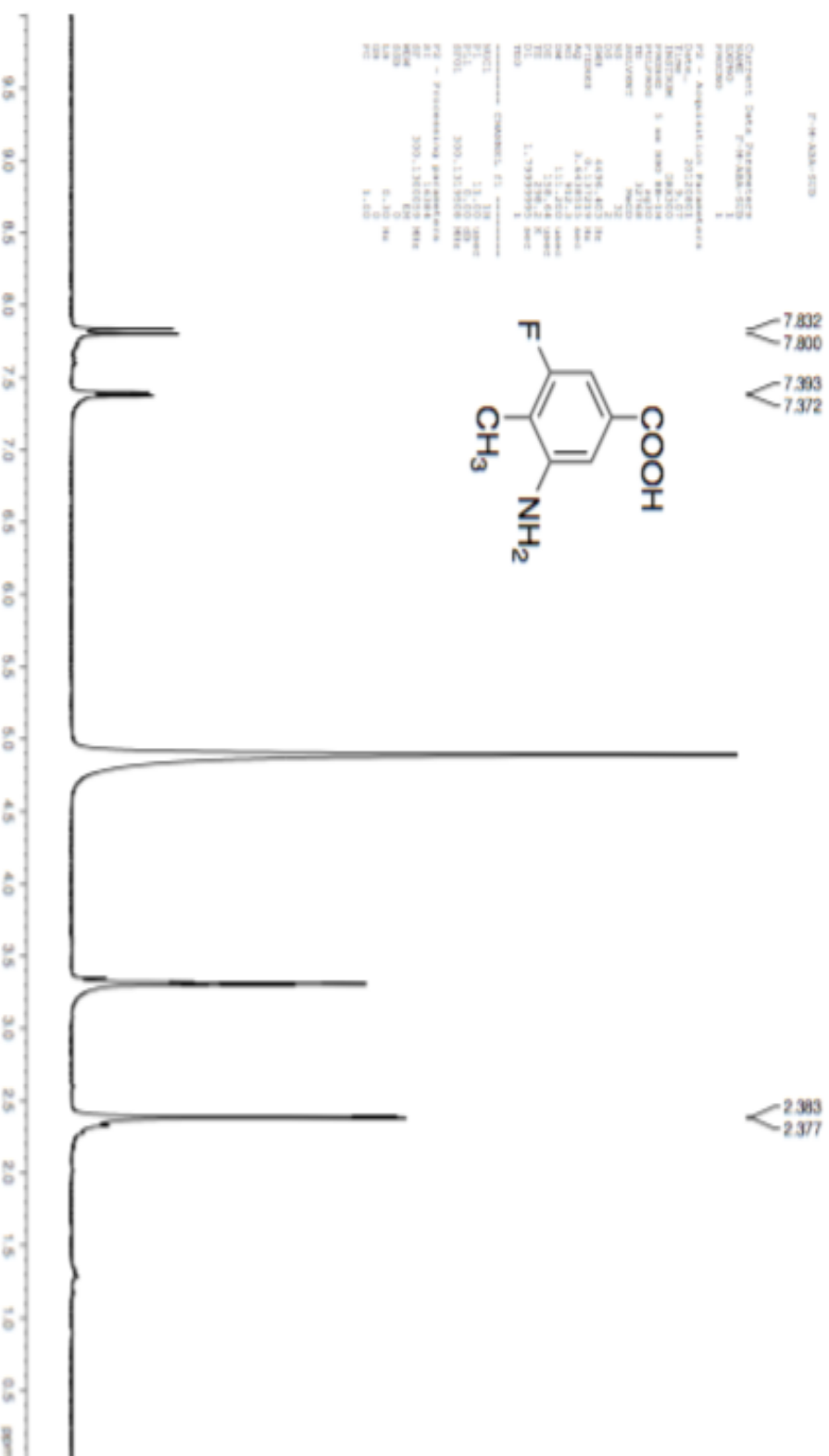
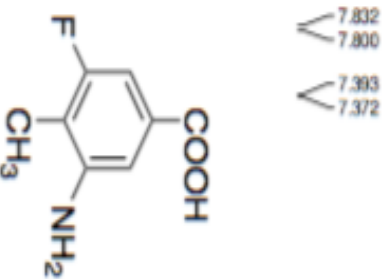


Figure 4.S7. ^1H NMR spectrum of 3-amino-4-methyl-5-fluorobenzoic acid.

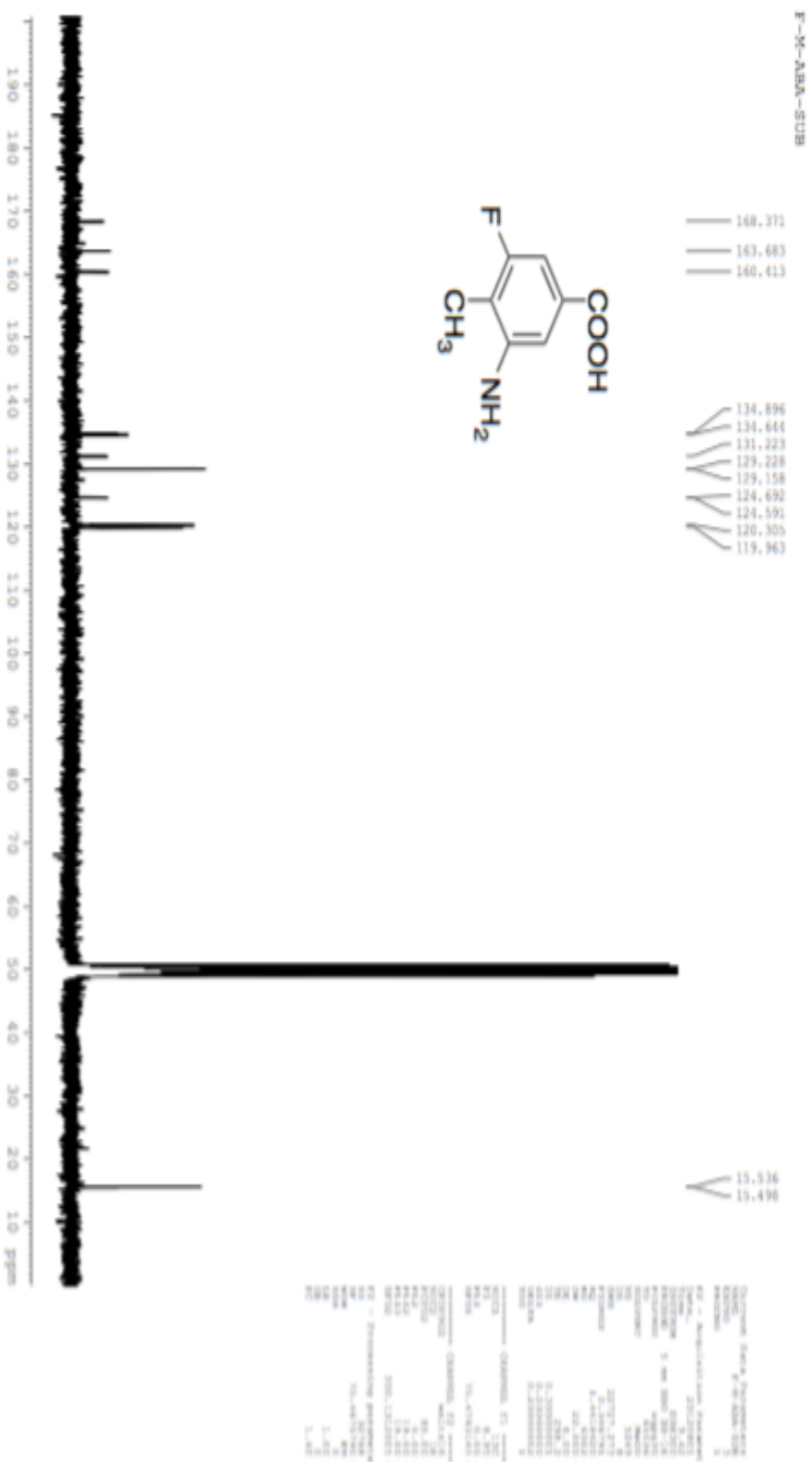


Figure 4.S8. ^{13}C NMR spectrum of 3-amino-4-methyl-5-fluorobenzoic acid.

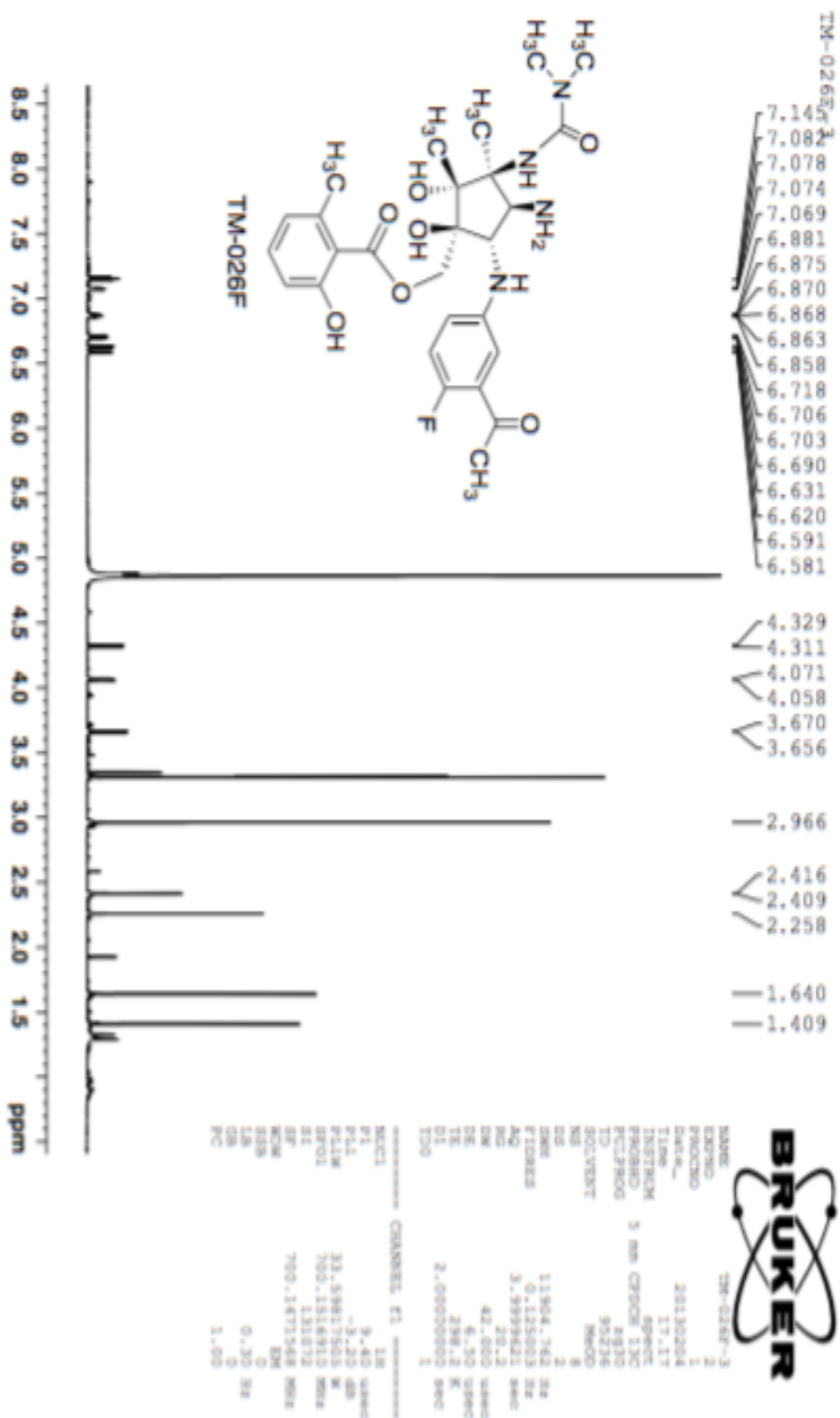


Figure 4.S9. ¹H NMR spectrum of TM-026F.

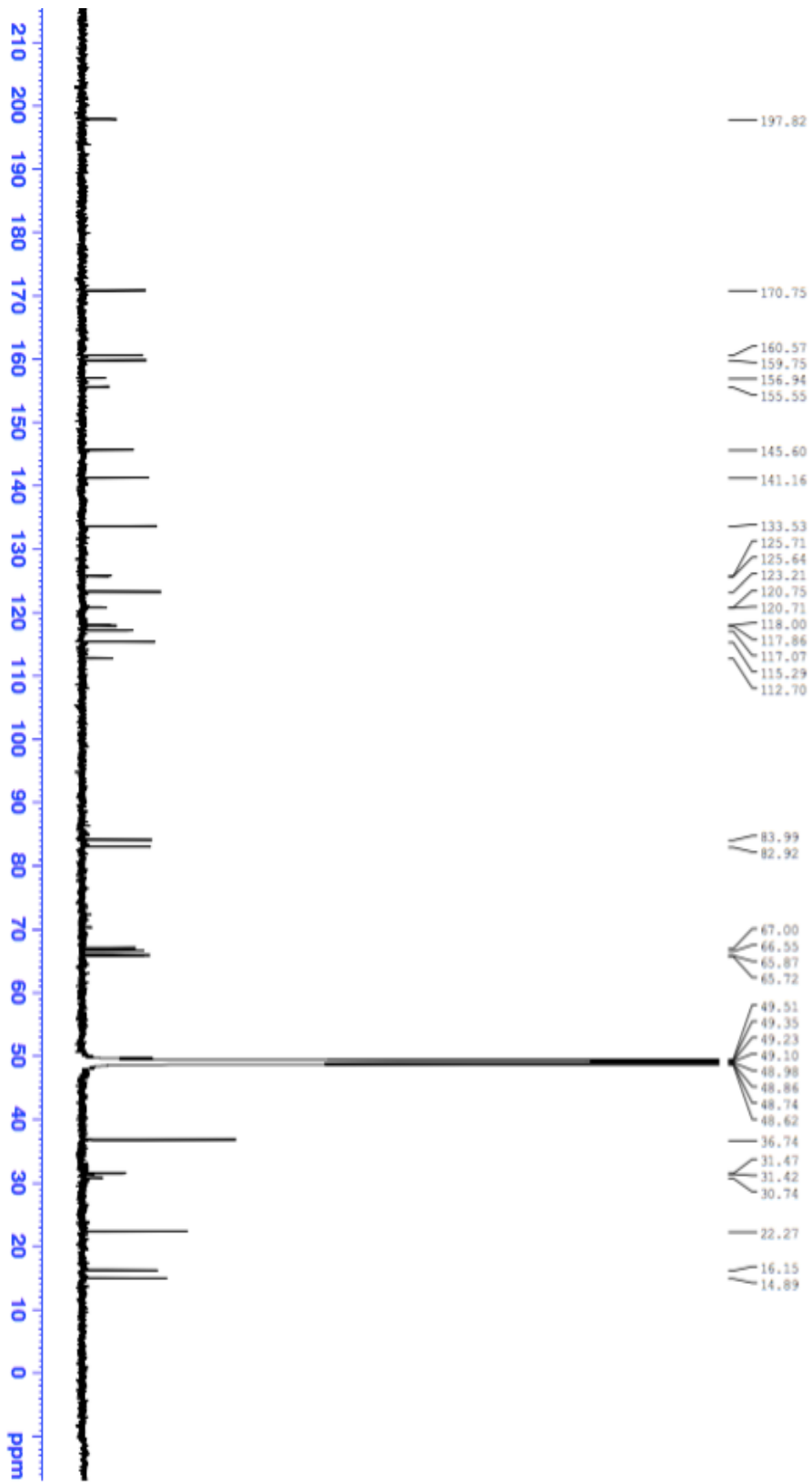


Figure 4.S10. ¹³C NMR spectrum of TM-026F.

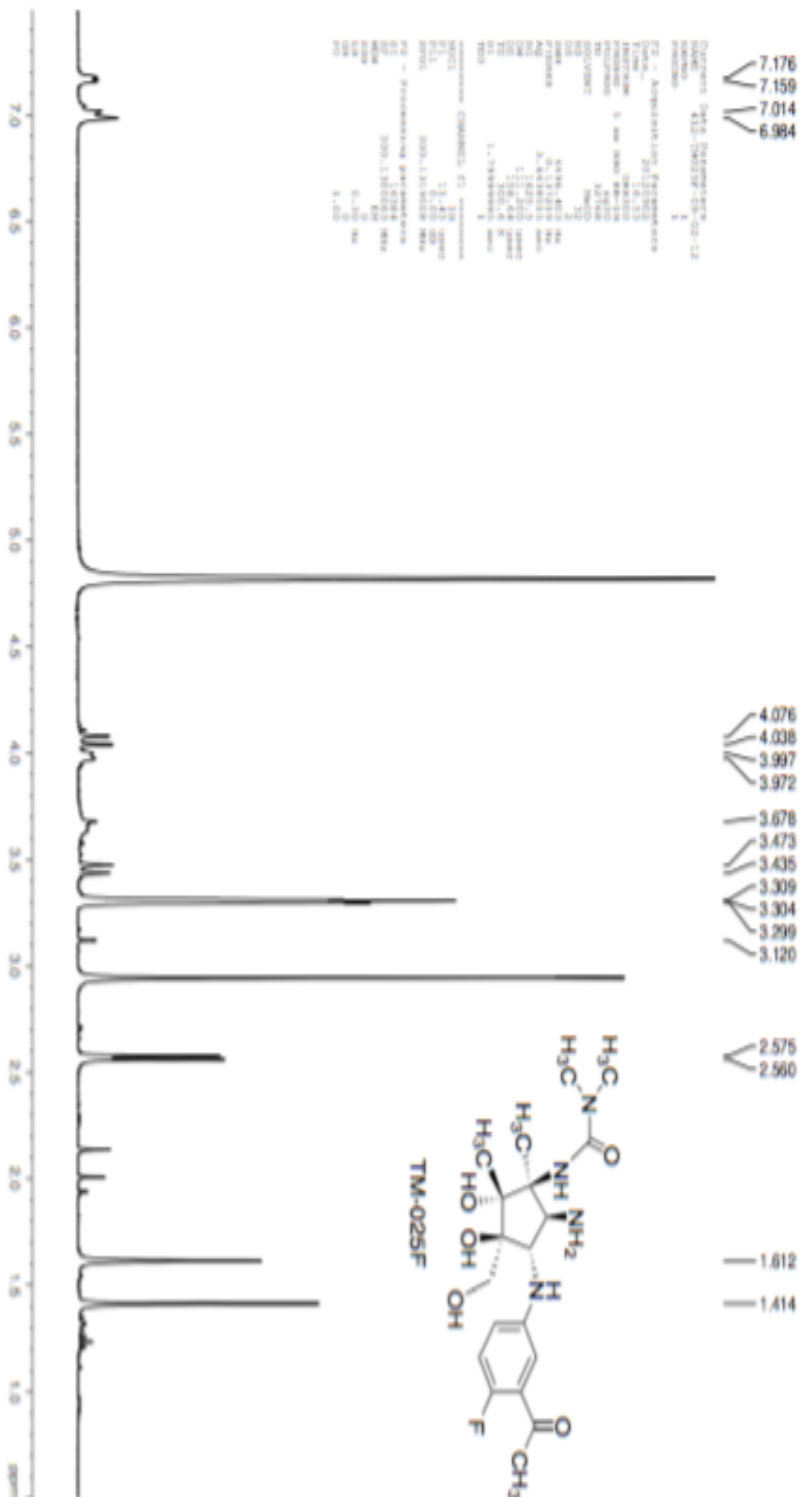


Figure 4.S11. ¹H NMR spectrum of TM-025F.

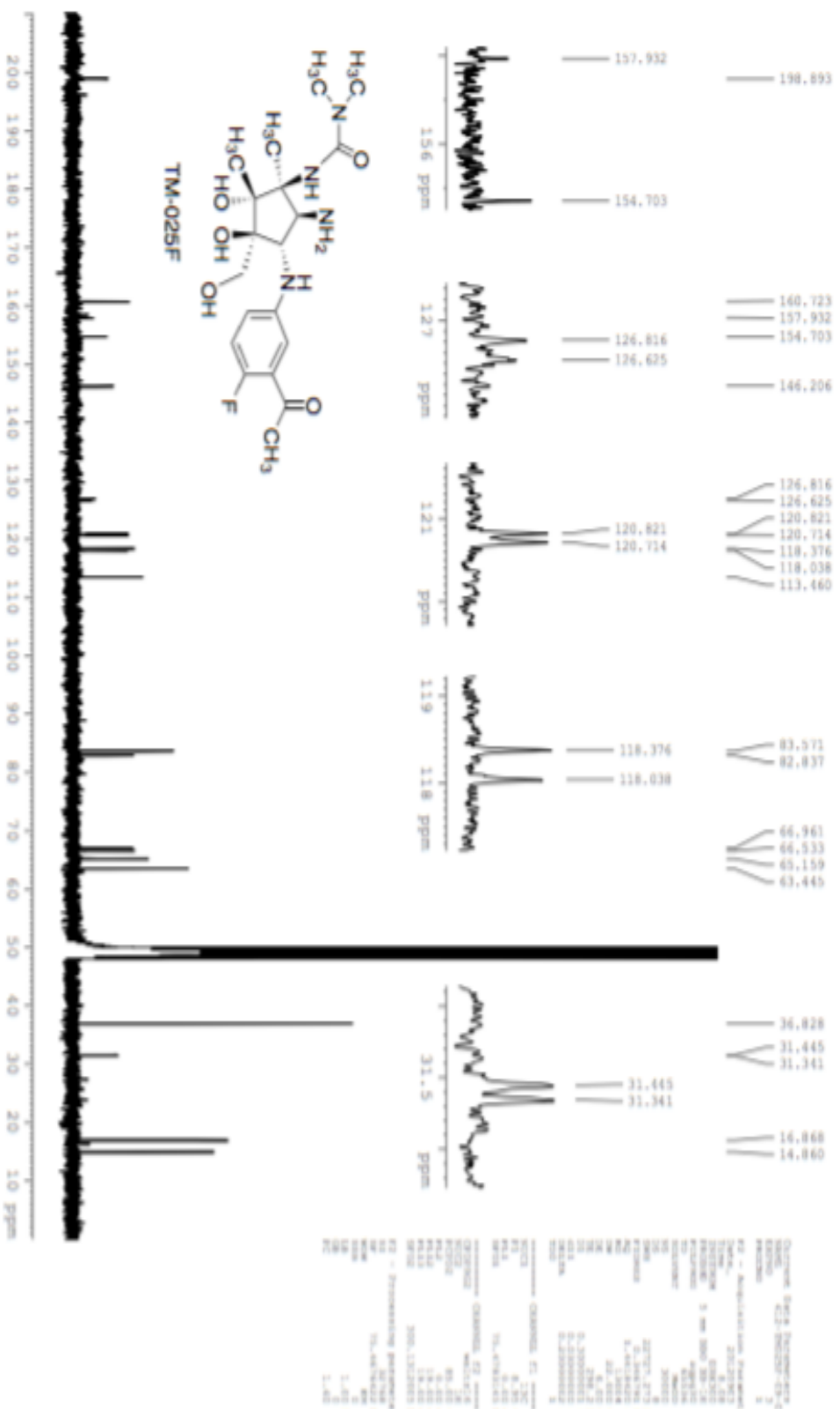


Figure 4.S12. ^{13}C NMR spectrum of TM-025F.

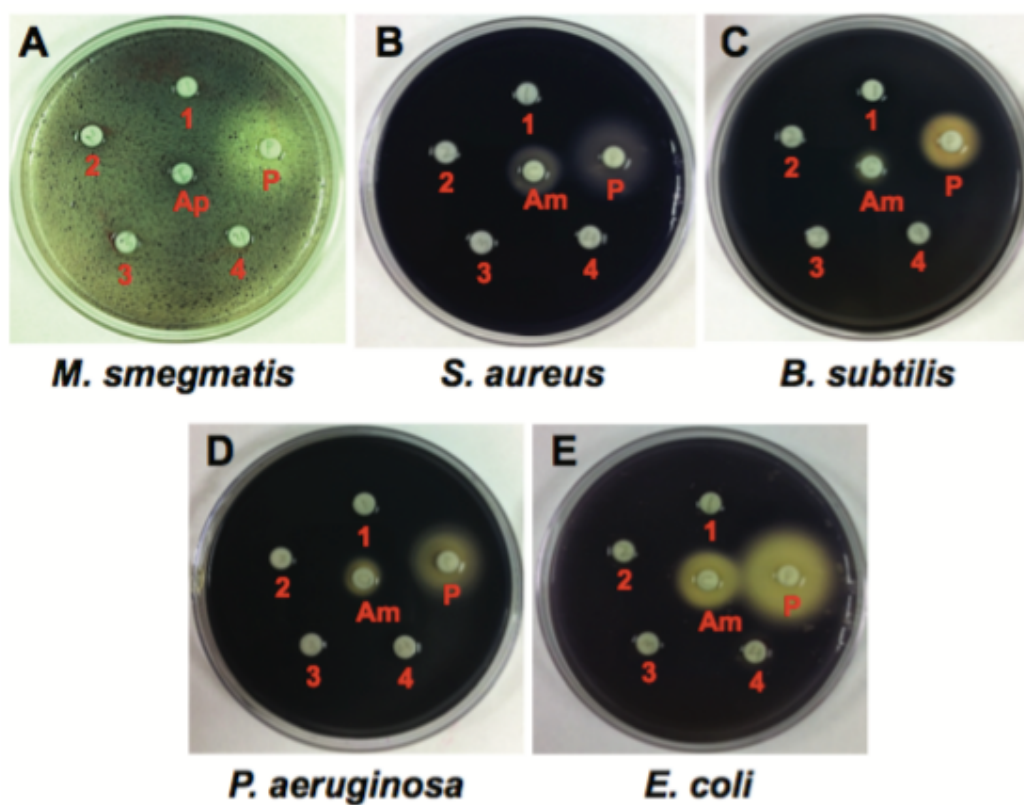


Figure 4.S13. Agar diffusion assay of pactamycin analogs. 1, TM-025; 2, TM-026; 3, TM-025F; 4, TM-026F; P, pactamycin; Am, ampicillin.

4.5 References

- Adams, E. S. and K. L. Rinehart (1994). "Directed biosynthesis of 5'-fluoropactamycin in *Streptomyces pactum*." J Antibiot (Tokyo) **47**(12): 1456-1465.
- Bhuyan, B. K. (1962). "Pactamycin production by *Streptomyces pactum*." Appl Microbiol **10**: 302-304.
- Brodersen, D. E., W. M. Clemons, Jr., A. P. Carter, R. J. Morgan-Warren, B. T. Wimberly and V. Ramakrishnan (2000). "The structural basis for the action of the antibiotics tetracycline, pactamycin, and hygromycin B on the 30S ribosomal subunit." Cell **103**(7): 1143-1154.
- Chan, K. K. and D. O'Hagan (2012). "The rare fluorinated natural products and biotechnological prospects for fluorine enzymology." Methods Enzymol **516**: 219-235.
- Dinos, G., D. N. Wilson, Y. Teraoka, W. Szaflarski, P. Fucini, D. Kalpaxis and K. H. Nierhaus (2004). "Dissecting the ribosomal inhibition mechanisms of edeine and pactamycin: the universally conserved residues G693 and C795 regulate P-site RNA binding." Mol Cell **13**(1): 113-124.
- Hanessian, S., R. R. Vakiti, S. Dorich, S. Banerjee and B. Deschenes-Simard (2012). "Total synthesis of pactamycin and pactamycate: a detailed account." J Org Chem **77**(21): 9458-9472.
- Hanessian, S., R. R. Vakiti, S. Dorich, S. Banerjee, F. Lecomte, J. R. DelValle, J. Zhang and B. Deschenes-Simard (2011). "Total synthesis of pactamycin." Angew Chem Int Ed Engl **50**(15): 3497-3500.
- He, Y., Z. Wang, L. Bai, J. Liang, X. Zhou and Z. Deng (2010). "Two pHZ1358-derivative vectors for efficient gene knockout in streptomyces." J Microbiol Biotechnol **20**(4): 678-682.
- Ito, T., N. Roongsawang, N. Shirasaka, W. Lu, P. M. Flatt, N. Kasanah, C. Miranda and T. Mahmud (2009). "Deciphering pactamycin biosynthesis and engineered production of new pactamycin analogues." Chembiochem **10**(13): 2253-2265.
- Kelly, J. X., M. J. Smilkstein, R. A. Cooper, K. D. Lane, R. A. Johnson, A. Janowsky, R. A. Dodean, D. J. Hinrichs, R. Winter and M. Riscoe (2007). "Design, synthesis, and evaluation of 10-N-substituted acridones as novel chemosensitizers in *Plasmodium falciparum*." Antimicrob Agents Chemother **51**(11): 4133-4140.
- Kieser, T., M. J. Bibb, M. J. Buttner, K. F. Chater and D. A. Hopwood (2000). ""Practical *Streptomyces* Genetics". The John Innes Foundation Norwich: England.
- Knapp, S. and Y. Yu (2007). "Synthesis of the oxygenated pactamycin core." Org Lett **9**(7): 1359-1362.
- Lu, W., N. Roongsawang and T. Mahmud (2011). "Biosynthetic studies and genetic engineering of pactamycin analogs with improved selectivity toward malarial parasites." Chem Biol **18**(4): 425-431.

Malinowski, J. T., S. J. McCarver and J. S. Johnson (2012). "Diastereocontrolled construction of pactamycin's complex ureido triol functional array." Org Lett **14**(11): 2878-2881.

Otoguro, K., M. Iwatsuki, A. Ishiyama, M. Namatame, A. Nishihara-Tukashima, S. Shibahara, S. Kondo, H. Yamada and S. Omura (2010). "Promising lead compounds for novel antiprotozoals." J Antibiot (Tokyo) **63**(7): 381-384.

Rinehart, K. L., Jr., M. Potgieter, D. L. Delaware and H. Seto (1981). "Direct evidence from multiple ^{13}C labeling and homonuclear decoupling for the labeling pattern by glucose of the m-aminobenzoyl (C7N) unit of pactamycin." J. Am. Chem. Soc. **103**: 2099-2101.

Sambrook, J. and D. W. Russell (2001). Molecular Cloning. A Laboratory Manual. New York, Cold Spring Harbor Laboratory Press.

Smilkstein, M., N. Sriwilaijaroen, J. X. Kelly, P. Wilairat and M. Riscoe (2004). "Simple and inexpensive fluorescence-based technique for high-throughput antimalarial drug screening." Antimicrob Agents Chemother **48**(5): 1803-1806.

Taber, R., D. Rekosh and D. Baltimore (1971). "Effect of pactamycin on synthesis of poliovirus proteins: a method for genetic mapping." J Virol **8**(4): 395-401.

White, F. R. (1962). "Pactamycin." Cancer Chemother Rep **24**: 75-78.

CHAPTER V

General Conclusion

Khaled H. Almabruk

Despite the fact that tuberculosis and malaria are treatable infectious diseases, the rate of morbidity and mortality resulting from these two infectious diseases worldwide is disturbingly high. While a number of global efforts to combat TB and malaria have started to show some encouraging results, the progress is decelerated by the increased cases of multidrug-resistant (MDR)-TB and malaria, which rendered many currently available treatments ineffective. Therefore, continued efforts to discover new drugs that can treat MDR-TB and malaria are acutely needed.

Accordingly, we have launched a drug discovery program focusing on bioactive natural products that have anti-TB and anti-malarial activities. Taking advantages of the advancements in the technology of molecular genetics, gene sequencing, and genetic engineering we employed biosynthetic approaches to access new analogs of natural products. This was successfully done with the rifamycin polyketide synthases as described in Chapter 2 and with the pactamycin biosynthetic machinery described in Chapter 4. Replacing the module 6 acyltransferase (AT) domain of the rif PKS with the module 2 AT domain of the rapamycin PKS has resulted in a mutant that was able to produce a new rifamycin analog, 24-desmethylrifamycin SV. Such a rifamycin analog, in which a modification occurred in the polyketide backbone, would have been difficult to produce synthetically. On the other hand, inactivation of genes responsible for tailoring processes in pactamycin biosynthesis has also resulted in mutants that produce analogs of

pactamycin. This approach is considered advantageous over the conventional total synthetic methods, as both rifamycin and pactamycin are highly complex natural products, which are intrinsically difficult to be synthesized. However, we have employed a semi-synthetic methodology to convert 24-desmethylrifamycin SV to 24-desmethylrifampicin. The latter compound was directly compared with rifampicin for their anti-TB activity against both rifampicin-sensitive and –resistant strains of *Mycobacterium tuberculosis*. To our delight, 24-desmethylrifampicin was active against both rifampicin-sensitive and -resistant strains of *M. tuberculosis*.

Similarly, some of the genetically engineered analogs of pactamycin also showed improved pharmacological properties. As shown in Chapter 4, TM-025 and TM-026 and their fluorinated analogs, which were produced by precursor-directed structure modifications (mutasynthesis) using a mutant strain of *Streptomyces pactum*, showed excellent anti-malarial activity and were 10-30 fold less toxic than pactamycin. These results underscore the utility of biosynthetic approaches to generate new analogs of complex natural products with potent biological activity.

In addition, we have employed a synthetic methodology to produce perbergin, a geranylated isoflavonone that may have antibacterial activity against *M. tuberculosis*. The synthesis of the reported perbergin as a racemic mixture was achieved in nine steps with an overall yield of 13.5%. However,

interestingly, upon the completion of this synthesis, we discovered that the NMR data for the synthetic products are different from those published for perbergin. Revisiting of the raw data for perbergin has led to the revision of its published chemical structure. While the synthetic compounds showed good activity and selectivity toward Gram-positive bacteria, including *Mycobacterium smegmatis*, they lack activity against *M. tuberculosis* at a concentration lower than 10 $\mu\text{g/mL}$. This is rather disappointing. However, the activity of the synthetic compounds against other Gram-positive bacteria including *Staphylococcus aureus* is encouraging. Further exploration of geranylated isoflavanones may lead to new antibacterial agents.

Appendices

Appendix A: Other scientific work published during Mr. Khaled Almabruk's Ph.D. program.

Asamizu, S.; Yang, J.; **Almabruk, K.**; Mahmud, T. Pseudoglycosyltransferase Catalyzes Non-Glycosidic C-N Coupling in Validamycin A Biosynthesis. *J. Am. Chem. Soc.* (2011) 133, 12124-12135.

Almabruk, K.; Asamizu, S.; Chang, A.; Varghese, S. G.; Mahmud, T. The alpha- Ketoglutarate/Fe(II) -Dependent Dioxygenase VldW Is Responsible for the Formation of Validamycin B. *ChemBioChem* (2012) 13, 2209-11.

Cavalier, M. C.; Yim, Y. S.; Asamizu, S.; Neau, D.; **Almabruk, K.**; Mahmud, T.; Lee, Y. H., Mechanistic insights into validoxylamine A 7'-phosphate synthesis by VldE using the structure of the entire product complex. *PLoS One* (2013) 7, e44934.

Osborn, A.;[§] **Almabruk, K.**;[§] Holzwarth, G.;[§] Asamizu, S.; LaDu, J.; Kean, K.; Karplus, P.; Tanguay, R.; Bakalinsky, A.; and Mahmud, T. De novo Synthesis of a Sunscreen Compound in Vertebrates. *eLife* (2015) 4:e0591.